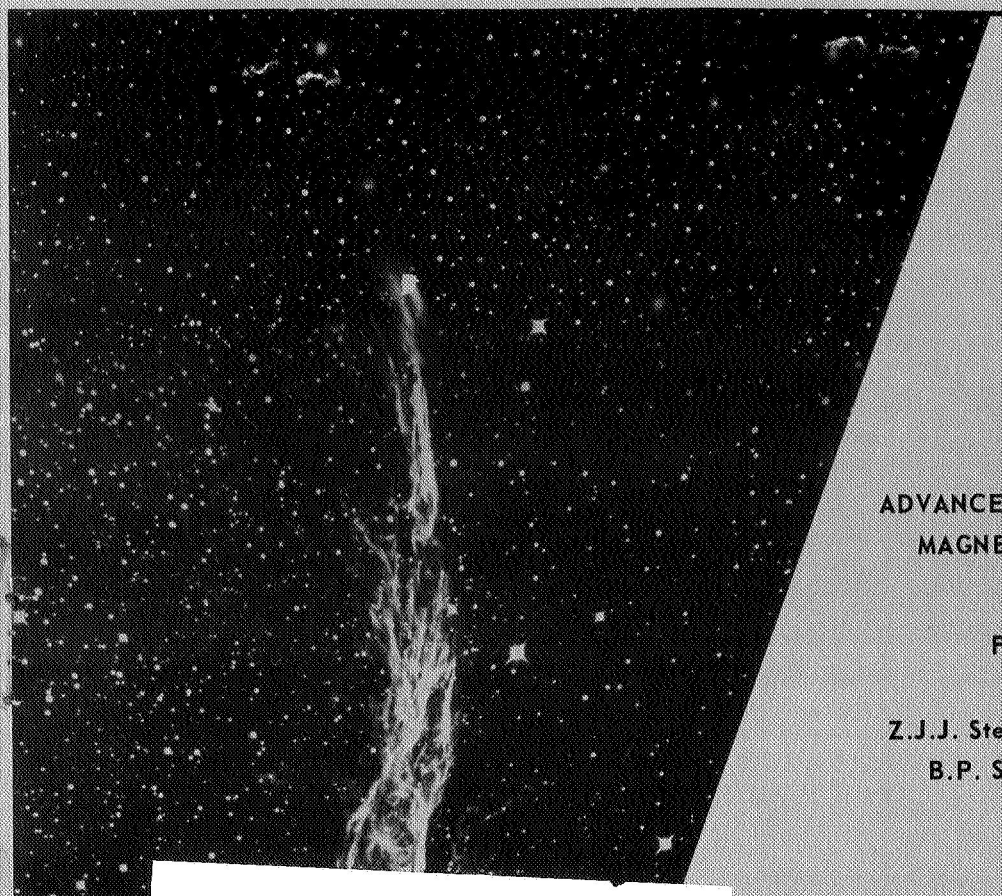

ADVANCED SUPERCONDUCTING MAGNETS INVESTIGATION

FINAL REPORT

Z.J.J. Stekly, R. Thome, E. Lucas,
B.P. Strauss and F. DiSalvo

Contract No. NAS 8-21037
April 1968

prepared for

GEORGE C. MARSHALL SPACE FLIGHT CENTER
NATIONAL AERONAUTICS AND SPACE ADMINISTRATION
Huntsville, Alabama

AVCO EVERETT RESEARCH LABORATORY
A DIVISION OF AVCO CORPORATION

ADVANCED SUPERCONDUCTING MAGNETS INVESTIGATION

FINAL REPORT

by

Z. J. J. Stekly, R. Thome, E. Lucas, B. P. Strauss
and F. Di Salvo

AVCO EVERETT RESEARCH LABORATORY
a division of
AVCO CORPORATION
Everett, Massachusetts

Contract No. NAS 8-21037

February 1968

prepared for

GEORGE C. MARSHALL SPACE FLIGHT CENTER
NATIONAL AERONAUTICS AND SPACE ADMINISTRATION
Huntsville, Alabama

FOREWORD

This report is the result of work performed under NASA Contract NAS 8-21037.

The authors wish to thank E. Urban and L. Lacey who monitored the program for the time, effort, and suggestions in regard to this program.

The 6-inch coil used in the experimental program was built by E. Lucas and T. deWinter under contract NAS 3-9684 with NASA Lewis Research Center and we wish to thank J. Lawrence for making this magnet available.

TABLE OF CONTENTS

LIST OF ILLUSTRATIONS

I. GENERAL INTRODUCTION

This report is a summary of the work done under Contract NAS 8-21037.

The main aim of the work performed was to develop analytically the steady state behavior of composite superconductors and to verify this behavior experimentally.

There are many effects which are observed in measurements of superconductors, and it is not the intent of the authors to claim that all of these can be explained by studying the steady state terminal characteristics. However, most of the work on the behavior of superconductors in coils is aimed at determining stability, and if stability is achieved then a steady state model should apply. As such, the conditions derived for stability or instability using a steady state model should provide a framework for study of superconductor behavior.

The first part of this report deals with the analysis of the behavior of a composite superconductor consisting of the superconductor itself and a highly conducting substrate in which all gradients along the conductor are neglected - this is referred to as the zero-dimensional analysis. It begins with the simplest case of a conductor exposed to a coolant which is assumed to have a heat transfer characteristic represented by a constant heat transfer coefficient. Even with this restriction this simple analysis is quite general, since the standard technique of using the heat transfer coefficient corresponding to the particular heat flux at each point can be readily applied if the heat transfer coefficient varies with heat flux.

Following this, the effect of the transition from nucleate to film boiling is investigated and a general steady state stability map is developed which is very useful in understanding the conductor characteristics.

The effect of poor thermal contact between the superconductor and the substrate as well as any temperature gradients in the superconductor itself are shown to be destabilizing effects, and lead to the conclusion that small superconducting filaments are desirable because of the increased area of contact as well as the reduced temperature gradients in the superconductor.

In most of the analyses an additional heat source is included for generality. This is done because heaters can be used very effectively as diagnostic tools, and also defects and joints can usually be represented as local heat sources.

Following the zero dimensional analyses, a one-dimensional model in which gradients along the conductor are taken into account was analyzed. This starts out with a constant heat transfer coefficient and analyzes the behavior of a conductor with a local heat source. The conditions required

for a local heat source to produce only local resistive regions are investigated in detail, and the effect of the transition from nucleate to film boiling is also considered.

Both the zero-dimensional as well as the one dimensional analyses assume heat transfer to a coolant which can convect heat away. In either of these cases it is not possible to conduct heat to a heat sink very far way without very large temperature gradients. In one dimension, the temperature drops linearly between the heat source and the heat sink, and in two dimensions it drops as the natural logarithm of the distance. It is only in three dimensions that conduction cooling alone can result in steady state solutions for finite amounts of heat generated. The case of three dimensional heat transfer was investigated, and the special case of only conduction cooling was solved.

The two dimensional case was formulated, but did not reduce to the simple meaningful results as in the case of one and three dimensions.

In addition to some preliminary experiments which are described in this report, the main experimental part of the program was aimed at verifying the predictions of the analytical model.

Specifically, tests were run on single wires heated locally to verify the results obtained in the one-dimensional analysis.

Another series of test involved the behavior of a 6-inch diameter coil wound with square copper stabilized Nb-Ti conductor. This coil was instrumented with heaters in the windings, and was operated in helium at various pressures and temperatures. A complete stability map was determined for this coil.

A paper has been accepted for publication in which the work under this contract is presented. This is reproduced in detail as an appendix to this report.

II. STEADY STATE STABILITY IN ZERO DIMENSIONS

A. Introduction

The behavior of a superconductor in a coil or as part of a circuit is determined by its terminal characteristics. These terminal characteristics are in general a function of the magnetic field and the relative degree to which the superconductor is cooled.

A superconducting material exposed to an external magnetic field can be characterized as having zero resistance up to its critical current. At this point the voltage rises very sharply at practically constant current. This in turn results in Joule heating raising the temperature of the superconductor.

Due to the high current densities characteristic of superconductors, the current must usually be considerably reduced before the sample can again cool down and return to fully superconducting behavior. The return to the superconducting state can be made at higher currents if an alternate path of low resistance is provided and the conductor is well cooled.

The analysis presented here concerns the behavior of a short sample of superconductor which has been stabilized by placing it in good electrical and thermal contact with a normally conducting substrate exposed to the liquid helium bath and in an externally applied magnetic field. Consider what must happen in such a conductor as the current is increased. At low currents, all the current flows in the superconductor until it reaches its maximum current carrying capacity. If the conductor is well cooled so that the conductor temperature rise can be neglected, then a further increase in current will result in a "spilling over" of the excess current from the superconductor to the normal substrate.

The net result is a sharing of the total current between the superconductor and the substrate. The superconductor must develop some resistance to limit its current, otherwise it would take on more current. Obviously, if not enough cooling is provided, the temperature rise due to current in the substrate will result in a lowering of the current carrying capacity of the superconductor resulting in more current in the substrate and a complete transfer of current to the substrate may occur.

To determine the stability of the conductor we must analyze the behavior of the conductor when current is shared between the substrate and the superconductor. To do this in a general fashion, we shall include a heating per unit length of q_h.

B. Linear Heat Transfer Characteristic of Liquid Helium

For this analysis the superconductor is initially assumed to be thin enough and to be in excellent thermal and electrical contact with a normal substrate of high thermal conductivity so that the temperature and voltage is the same in the superconductor and substrate at any point of the composite cross section. These assumptions imply that temperature and voltage gradients within the conductor may be neglected. The assumption of no temperature gradients will later be relaxed.

If we define $0 \leq f \leq 1$ as being the fraction of the total current I which flows in the substrate, then the voltage per unit length of the conductor is:

$$v = \rho \, If/A \qquad \text{(II-1)}$$

where ρ and A are the resistivity and cross sectional area of the substrate.

We now consider a heat balance on a unit length of the conductor

$$hP(T-T_b) = vI + q_h = \frac{\rho I^2 f}{A} + q_h \qquad \text{(II-2)}$$

where h is the heat transfer per unit surface area per unit temperature rise from the conductor to the cooling bath at a temperature T_b and is assumed to be a constant.* The perimeter of the conductor that is exposed to the cooling bath is P.

From this we can find the temperature rise at the wire

$$T-T_b = \frac{vI + q_h}{hP} = \frac{\rho I^2 f}{hPA} + \frac{q_h}{hP} \qquad \text{(II-3)}$$

Under conditions of current sharing between superconductor and substrate, the temperature T, and the externally applied magnetic field determine the current in the superconductor.

Let us define $I_{ch}(T_b)$ as the maximum current a superconductor can carry at the bath temperature T_b and in an externally applied magnetic field, H. This is the so-called short sample or H-I curve of the superconductor. The current in the superconductor I_s is given by the following relationship:

$$I_s/I_{ch} = g\left[(T - T_b)/(T_{ch} - T_b)\right] \qquad \text{(II-4)}$$

it follows that $g(0) = 1$ and $g(1) = 0$. Here T_{ch} is the superconductor critical temperature (with zero current flowing through it) in a field H and g represents

*The case of a heat transfer coefficient which varies with heat flux can be handled by using the value of heat transfer coefficient corresponding to the particular heat flux at each point.

the functional relationship between the superconductor current and temperature. For most superconductors the functional relationship is well approximated by a straight line:

$$I_s/I_{ch} = \left[1 - (T - T_b)/(T_{ch} - T_b)\right] \qquad \text{(II-5)}$$

It is useful to introduce a stability parameter.

$$\alpha \equiv \frac{\rho I_{ch}^2}{hPA\,(T_{ch} - T_b)}$$

Use of Eqs. (II-1) and (II-3) and the definition of α result in the following expressions after some simplification:

$$f = \frac{\tau \quad - 1 + Q_h}{\tau \quad \left[1 - \alpha\, \tau \quad\right]} \qquad \text{(II-6)}$$

$$vA/\rho I_{ch} = \frac{\tau \; - 1 + Q_h}{1 - \alpha \tau} \qquad \text{(II-7)}$$

$$\theta = \frac{\alpha \tau\, (\tau - 1 + Q_h)}{1 - \alpha\, \tau} \qquad \text{(II-8)}$$

where

$$Q_h = \frac{q_h}{hP\,(T_{ch} - T_b)}$$

$$\tau = I/I_{ch}$$

$$\theta = (T - T_b)\ /\ (T_{ch} - T_b)$$

Equations (II-6), (II-7), and (II-8) are shown plotted in Figs. II-1, II-2, and II-3 respectively, for several values of α for $Q_h = 0$ and for several values of Q_h for $\alpha = 2$.

Figure II-2 shows the voltage-current characteristics of a unit length of the conductor. Since we are interested in the behavior of this conductor in a coil which is inductive, we should examine the stability at constant current.

Two distinct types of operation are possible for no heat input ($q_h = 0$) depending on the value of α. For $\alpha < 1.0$ no voltage appears until $I = I_{ch}$ (the superconductor current carrying capacity). For $I > I_{ch}$ the voltage increases gradually with current. The characteristic is everywhere single valued. For $\alpha > 1.0$ the operation is more complicated:

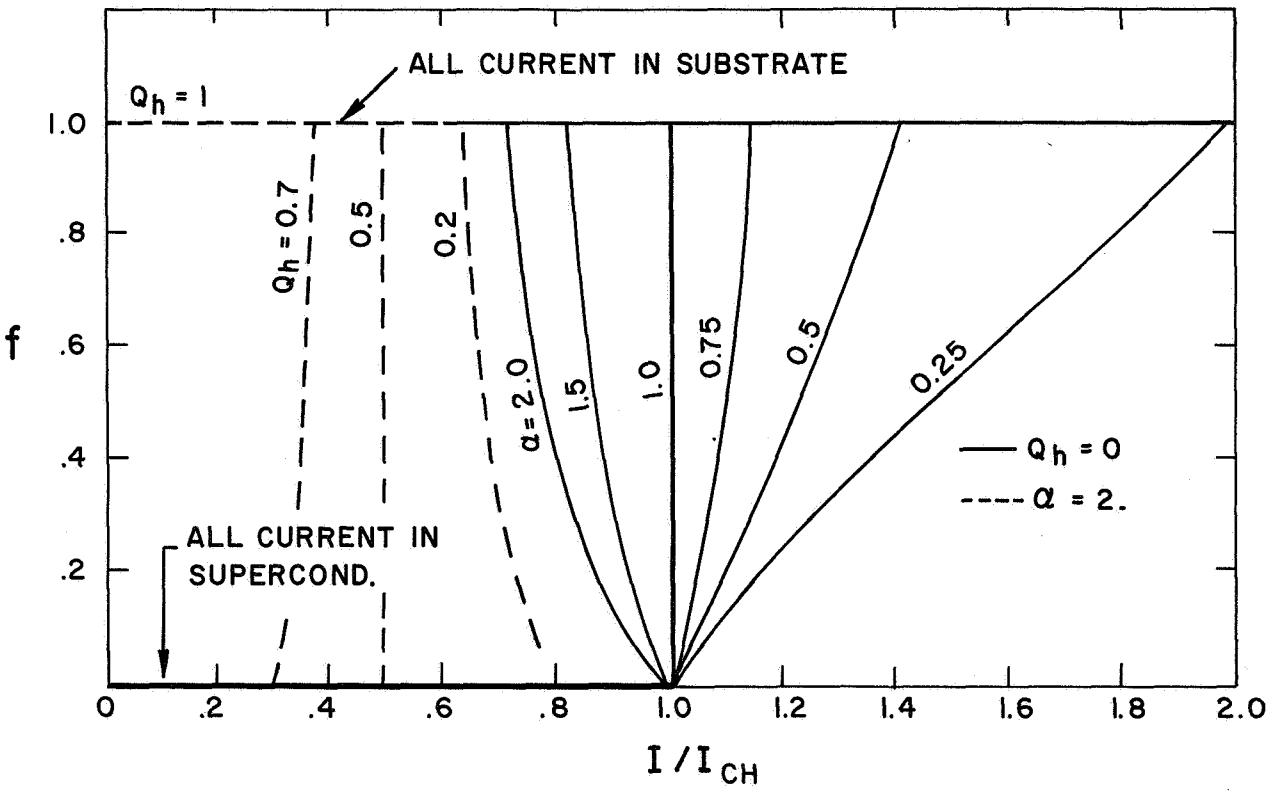

Fig. II-1 Current sharing between a stabilized superconductor and a cooled substrate. The dependent variable f is the fraction of the total current conducted by the substrate.

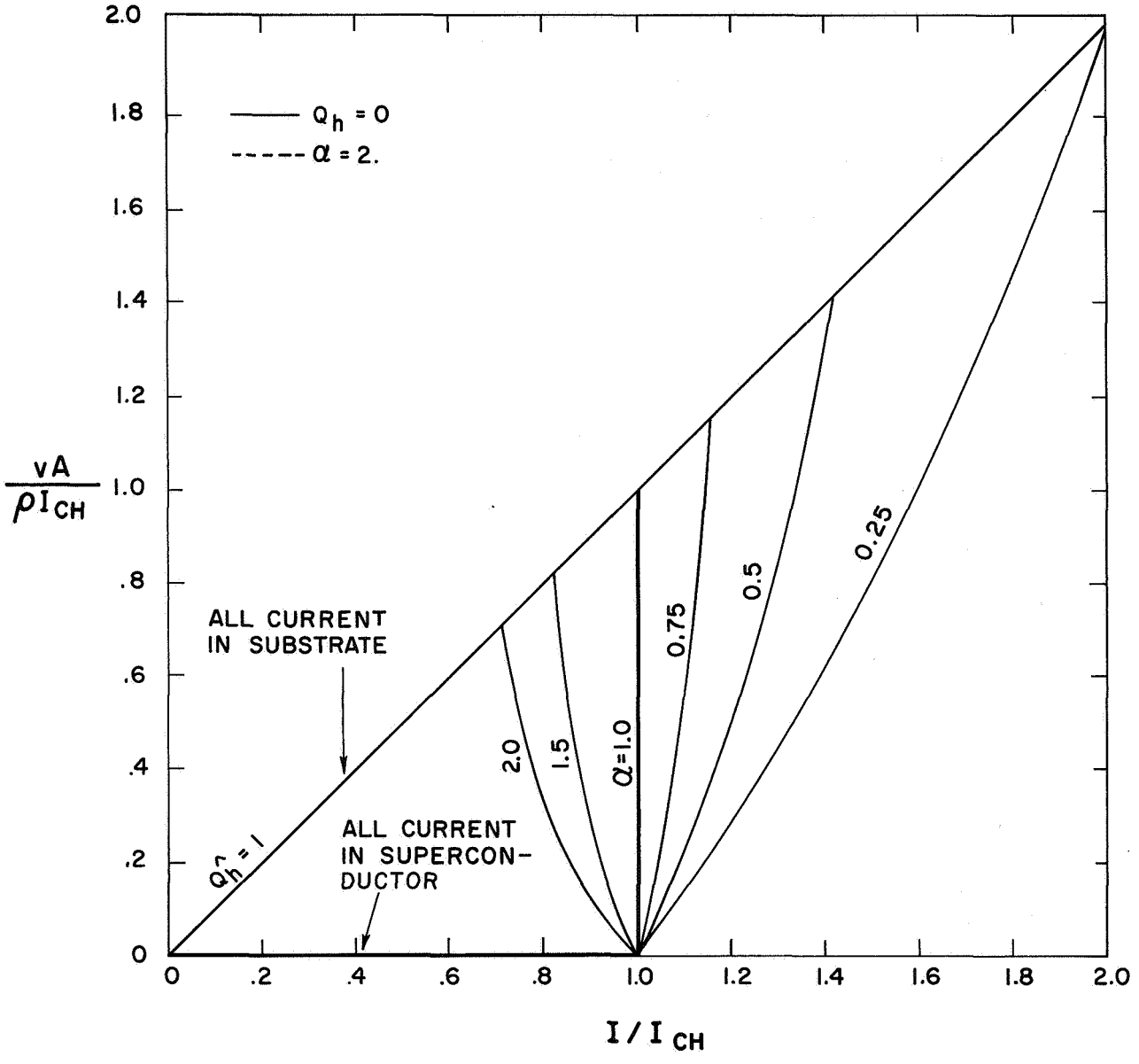

Fig. II-2 Voltage - current characteristics for a stabilized superconductor - substrate combination

For: $$0 < \tau \leq \frac{1}{\sqrt{\alpha}}$$

Single valued operation results with all the current in the superconductor (v = 0).

For: $$\frac{1}{\sqrt{\alpha}} \leq \tau \leq 1$$

Double valued operation results with either all the current in the superconductor or all the current in the substrate.*

For: $$\tau > 1$$

Single valued operation results with all the current in the substrate.

Completely stable operation results for $\alpha \leq 1.0$. For $\alpha > 1.0$ stable operation is limited to currents up to $I_{ch}/\sqrt{\alpha}$. In the region of current above $I_{ch}/\sqrt{\alpha}$ steady operation with all the current in the superconductor is still possible up to I_{ch}; however, should the conductor suffer a disturbance then all the current will immediately switch to the substrate.

The effect of heat is easily summarized by the following behavior:

(1) Current begins to transfer out of the superconductor at a total current of

$$\tau = 1 - Q_h \Big]_{f = 0+}$$

which simplifies to $I/I_{ch} = 1$ for $Q_h = 0$. If $Q_h = 1.0$ then a voltage exists for all values of $I/I_{ch} > 0$. The physical interpretation of this is that enough heat is supplied to raise the temperature to its critical value even with no current flowing. This means that the range of interest is $0 < Q_h < 1.0$.

(2) The amount of heat necessary to completely drive the current out of the superconductor at any current is:

$$Q_h \Big]_{f = 1.0} = 1 - \alpha \tau^2$$

(3) The slope of the voltage-current characteristic at the first appearance of voltage is:

$$\frac{d\,(vA/\rho I_{ch})}{d\,(I/I_{ch})}\Bigg]_{v = 0+} = \frac{1}{1 - \alpha\,(1 - Q_h)}$$

*Operation on the negative resistance part of the curve is unstable for a constant current type of operation.

since α is multiplied by $(1 - Q_h)$ the effect of heat is to reduce the slope of the voltage-current curve at the first appearance of voltage. However, this is done at the expense of lowering the current at which voltage first appears.

To illustrate this behavior Figs. II-1, II-2, and II-3 also show with dotted lines how f, v, and θ change at $\alpha = 2.0$ with varying heat input Q_h. As can be seen in these plots we can control the initial slope of all of these curves, and particularly the voltage, to a finite positive value by increasing the heat input. However, this lowers the range of (I/I_{ch}) at which the composite is fully superconducting ($f=0$). For $Q_h = 1$ the composite acts as a normal metal.

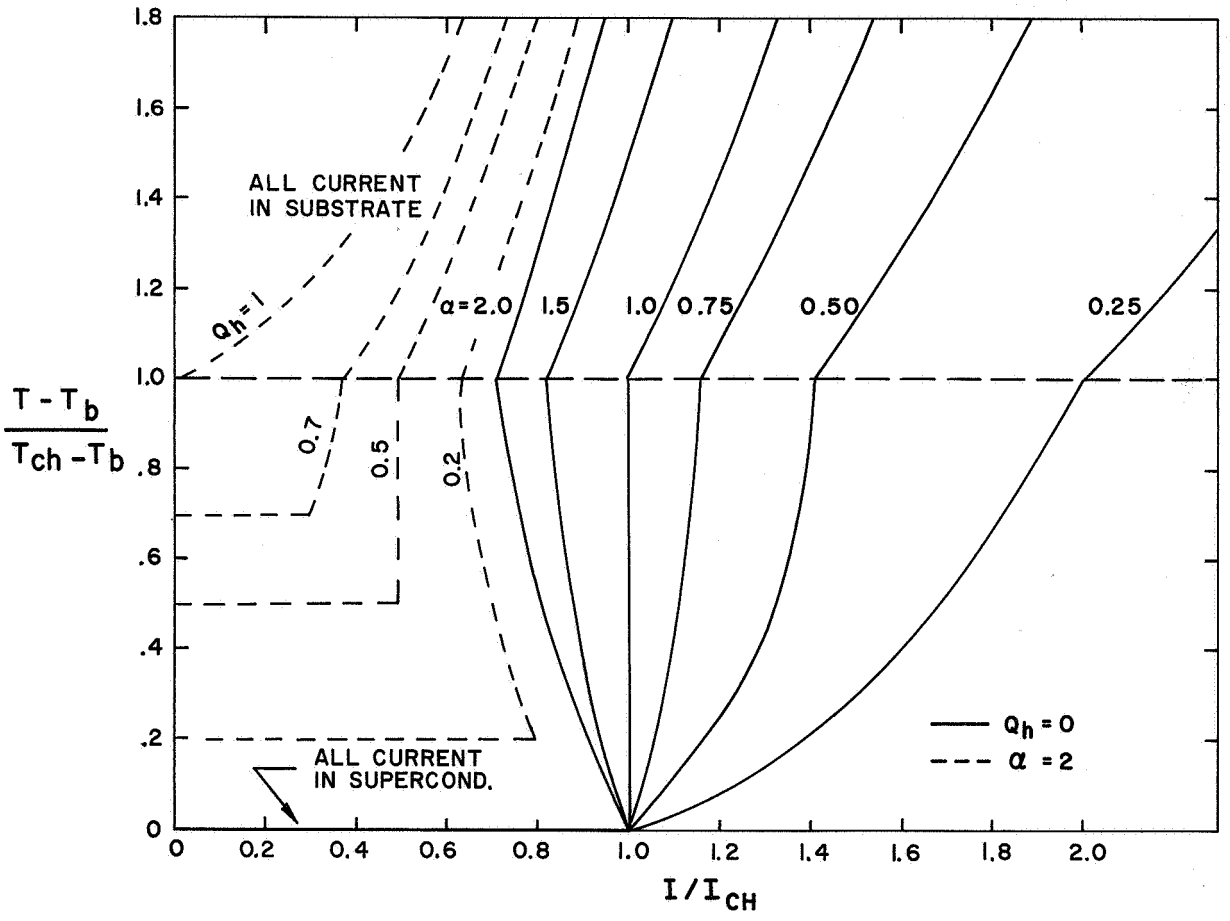

Fig. II-3 Temperature rise of a stabilized superconductor as a function of current and cooling parameter

C. Nonlinear Heat Transfer Characteristic of Liquid Helium

The case of a superconductor surrounded by a liquid helium bath will now be extended to take into account a nonlinear heat transfer coefficient. The nonlinear characteristic of the boiling curve of liquid helium can, to a first approximation, be represented by a region of constant heat transfer coefficient up to a surface temperature T_m which is the maximum temperature at which nucleate boiling can occur; above this temperature a transition to film boiling will occur, and to a first approximation we can assume a constant heat flux per unit area, q''_m. This is justified by the fact that in a coil magnetic field gradients exist so that adjacent turns will be at different conditions. In such a situation if the surface goes into the film boiling region locally, conduction to adjacent turns will result and a plot of local heat flux per unit area (based only on the area of the conductor in question) versus local temperature will exhibit a characteristic which can be approximated as a constant heat flux per unit area of the conductor exposed to helium.

The idealized heat transfer characteristic is shown in Fig. II-4.

In the region of constant heat transfer coefficient the solution for the terminal characteristics with a heat addition q_h per unit length of conductor has been derived in the previous section.

1) The Region of Constant Heat Flux ($T > T_m$)

For constant heat flux:

$$q'' = q_m'' = h\,(T_m - T_b) \qquad \text{(II-9)}$$

This represents a constant power dissipation, therefore:

$$hP\,(T_m - T_b) = \frac{\rho I^2 f}{A} + q_h \qquad \text{(II-10)}$$

Solving Eq. (II-10) and putting it into the usual dimensionless form we find:

$$f = \frac{\theta_m - Q_h}{\alpha \tau^2} \qquad \text{(II-11)}$$

$$\frac{vA}{\rho I_{ch}} = f\tau = \frac{\theta_m - Q_h}{\alpha \tau} \qquad \text{(II-12)}$$

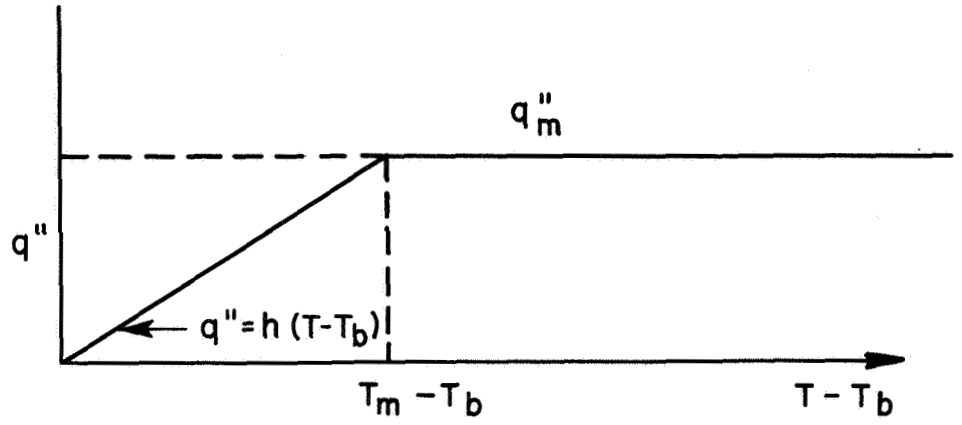

Fig. II-4 The idealized heat transfer characteristic - first approximation

By substituting the constant heat flux expression into Eq. (II-2) and expressing f in terms of θ we can find an expression for θ in the range above nucleate boiling

$$\theta = \frac{\theta_m + \alpha\tau\,(1 - \tau) - Q_h}{\alpha\tau} \qquad \text{(II-13)}$$

where θ_m and Q_h are defined as:

$$\theta_m = \frac{T_m - T_b}{T_{ch} - T_b}$$

$$Q_h = \frac{q_h}{h\,P\,(T_{ch} - T_b)}$$

2) Terminal Characteristics

Using the above equations the terminal characteristics of a conductor can be calculated. Figure II-5 shows the results for the case of no heating ($Q_h = 0$) and for $\theta_m = 0.25$.

For $\alpha < 1$, no voltage appears until the current reaches the critical value, ($I/I_{ch} = 1$) the voltage then rises gradually until the limit of nucleate boiling is reached; at this point all the current is expelled suddenly from the superconductor and transferred to the copper. If the current is then reduced, a recovery occurs in which all or most of the current transfers back into the superconductor. (This cycle is shown in Fig. II-5 for $\alpha = 0.5$.) For $\alpha > 1$, no voltage appears until the current reaches the critical value; then the current transfers abruptly out of the superconductor. Lowering of the current to a recovery value will again result in a return of all the current into the superconductor.

There are three points which characterize the behavior of a particular conductor exposed to a magnetic field.

a) The critical current

This occurs at $I/I_{ch} = 1.0$ (II-14)

b) The transition from nucleate boiling to film boiling from the region where current is shared between the superconductor and its substrate.

This occurs at a current which is found by equating Eqs. (II-12) and (II-7) and solving

$$\frac{I}{I_{ch}} = \frac{1 - \theta_m}{2} + \sqrt{\left(\frac{1 - \theta_m}{2}\right)^2 + \frac{\theta_m - Q_h}{\alpha}} \qquad \text{(II-15)}$$

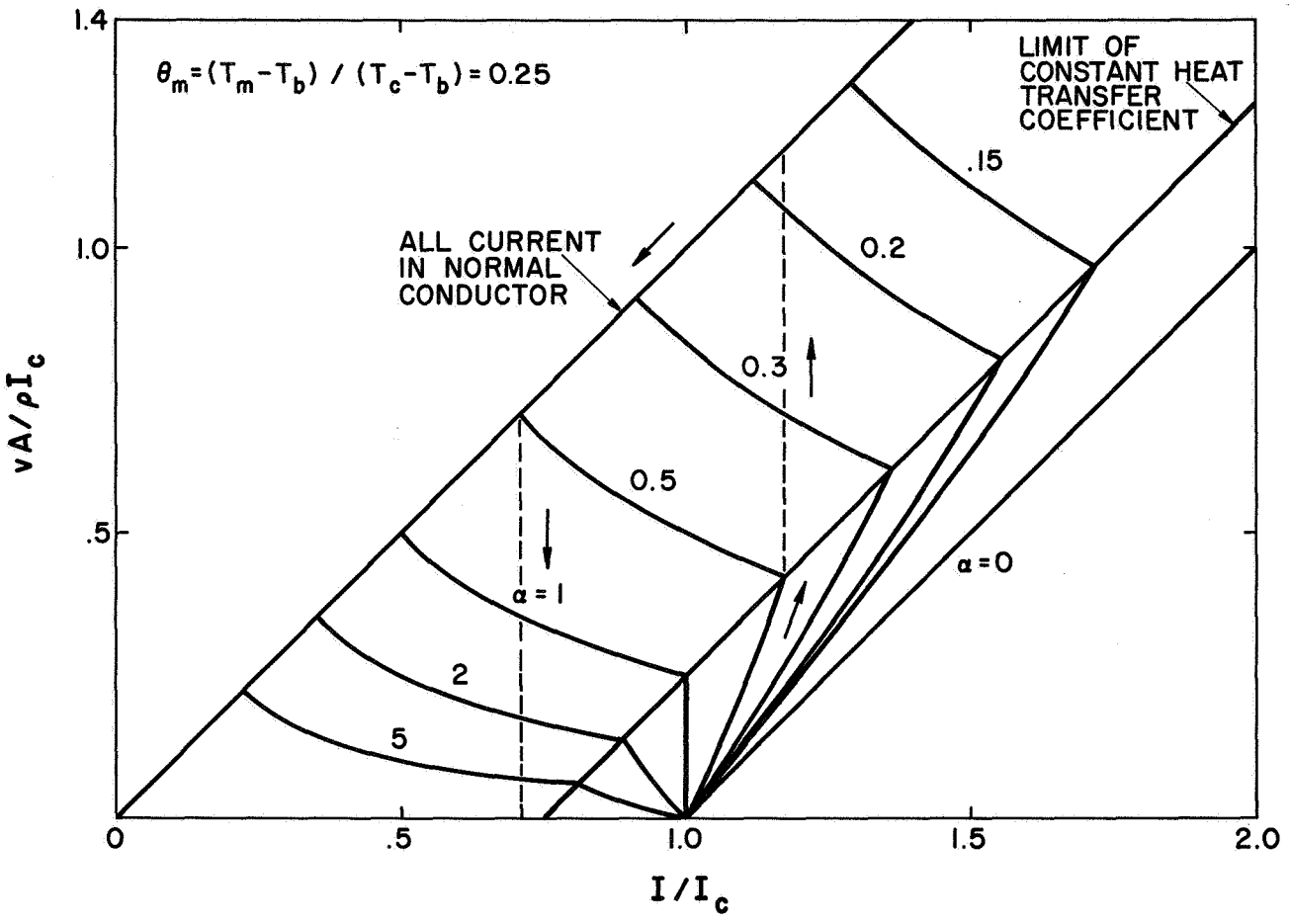

Fig. II-5 Dimensionless terminal characteristics of a conductor taking into account through a simplified model the change in heat transfer characteristics resulting from a transition from nucleate to film boiling

c) The recovery from film boiling to nucleate boiling with all the current in the normal substrate.

This is simply the f = 1 point, which from Eq. (II-11) results in:

$$\frac{I}{I_{ch}} = \sqrt{\frac{\theta_m - Q_h}{\alpha}} \qquad \text{(II-16)}$$

Hysteresis in the boiling curve which results in a transition from nucleate to film at a different heat flux than the recovery transition from film to nucleate can be easily taken into account. These two points correspond to the takeoff point, which can be characterized by a value of q''_m and ΔT_m (which determine α and θ_m), and the recovery point which can be characterized by a different value of the same parameters. Operation of a coil never occurs between these two points since the slope of the V-I characteristic is negative, hence, the details of the curve are not important. It can therefore be concluded that the important characteristics of the heat transfer curve are the constant heat transfer coefficient part, the limit of nucleate boiling, and the recovery to nucleate boiling.

3. Behavior Map

A map can now be drawn up of the different regions of operation for a particular conductor. This type of map is shown schematically in Fig. II-6. The map must take into account the variation of the critical temperature at zero current T_{ch} and the restivity of the substrate ρ with magnetic field.

The behavior of a typical superconductor has the following regions and curves:

a) An I-H curve - represents the current-carrying capacity of the superconductor at the bath temperature.

b) A recovery curve - defined by the condition for maximum nucleate boiling heat flux, with all the current in the normal substrate; conduction of heat between adjacent turns must be taken into account by using an effective value for the maximum heat flux. (Eq. II-16)

c) The takeoff curve - defined by the condition for maximum nucleate boiling heat flux under conditions of current sharing between the superconductor and the normal substrate. Conduction between turns must also be taken into account in calculation of this curve. (Eq. II-15)

d) Stable zero resistance region - below the recovery curve and the I-H curve.

e) Stable resistive region - above the I-H curve and below the recovery curve.

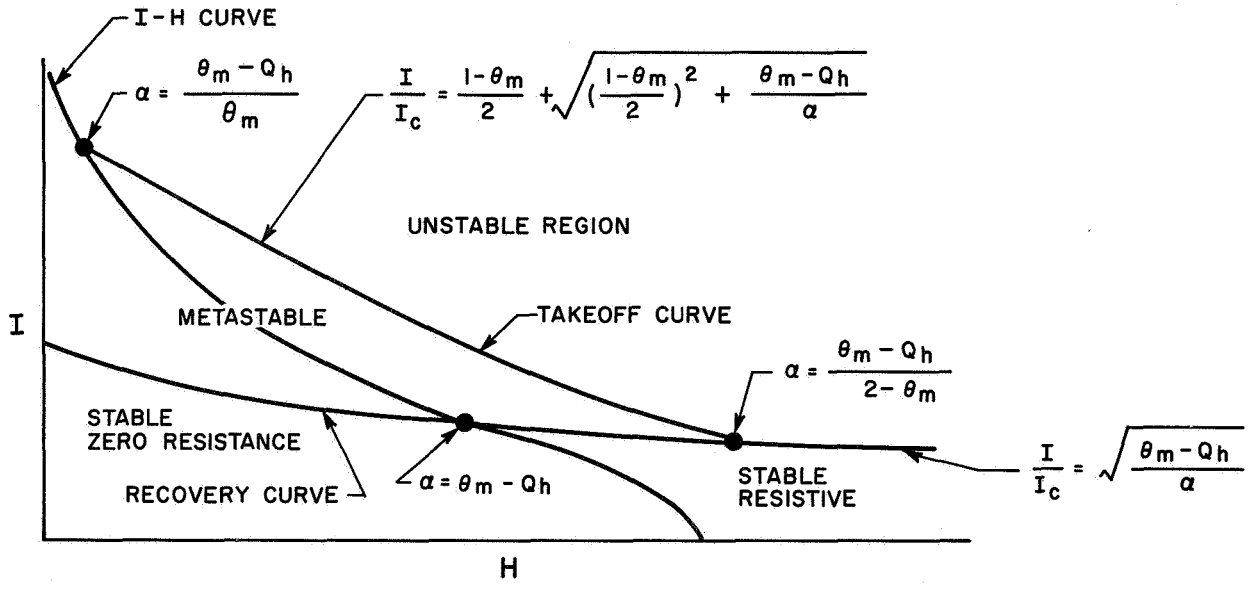

Fig. II-6 Map indicating modes of behavior as predicted by a zero-dimensional analysis incorporating a nonlinear heat transfer characteristic

f) Metastable region - between the takeoff and recovery curves; either below or above the I-H curve in which the conductor can be triggered by a disturbance from the fully superconducting region (below the I-H curve) or from the nucleate boiling region (above the I-H curve) into the film boiling region with the simultaneous local transfer of the current from the superconductor into the normal conductor.

g) Unstable region - operation in this region is possible only with all the current in the normal conductor.

D. Effect of Thermal Contact Resistance

In all previous analyses, it has been stated that the superconductor is in good thermal contact with the substrate. This is equivalent to assuming that there is no discontinuity in temperature at the interface. This section presents a simple model which exhibits the effects of a finite thermal contact resistance.

Using the notation of the previous sections, the heat generated per unit length in the superconducting portion of a composite conductor is

$$q_s = v\,I\,(1-f) = \frac{\rho I^2}{A} f\,(1-f) \qquad \text{(II-17)}$$

and the heat generated per unit length in the substrate is

$$q_n = v\,I\,f = \frac{\rho}{A} I^2 f^2 \qquad \text{(II-18)}$$

Assuming that the heat generated in the superconductor must be transferred to the normal substrate through a contact heat transfer coefficient, h_i, over an interface perimeter, P_i, the difference in temperature between the superconductor and substrate is

$$T_s - T_n = \frac{\rho I^2}{h_i P_i A} f\,(1-f) \qquad \text{(II-19)}$$

The total heat generated in the conductor, $(q_s + q_n)$ must be transferred to the liquid helium bath over a perimeter, P, and with a heat transfer coefficient, h, which is assumed to include the thermal resistance of any insulation. The temperature rise of the substrate above the liquid helium bath is, then:

$$T_n - T_b = \frac{\rho I^2 f}{h\,P\,A} \qquad \text{(II-20)}$$

Adding Eqs. (II-19) and (II-20) yields the temperature difference between the superconductor and the bath.

$$T_s - T_b = \frac{\rho I^2}{h\,P\,A} f + \frac{\rho I^2}{h_i P_i A} f\,(1-f) \qquad \text{(II-21)}$$

The following equation may now be developed using Eqs. (5), (21) and the definition of f,

$$\alpha_i \left(\frac{I}{I_{ch}}\right)^2 f^2 - \left[(\alpha+\alpha_i)\frac{I}{I_{ch}} - 1\right]\left(\frac{I}{I_{ch}}\right) f + 1 - \frac{I}{I_{ch}} = 0 \qquad \text{(II-22)}$$

where:

$$\alpha = \frac{\rho I_{ch}^2}{h P A (T_{ch} - T_b)}$$

$$\alpha_i = \frac{\rho I_{ch}^2}{h_i P_i A (T_{ch} - T_b)}$$

Equation (II-22) may be solved for f. Then the expression for the voltage, the voltage per unit length and the superconductor temperature may be determined. The results are:

$$f = \frac{1}{2}\left\{\frac{\alpha + \alpha_i}{\alpha_i} - \frac{1}{\alpha_i \cdot \tau} \pm \sqrt{\left(\frac{\alpha + \alpha_i}{\alpha_i} - \frac{1}{\alpha_i \tau}\right)^2 - 4\left(\frac{1 - \tau}{\alpha_i \tau^2}\right)}\right\} \qquad \text{(II-23)}$$

$$V = \frac{vA}{\rho I_{ch}} = f\tau = \frac{1}{2}\tau\left\{\frac{\alpha + \alpha_i}{\alpha_i} - \frac{1}{\alpha_i \tau} \pm \sqrt{\left(\frac{\alpha + \alpha_i}{\alpha_i} - \frac{1}{\alpha_i \tau}\right)^2 - 4\left(\frac{1 - \tau}{\alpha_i \tau^2}\right)}\right\} \qquad \text{(II-24)}$$

$$\theta = \frac{T_s - T_b}{T_{ch} - T_b} = 1 - \tau + \frac{1}{2}\tau\left\{\frac{\alpha + \alpha_i}{\alpha_i} - \frac{1}{\alpha_i \cdot \tau} \pm \sqrt{\left(\frac{\alpha + \alpha_i}{\alpha_i} - \frac{1}{\alpha_i \tau}\right)^2 - 4\left(\frac{1 - \tau}{\alpha_i \tau^2}\right)}\right\} \qquad \text{(II-25)}$$

where:

$$\tau = \frac{I}{I_{ch}}$$

In searching for a stability criterion, we require that condition which corresponds to the onset of a positive resistance in a composite conductor when the current reaches the short sample critical current of the super-

conductor. We, therefore, examine $\frac{\partial V}{\partial \tau}$ at $\tau = 1$ and f = 0. This may be shown from Eq. (22) to be:

$$\left.\frac{\partial V}{\partial \tau}\right|_{\substack{\tau = 1 \\ f = 0}} = \frac{1}{1 - (\alpha + \alpha_i)} \qquad \text{(II-26)}$$

In order for the slope of voltage vs current to be positive at the critical current, then, it is necessary that

$$\alpha + \alpha_i < 1 \qquad \text{(II-27)}$$

Equation (II-27) is the required condition for stability.

Typical behavior is illustrated in Fig. II-7 which was obtained by plotting Eq. (II-24) for $\alpha = 0.5$ and various values of α_i. For this case, if $\alpha_i \leq 0.5$ then the voltage will remain zero until τ reaches one. At this point, a voltage will appear and will increase continuously and controllably as τ increases further. For $\alpha_i > .5$ (in general, for $\alpha + \alpha_i > 1$), the voltage current curves are double valued. Since operation on the part of a particular curve (specified α, α_i) which corresponds to negative resistance is impossible, it may be expected that for

1) $\tau \leq \tau_r = \tau_r(\alpha, \alpha_i)$, all current will flow in the superconductor,

2) for $\tau_r \leq \tau < 1$, however, the current will transfer to the substrate if a disturbance occurs. The voltage will then rise discontinuously from zero to that determined by the positive resistance portion of the curve specified by α and α_i. In order to recover to a fully superconducting state, it is then necessary to lower τ to τ_r where the voltage will discontinuously decrease to zero. (Note that if no disturbance occurs, then the voltage must still rise discontinuously when τ reaches one.)

The function $\tau_r = \tau_r(\alpha, \alpha_i)$ may be found from Eqs. (II-23), (II-24), or (II-25) under the condition that f, V, or θ must be single valued at $\tau = \tau_r$. This "recovery" condition may be shown to be:

$$\tau_r = \left(\frac{I}{I_{ch}}\right)_r = \frac{(\alpha - \alpha_i) \pm 2\sqrt{-\alpha\,\alpha_i + \alpha_i(\alpha + \alpha_i)^2}}{(\alpha + \alpha_i)^2} \qquad \text{(II-28)}$$

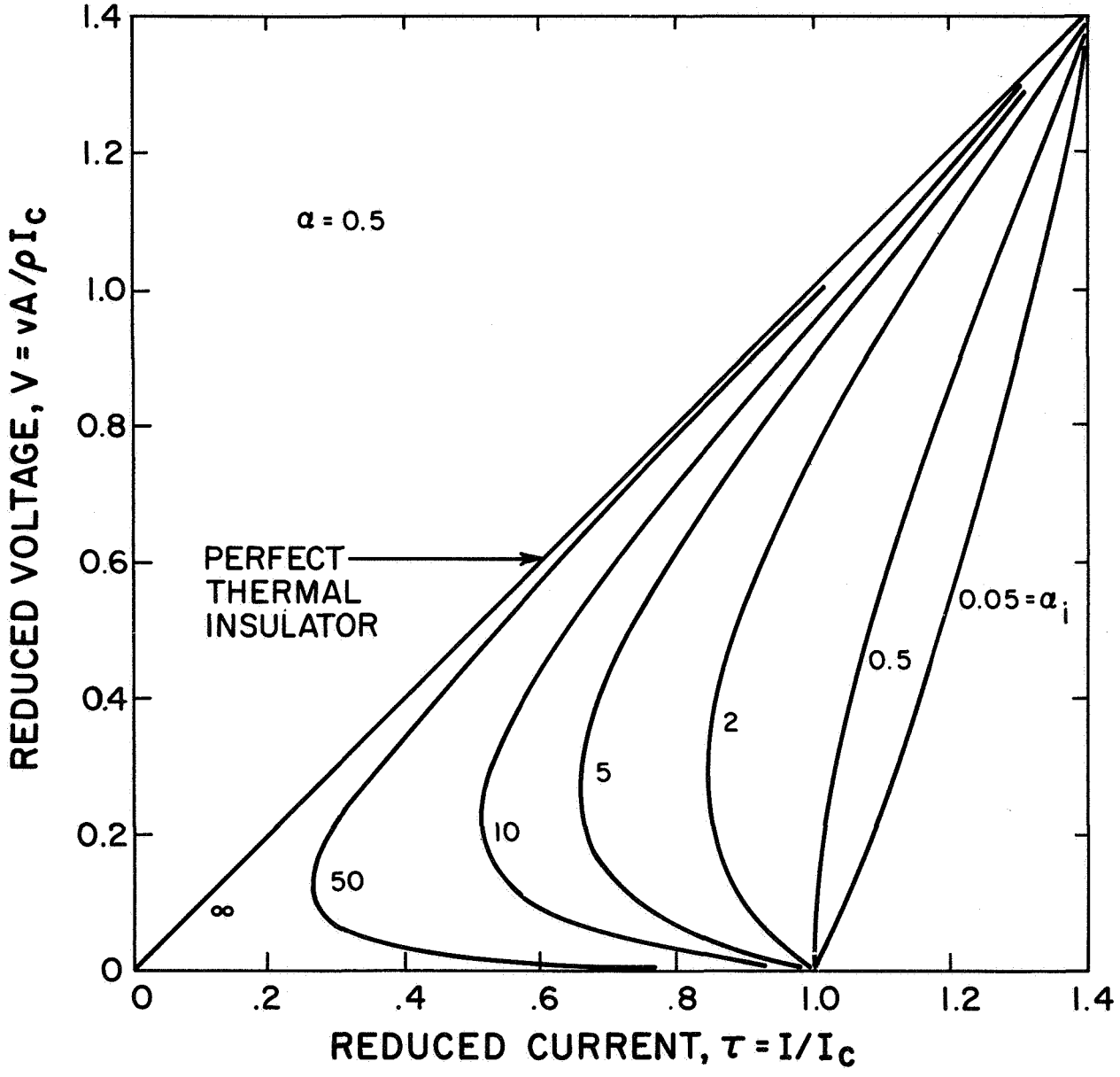

Fig. II-7 Illustration of the effect of thermal contact resistance between the superconductor and substrate

A7458

It is important to determine the effect on the stability criterion due to the possibility of self-generated heat as may occur, for example, in a contact. From another viewpoint, a heater may be used for diagnostic purposes. To consider this effect, assume that any heat generated flows into the substrate and from there to the helium bath, so that the temperature difference between the superconductor and substrate is still given by Eq. (II-19).

If an amount of heat, q_h, is generated per unit length, then Eq. (II-21) becomes

$$T_s - T_b = \frac{\rho I^2 f}{h P A} + \frac{\rho I^2}{h_i P_i A} f(1 - f) + \frac{q_h}{hP} \qquad \text{(II-29)}$$

A relation for f, τ, α, and α_i analogous to Eq. (II-22) may now be found.

$$\alpha_i \tau^2 f^2 - \left[(\alpha + \alpha_i)\ \tau - 1\right]\ \tau\ f + 1 - \tau - Q_h = 0 \qquad \text{(II-30)}$$

where

$$Q_h = \frac{q_h}{h P (T_c - T_b)}$$

By setting f = 0 in Eq. (II-30), it is clear that current begins to transfer into the substrate when

$$\tau = 1 - Q_h \qquad \text{(II-31)}$$

If we then require that $\frac{\partial V}{\partial \tau}$ at $\tau = 1 - Q_h$ and f = 0 represent positive resistance, the stability criterion will be established. In this way, it may be shown that

$$\left.\frac{\partial V}{\partial \tau}\right|_{\substack{\tau = 1 - Q_h \\ f = 0}} = \frac{1}{1 - (1 - Q_h)(\alpha + \alpha_i)} \qquad \text{(II-32)}$$

Hence, stability requires that

$$(1 - Q_h)(\alpha + \alpha_i) = \tau(\alpha + \alpha_i) < 1 \qquad \text{(II-33)}$$

This implies that a conductor, which is subjected to enough heating to produce a normal region, will exhibit stable, positive resistance behavior for current

$$\tau < \frac{1}{\alpha + \alpha_i}$$

Equation (II-28) holds if $(\alpha - \sqrt{\alpha})/\alpha_i < 1$; however if $(\alpha - \sqrt{\alpha})/\alpha_i < 1$ then

$$\tau_r = \sqrt{\alpha} \quad \text{independent of } \alpha_i$$

and $f_r = 1$.

The results of the above analyses are best summarized graphically in maps (Figs. II-8 and II-9) having α and α_i as coordinates and lines of constant recovery conditions on it. Given α and α_i, the recovery current, its distribution, and conductor voltage per unit length may be read off directly. Conversely, the graph may be used to determine the effective values of α and α_i from the fraction of short sample current at recovery and the voltage per unit length at recovery. Note that, in Fig. II-8 above the line given by $(\alpha - \sqrt{\alpha})/\alpha_i = 1$, $V_r = \tau_r$ since $f_r = 1$.

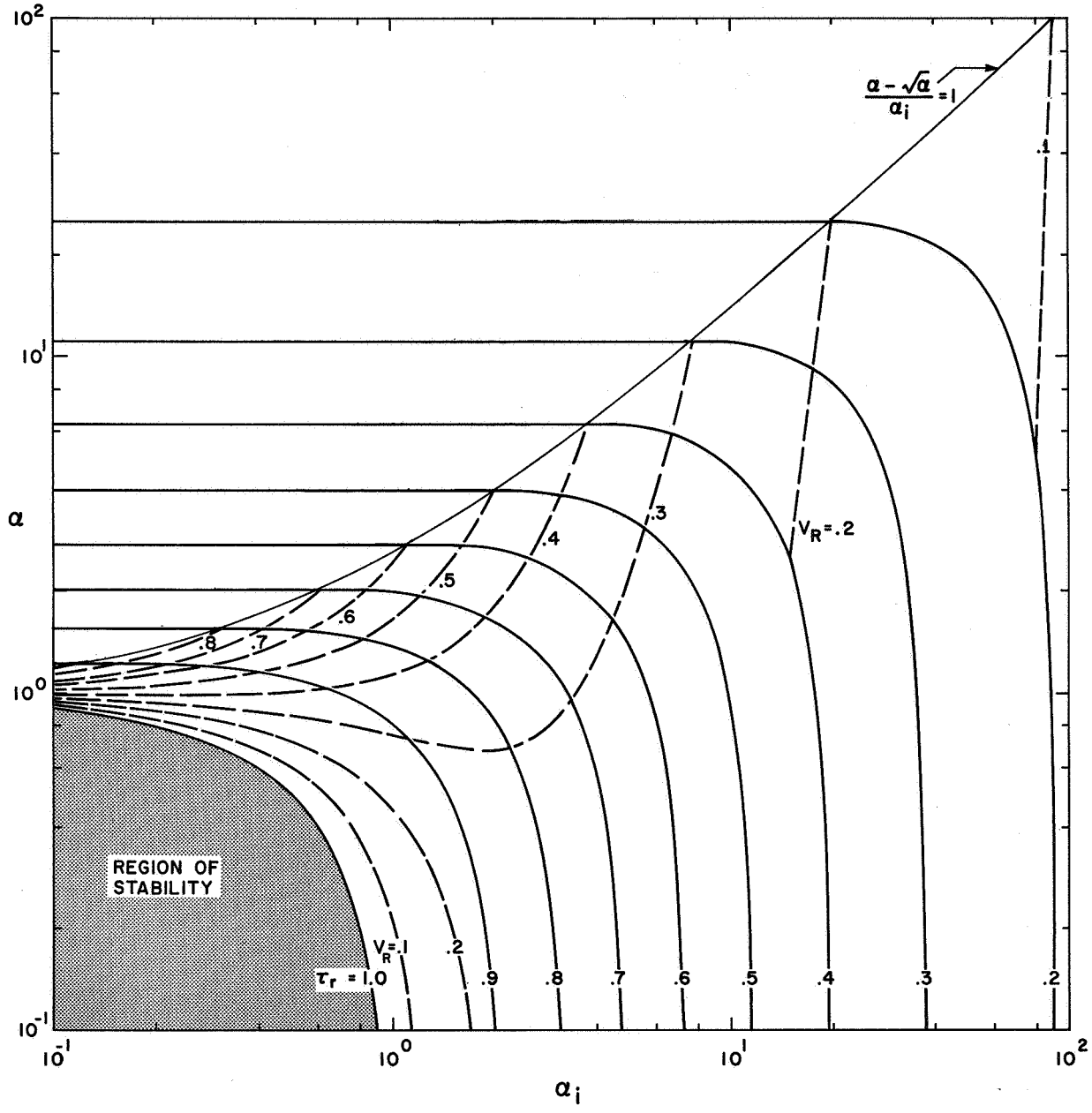

Fig. II-8 Recovery current τ_r and recovery voltage V_r as a function of α and α_1

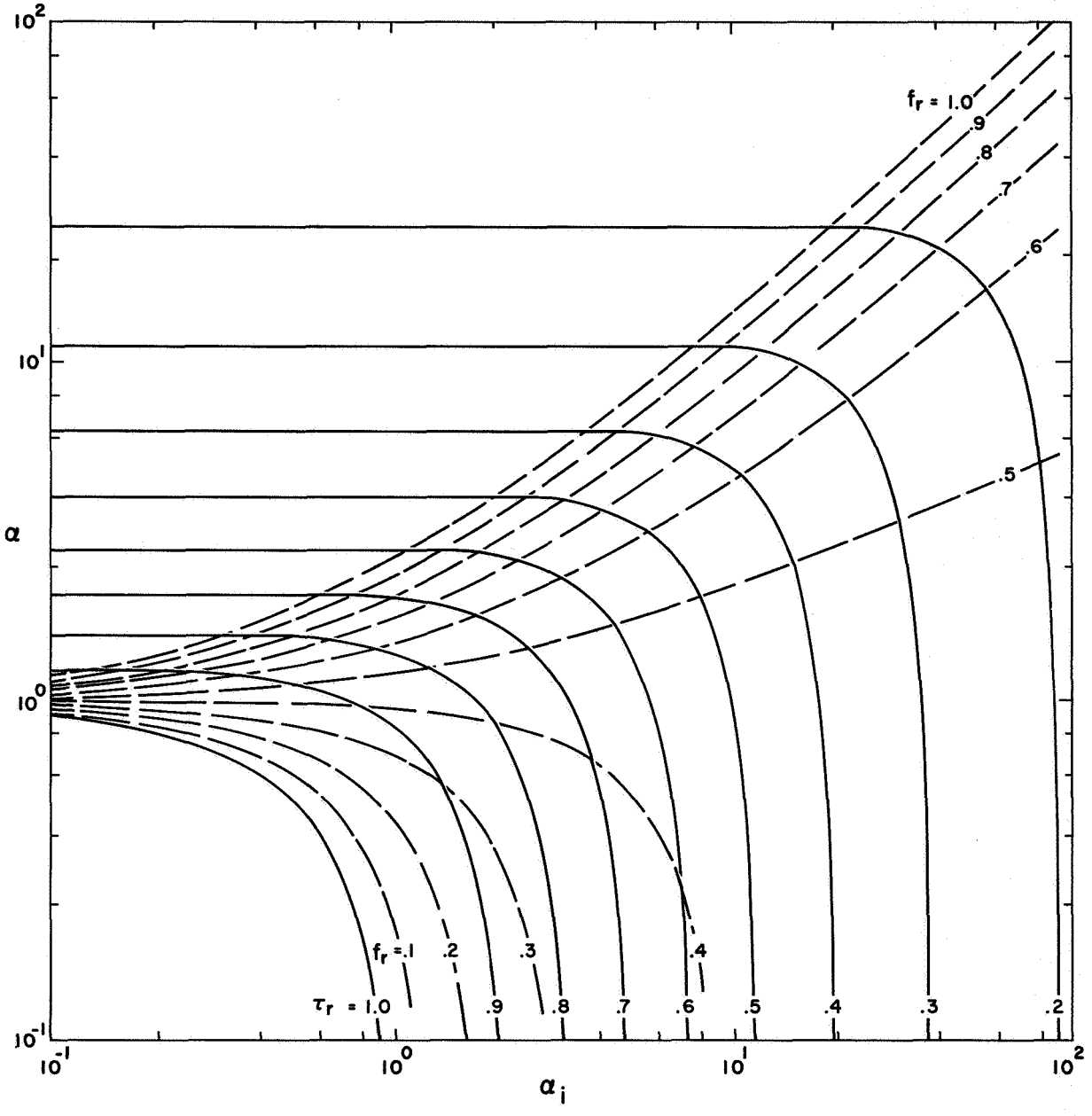

Fig. II-9 Recovery current and recovery current distribution as a function of α and α_1

E. Effect of a Gradual Resistance Rise in the Superconductor at Currents Greater Than the Critical Current

The previous analyses assumed that the superconductor current is just the critical current of the superconductor at the superconductor temperature. The resistivity of the superconductor at constant applied magnetic field and temperature is then a function of superconductor current as shown in Fig. II-10A. For currents below the critical current, the resistivity is zero, at the critical current the resistivity rises with an infinite slope. Experimental evidence[1] indicates that the resistivity increases gradually with current above the critical current. We shall now derive the zero dimensional terminal characteristics of a composite conductor taking into account a gradual appearance of resistance as shown in Fig. II-10B. This particular approximation to the gradual appearance superconductor resistance used, is intended as a measure of the effect of the slope on the terminal characteristics rather than an exact model of the superconductor behavior.

The superconductor resistivity at currents above the critical current at the applied magnetic field and composite temperature is given by

$$\rho_s = \kappa (I'_s - I_s) \qquad \text{(II-35)}$$

where I'_s = actual superconductor current

I_s = superconductor critical current at the superconductor temperature and in the presence of whatever applied magnetic field

κ = slope of resistivity increase-to be experimentally determined

ρ_s = superconductor resistivity

It is expected that as $\kappa \to \infty$, the previous results will be reproduced.

The voltage per unit length must be the same in the superconductor and substrate since they are in parallel, thus:

$$\frac{\kappa}{A_s}\left[(1-f)\,I - I_s\right] = \frac{\rho}{A}\,\frac{f}{1-f} \qquad \text{(II-36)}$$

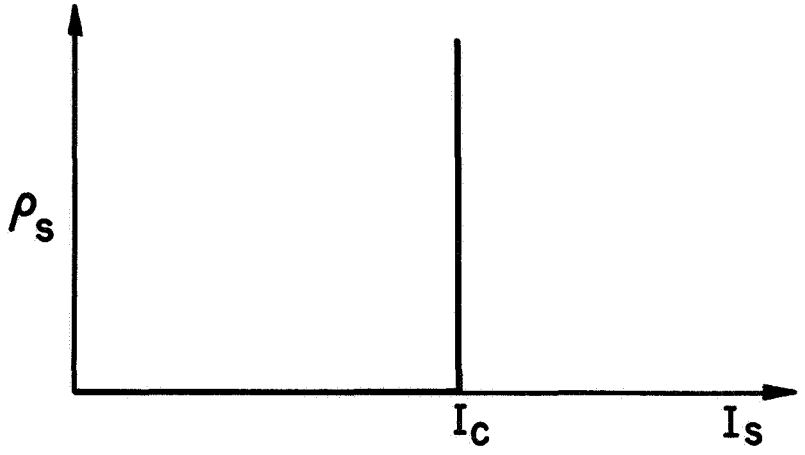

A. ASSUMED RESISTIVITY OF THE SUPERCONDUCTOR

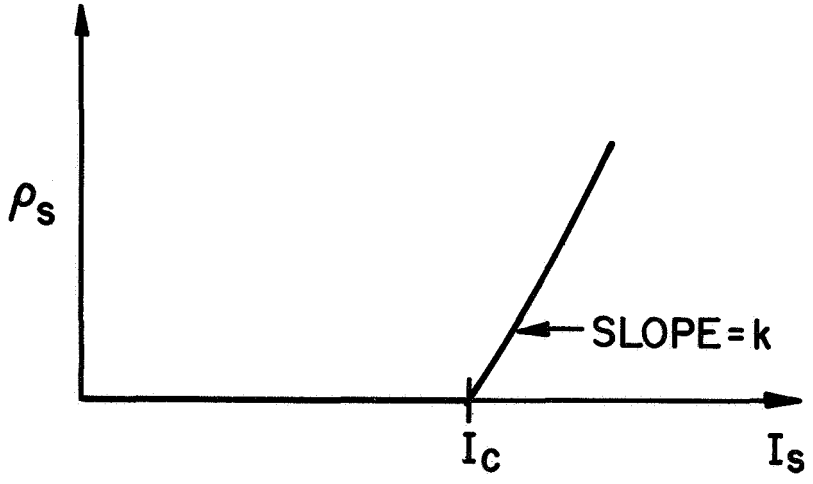

B. THE RESISITIVITY OF THE SUPERCONDUCTOR SHOWING AN INCREASING RESISITIVITY WITH CURRENT

Fig. II-10 Models for the resistivity of the superconductor as a function of the superconductor current

where

A_s = cross-sectional area of superconductor

A = cross-sectional area of a substrate

I = total composite current

ρ = resistivity of substrate

f = fraction of current in the substrate

We assume that the variation of the superconductor critical current I_s with temperature can be approximated by a linear relationship as before.

$$I_s = I_{ch} \left(1 - \frac{T_s - T_b}{T_{ch} - T_b}\right) \tag{II-37}$$

The heat produced in the sample due to joule losses must be transferred to the helium bath. If we assume a constant heat transfer coefficient h for the helium we have:

$$\frac{\rho}{A} I^2 f = hP (T_s - T_b) \tag{II-38}$$

where the parameters h, P have already been defined. Manipulation of the equations yields:

$$\alpha f \tau^2 + (1-f) \tau - \left(1 + \frac{\gamma f}{1-f}\right) = 0 \tag{II-39}$$

where α, τ have been defined previously, and γ

$$\gamma = \frac{\rho A_s}{\kappa A I_c} \tag{II-40}$$

To determine the effect of the gradual rise in superconductor resistance, we determine the rate of voltage increase with current at $\tau = 1$ and $f = 0$.

When the voltage first appears, the current is just beginning to exceed the critical current, and the superconductor resistance is "small". At this point, then, the effect of the gradual rise in resistance is most pronounced. We have:

$$\left.\frac{d\left(\frac{v A}{\rho I_c}\right)}{d\tau}\right|_{\substack{\tau = 1 \\ f = 0}} = \left.\frac{df}{d\tau}\right|_{\substack{\tau = 1 \\ f = 0}} = \frac{1}{1 + \gamma - \alpha} \tag{II-41}$$

where v is the voltage per unit length. From the model neglecting the slope, we would have obtained:

$$\left.\frac{df}{d\tau}\right]_{\substack{\tau = 1 \\ f = 0}} = \frac{1}{1-\alpha} \qquad \text{(II-42)}$$

Unless γ is comparable to unity the effect of a gradual resistance increase with current above the short sample current carrying capacity can be neglected, and the results using the former model are sufficient for calculating purposes.

Nonlinear Heat Transfer Characteristic

We extend the treatment of the gradual appearance of normal state resistance in the superconductor to the case of nonlinear heat transfer. As before, the constant h case applies up to a limit. Beyond this limit we assume a constant heat flux per unit area:

$$q = q_m = h\,(T_m - T_b) \qquad \text{(II-43)}$$

Substitution of this value into Eq. (II-2) yields:

$$\frac{\rho}{A}\, I^2 f = h P\,(T_m - T_b) \qquad \text{(II-44)}$$

Solving for f and introducing our usual dimensionless parameters we find:

$$f = \frac{\theta_m}{\alpha \tau^2} \qquad \text{(II-45)}$$

It is well to note here that this result for f is the same as that found for the case of steep return of resistance ($\gamma = 0$) and is independent of the value of γ.

At $T = T_m$ the locus of points for the transfer from nucleate to film boiling may be found by substituting the value θ_m into Eqs. (II-36), (II-37), and (II-38) yields:

$$\tau\,(1 - f) - 1 + \theta_m = \gamma \frac{f}{1 - f} \qquad \text{(II-46)}$$

Substituting $V = f\tau$ and the value for f in Eq. (II-45) into the above equation we find

$$V = \tau - (1 - \theta_m) - \frac{\gamma\ \theta_m}{\alpha \tau^2 - \theta_m} \qquad \text{(II-47)}$$

For $\gamma = 0$ this is a straight line intersecting the τ-axis at $(1 - \theta_m)$. For finite γ the relationship is more complicated. Figure II-11 shows the effect of finite γ on the voltage-current characteristic. For each value of α the initial slope at the onset of resistance is lower for finite γ, as expected. However, as can be seen in Fig. II-11 the effect is small.

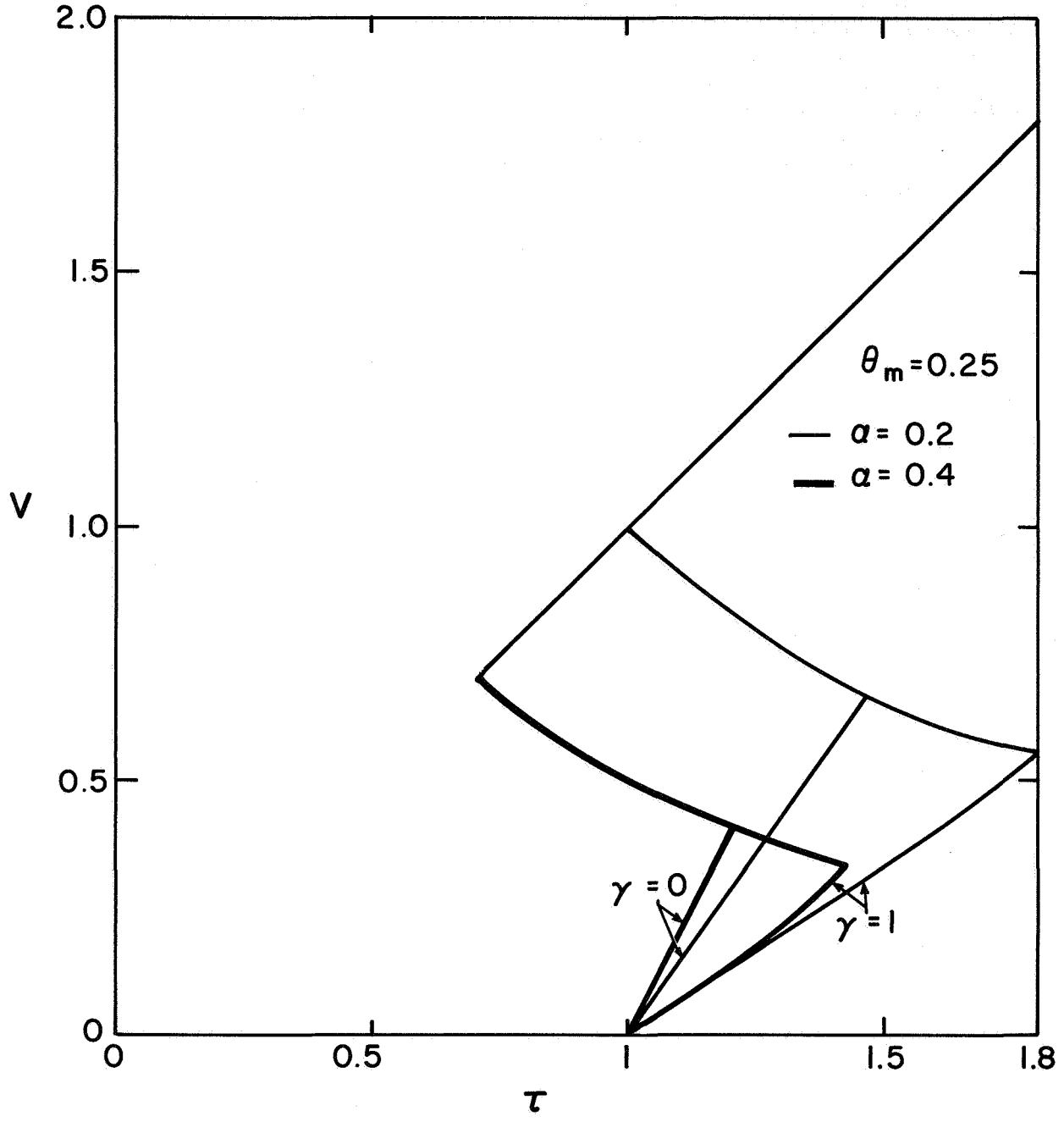

Fig. II-11 The terminal voltage of a superconducting composite incorporating the gradual appearance of resistance and maximum heat flux

F. The Effect of Superconductor Size on Steady State Stability

The following analysis concerns the behavior of a short unclad sample of superconductor exposed to a liquid helium bath. The properties of the superconductor are assumed to have the usual dependence upon current, magnetic field, and temperature. We are concerned with the cooling effectiveness of the superconductor, its current and temperature distribution, and its optimum size from a stability standpoint. It should be noted that superconductors have poor thermal conductivity and this will lead to rather steep temperature gradients within the sample.

The analysis carried out below is for a round superconducting wire operating in the critical state. Under these conditions there will be a voltage per unit length, which will result in internal heating of the superconductor. This internal heating will be conducted outward toward the surface. The higher temperatures within the wire will result in a lowering of the current carrying capacity (assuming all parts of the wire remain in the critical state).

The heating and temperature distribution in the wire will vary with the voltage per unit length v.

In previous analyses we assumed that the superconductor was all at one temperature. In this case the assumption is removed and the superconductor is locally characterized by a current density j_s which we shall assume to vary linearly with temperature:

$$j_s = j_{ch}\left(1 - \frac{T - T_b}{T_{ch} - T_b}\right) = j_{ch}(1 - \theta) \qquad \text{(II-48)}$$

Referring to Fig. II-12, the heat per unit length generated in a circular shell parallel to the current axis of the wire is:

$$dq = 2\pi\ r\ v\ j_s\ dr \qquad \text{(II-49)}$$

which gives:

$$\frac{dq}{dr} = 2\pi\ r\ v\ j_s \qquad \text{(II-50)}$$

Let us now set up a heat balance equating this to the radial heat conduction from this same shell.

$$\frac{dq}{dr} = 2\pi r v j_s = -2\pi k \frac{d}{dr}\left(r\frac{dT}{dr}\right) = -2\pi k(T_{ch} - T_b)\frac{d}{dr}\left(r\frac{d\theta}{dr}\right) \qquad \text{(II-51)}$$

where k is the thermal conductivity of the superconductor and is assumed to be constant.

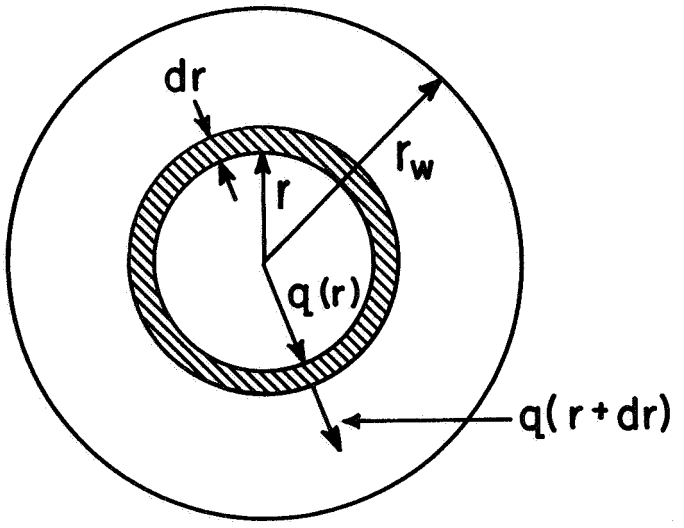

Fig. II-12 Element on which a radial heat balance is taken

Simplifying Eq. (II-51) we find:

$$\frac{1}{r}\frac{d}{dr}\left(r\frac{d\theta}{dr}\right) = -\frac{v\, j_{ch}\,(1-\theta)}{k(T_{ch}-T_b)} \qquad \text{(II-52)}$$

Let us now define a characteristic size r_c:

$$r_c^2 = \frac{k(T_{ch}-T_b)}{v\, j_{ch}} \qquad \text{(II-53)}$$

r_c is a measure of the ability of the superconductor to conduct heat away. If r_c is larger than the radius r_w of the wire, then conduction prevails and the temperature rise in the superconductor is small, and the assumption of superconductor temperature equal to its surface temperature is good. However if r_c is smaller than r_w, then the temperature rise in the superconductor cannot be neglected.

Figure II-13 is a plot of v vs. the critical radius, r_c. This plot is taken for Nb - Ti at 50 kG. At this field $j_{ch} = 1.3 \times 10^5$ A/cm^2 and $T_{ch} = 6.8^\circ$K. The thermal conductivity was taken at 6 milli watts/cm$^\circ$K which is representative for materials of this type.

We let $r = u\, r_c$ and Eq. (II-52) becomes:

$$\frac{1}{u}\frac{d}{du}\left(u\frac{d\theta}{du}\right) = -(1-\theta) \qquad \text{(II-54)}$$

$$\frac{d^2\theta}{du^2} + \frac{1}{u}\frac{d\theta}{du} + (1-\theta) = 0 \qquad \text{(II-55)}$$

Multiplying Eq. (II-55) by u^2 will put it into a form of Bessel's equation of the zeroth order.

$$u^2\frac{d^2\theta}{du^2} + u\frac{d\theta}{du} + u^2(1-\theta) = 0 \qquad \text{(II-56)}$$

We let $U = 1 - \theta$ and the above equation becomes:

$$u^2\frac{d^2U}{du^2} + u\frac{dU}{du} - u^2 U = 0 \qquad \text{(II-57)}$$

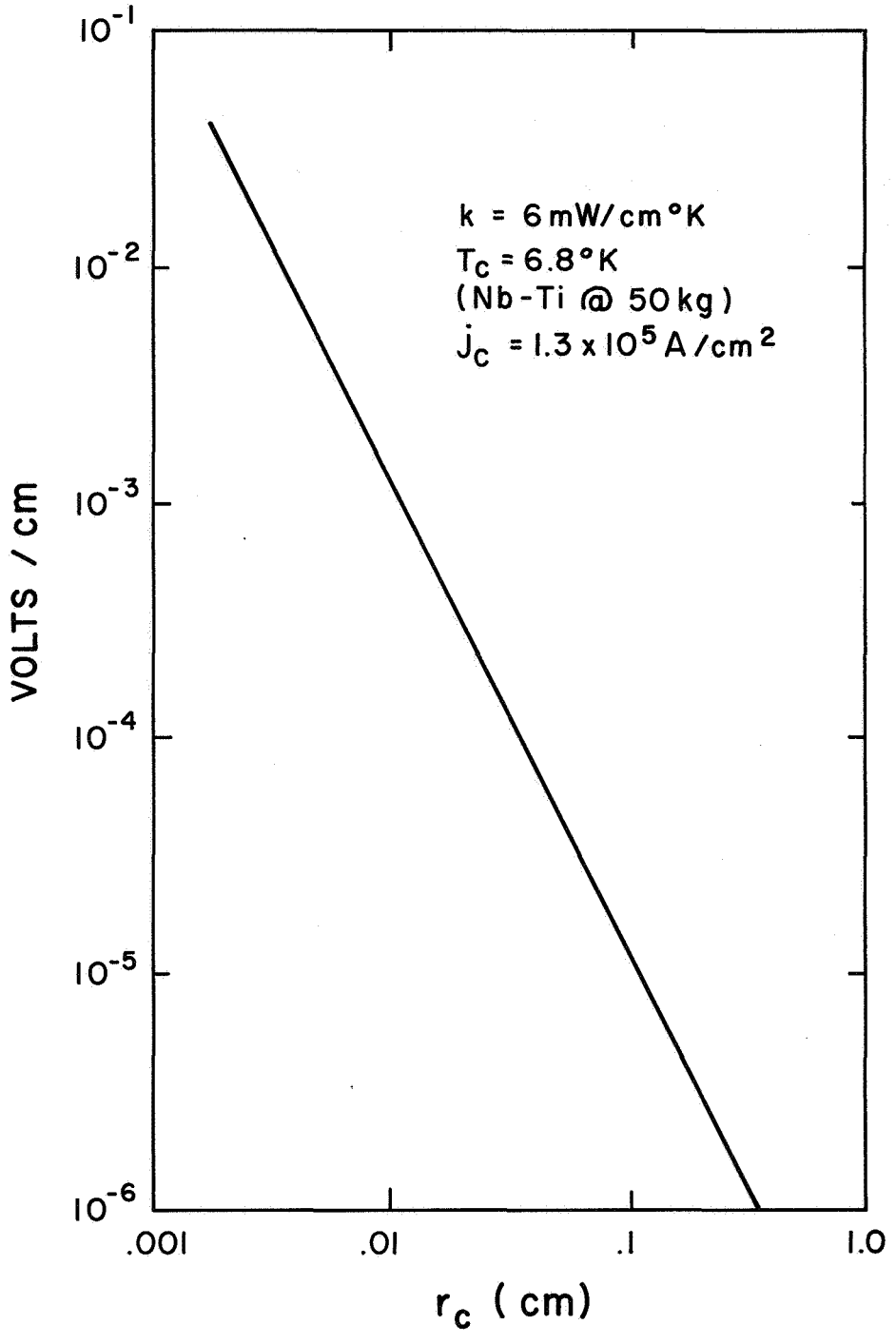

Fig. II-13 The voltage, v, corresponding to the critical radius r_c

This equation has the solution:

$$U = C_1 I_0(u) + C_2 K_0(u) \tag{II-58}$$

$$\theta = 1 + C_1 I_0(u) + C_2 K_0(u) \tag{II-59}$$

where I_0 is the modified Bessel function of the first kind of order zero and K_0 is the modified Bessel function of the second kind, of order zero. Since $K_0(0) \longrightarrow \infty$ we let $C_2 = 0$. To find the constant C_1, we arbitrarily set the temperature at the surface of the wire, $r = r_w$, or $(u = u_w = \frac{r_w}{r_c})$, equal to: $\theta_w = (T_w - T_b)/(T_{ch} - T_b)$ and obtain the following:

$$\theta_w = 1 + C_1 I_0(u_w) \tag{II-60}$$

and,

$$C_1 = - \frac{1 - \theta_w}{I_0(u_w)} \tag{II-61}$$

Thus Eq. (II-59) becomes

$$\theta = 1 - \frac{1 - \theta_w}{I_0(u_w)} I_0(u) \tag{II-62}$$

We are interested in the total transport current that the wire can carry. To find this we integrate the current density j_s over the cross-section of the wire.

$$I_s = \int_0^{r_w} j_s \, 2\pi r \, dr = 2\pi j_c r_c^2 \int_0^{r_w/r_c} (1 - \theta) u \, du \tag{II-63}$$

We substitute the relation (II-62) for θ

$$I_s = 2\pi j_c r_c^2 \int_0^{r_w/r_c} -C_1 u I_0(u) \, du \tag{II-64}$$

$$I_s = -C_1 \, 2\pi j_c r_c^2 [u_w I_1(u_w)] \tag{II-65}$$

$$I_s = 2\pi r_w (1 - \theta_w)\sqrt{\frac{k j_{ch}(T_{ch} - T_b)}{v}}\,\frac{I_1(u_w)}{I_0(u_w)} \qquad \text{(II-66)}$$

$I_1(u_w)$ is the modified Bessel function of the first kind and first order. The maximum temperature will be found at the center of the wire:

$$\theta_{max} = 1 + C_1 I_0(0) = 1 + C_1 = 1 - \frac{1 - \theta_w}{I_0(u_w)} \qquad \text{(II-67)}$$

For small u_w, $I_0(u_w) \rightarrow 1$ so

$$\theta_{max} \approx \theta_w$$

As expected, for small $u_w = r_w/r_c$ the temperature rise in the superconductor can be neglected.

CASE 1

Assume there is excellent heat transfer at the wire surface such that $T_w = T_b$, $\theta_w = 0$. From Eq. (II-66) with $\theta_w = 0$, after some simplification

$$I_s = 2 I_{ch} \frac{r_c}{r_w} \frac{I_1(r_w/r_c)}{I_0(r_w/r_c)} \qquad \text{(II-68)}$$

This is shown plotted in Fig. II-14 along with the maximum dimensionless temperature θ_{max}.

CASE 2

For this case let a finite heat transfer coefficient, h, exist at the surface of the wire. This heat transfer coefficient can be an effective one such as might exist in the case of a wire imbedded in a substrate. In the case of a substrate, however, shunting of current occurs which is a more complex situation. If this shunting is neglected, then h can be an effective value of the heat transfer coefficient from the surface of the wire to the helium, taking into account the larger perimeter of contact between the substrate and the helium. If h_{He} is the heat transfer coefficient from the substrate to the helium over a cooled perimeter of substrate P, then the effective heat transfer coefficient at the surface of the superconductor is $h_{eff} = h_{He} \cdot \frac{P}{2\pi r_w}$. We first set up a heat balance between the heat generated in the wire and that transferred at the superconductor surface.

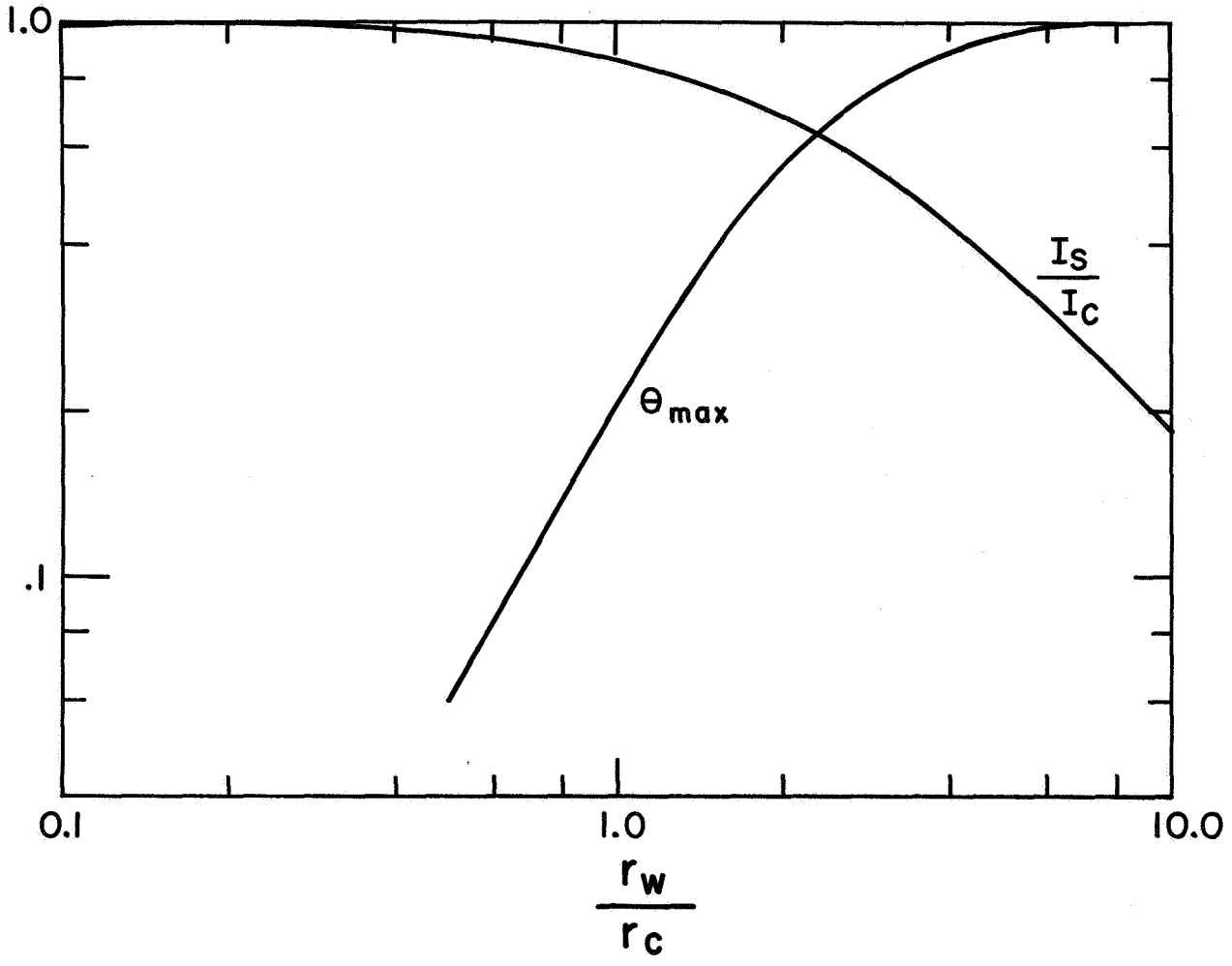

Fig. II-14 Reduced critical current and θ_{max} as a function of (r_w/r_c)

$$v\, I_s = h\, 2\pi\, r_w \left(\frac{T_w - T_b}{T_{ch} - T_b}\right)(T_{ch} - T_b)$$

$$v\, I_s = 2\pi\, r_w\, h(T_{ch} - T_b)\theta_w \tag{II-69}$$

Solving for I_s

$$I_s = \frac{2\pi\, r_w\, h(T_{ch} - T_b)}{v}\, \theta_w$$

We now set this equal to Eq. (II-66)

$$\frac{2\pi\, r_w\, h(T_{ch} - T_b)}{v}\, \theta_w = \frac{2\pi(1 - \theta_w)\, r_w^2\, j_{ch}\, I_1\left(\frac{r_w}{r_c}\right)}{\frac{r_w}{r_c} \cdot I_0\left(\frac{r_w}{r_c}\right)} \tag{II-70}$$

Solving for θ_w we find

$$\theta_w = \frac{1}{1 + \frac{h(T_{ch} - T_b) I_0(r_w/r_c)}{v\, r_c\, j_{ch}\, I_1(r_w/r_c)}} \tag{II-71}$$

and

$$1 - \theta_w = \frac{1}{1 + \frac{v\, r_c\, j_{ch}\, I_1(r_w/r_c)}{h(T_{ch} - T_b) I_0(r_w/r_c)}} \tag{II-72}$$

Let us now substitute the value for $(1 - \theta_w)$ back into Eq. (II-65). We find

$$I_s = 2\, I_c \frac{r_c}{r_w} \frac{I_1(r_w/r_c)}{I_0(r_w/r_c)} \left\{ \frac{1}{1 + \frac{v\, r_c\, j_{ch}\, I_1(r_w/r_c)}{h(T_{ch} - T_b) I_0(r_w/r_c)}} \right\} \tag{II-73}$$

For high values of the heat transfer coefficient this equation becomes Eq. (II-68) as it should.

After some simplification Eq. (II-73) may be expressed as follows:

$$\frac{I_s}{I_c} = \frac{2\, I_1(u_w)}{u_w\, I_0(u_w)} \left[\frac{1}{1 + \frac{k\, I_1(u_w)}{h\, r_c\, I_0(u_w)}} \right]$$

CASE 3

We now consider a composite superconductor. The normal substrate is assumed to have a high thermal conductivity and low resistivity. Assuming no temperature gradients in the substrate, the temperature of the surface of the superconductor is equal to the substrate temperature T_w.

The heat balance at the surface of the substrate is:

$$hP(T_w - T_b) = v\, I = \frac{\rho}{A} I^2 f$$

where

$$f = \frac{I - I_s}{I} = 1 - \frac{I_s}{I} = 1 - \frac{I_s/I_{ch}}{\tau}$$

substituting for f and solving for the temperature T_W results in:

$$\theta_w = \frac{T_w - T_b}{T_c - T_b} = a \left[\tau^2 - \tau \frac{I_s}{I_{ch}} \right] \qquad \text{(II-74)}$$

From previous analyses:

$$\frac{I_s}{I_c} = (1 - \theta_w) \frac{2\, I_1(u_w)}{u_w\, I_0(u_w)} \qquad \text{(II-66)}$$

substitution for θ_w and simplification yields:

$$\frac{I_s}{I_c} = \frac{\beta(1 - a\, \tau^2)}{1 - a\, \tau\, \beta} \qquad \text{(II-75)}$$

where

$$\beta = \frac{2\, I_1(u_w)}{u_w\, I_0(u_w)} \qquad \text{(II-76)}$$

Substitution into the expression for f yields:

$$f = 1 - \frac{\beta(1 - \alpha \tau^2)}{\tau(1 - \alpha \tau \beta)} \qquad \text{(II-77)}$$

as u_w approaches zero, β approaches unity, and all the results above degenerate into those for which it was assumed that no temperature gradients exist in the superconductor.

We now need to derive an expression for the voltage current characteristic. In doing so we shall use the same nomenclature as before.

The voltage per unit length is

$$v = \frac{\rho}{A} I f$$

or in dimensionless form:

$$V = \frac{v A}{\rho I_{ch}} = \tau \cdot f = \frac{\tau - \beta}{1 - \alpha \tau \beta} \qquad \text{(II-78)}$$

For $\beta = 1$ ($u_w \longrightarrow 0$) the above equation is identical with Eq. (II-8).

The quantity u_w is related to the dimensionless voltage V as:

$$u_w = \frac{r_w}{\sqrt{\frac{k(T_{ch} - T_b)}{v j_{ch}}}} = \frac{r_w}{\sqrt{\frac{k A^2 (T_{ch} - T_b)}{\rho I_{ch}^2}}} \sqrt{V} \qquad \text{(II-79)}$$

Substitution and rearrangement results in the following form which is convenient for plotting:

$$\tau = \frac{V + \frac{2}{\frac{r_w}{r_{cs}}\sqrt{V}} \frac{I_1(\frac{r_w}{r_{cs}}\sqrt{V})}{I_0(\frac{r_w}{r_{cs}}\sqrt{V})}}{1 + \alpha V \cdot \left[\frac{2}{\frac{r_w}{r_{cs}}\sqrt{V}} \frac{I_1\left(\frac{r_w}{r_{cs}}\sqrt{V}\right)}{I_0\left(\frac{r_w}{r_{cs}}\sqrt{V}\right)}\right]} \qquad \text{(II-80)}$$

where r_{cs} is defined as:

$$r_{cs} = \frac{A}{I_{ch}}\sqrt{\frac{k(T_{ch} - T_b)}{\rho}} \qquad \text{(II-81)}$$

where A and ρ refer to the substrate, and I_c, k refer to the superconductor.

Using the above equation, a plot of τ versus v can be easily obtained. This is done in Figs. II-15 and II-16. for several values of r_w/r_{cs}.

The slope can be obtained at $\tau = 1$ where V = 0 relatively simply. Taking the derivative of τ with respect to V yields:

$$\left.\frac{d\tau}{dV}\right]_{\tau=1} = 1 - \alpha - \frac{1}{8}\left(\frac{r_w}{r_{cs}}\right)^2 \qquad \text{(II-82)}$$

or in the more conventional form:

$$\left.\frac{dV}{d\tau}\right]_{\tau=1} = \frac{1}{1 - \alpha - \frac{1}{8}\left(\frac{r_w}{r_{cs}}\right)^2} \qquad \text{(II-83)}$$

The condition for stability is that the slope be positive at the critical current, and we have:

$$\alpha + \frac{1}{8}\left(\frac{r_w}{r_{cs}}\right)^2 < 1. \qquad \text{(II-84)}$$

As an example let us consider a case of a .020 in diameter wire consisting of superconductor and copper with a cross sectional area of copper three times that of the superconductor. The sample is assumed to be at 50 kilogauss where the superconductor has a critical current of 60 amperes.

We then have the following:

P $= \pi(.02 \times 2.54) = .16\ \text{cm}^2$

A $= \frac{3}{4}\left(\frac{\pi}{4}\right)(.02 \times 2.54)^2 = 1.52 \times 10^{-3}\ \text{cm}^2$

I_{ch} $= 60\text{A}$

k $= .01\ \text{W/cm}\ ^{\circ}\text{K}$

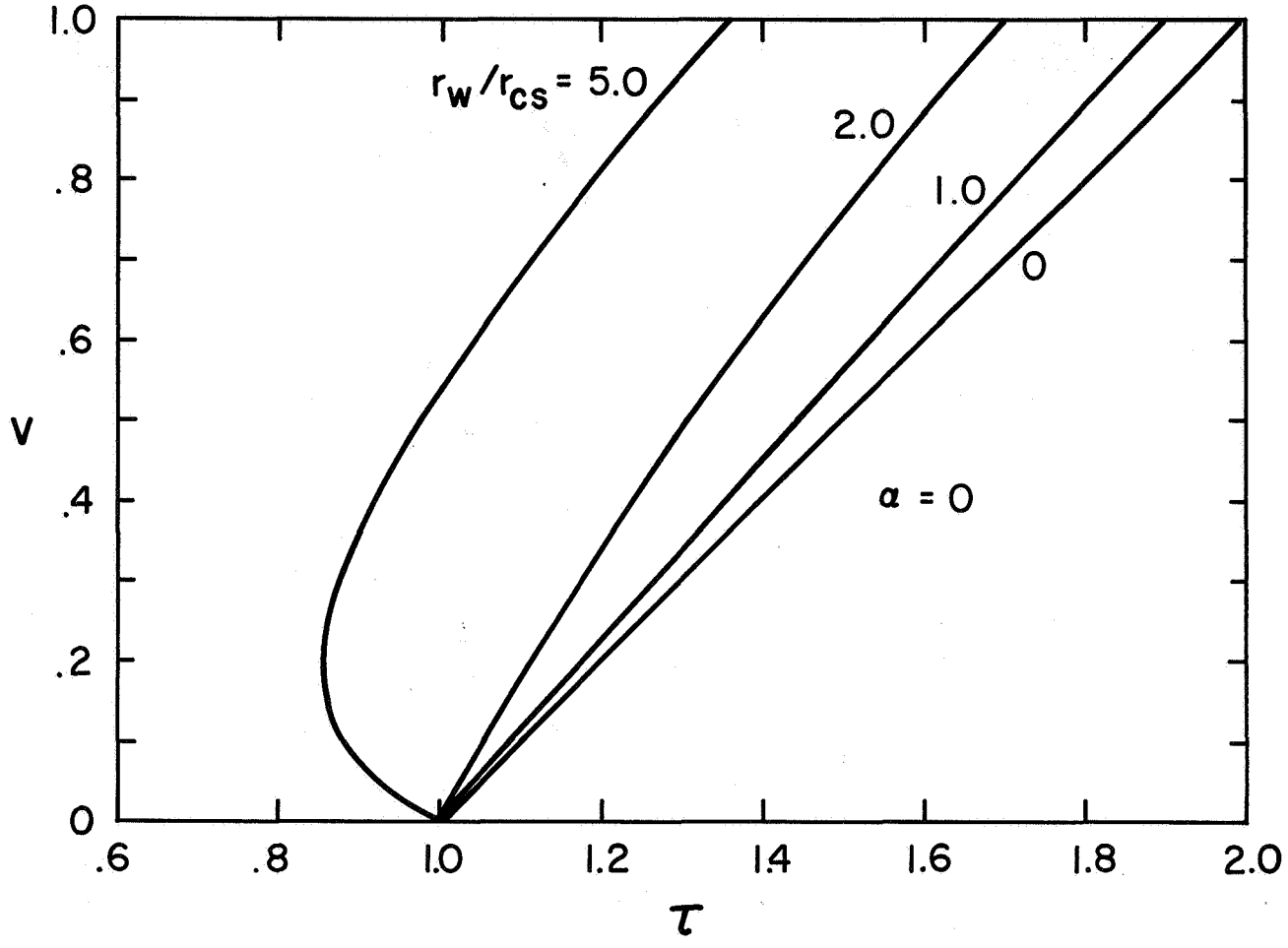

Fig. II-15 The voltage current characteristic as determined from Eq. (II-80) for the case $\alpha = 0$.

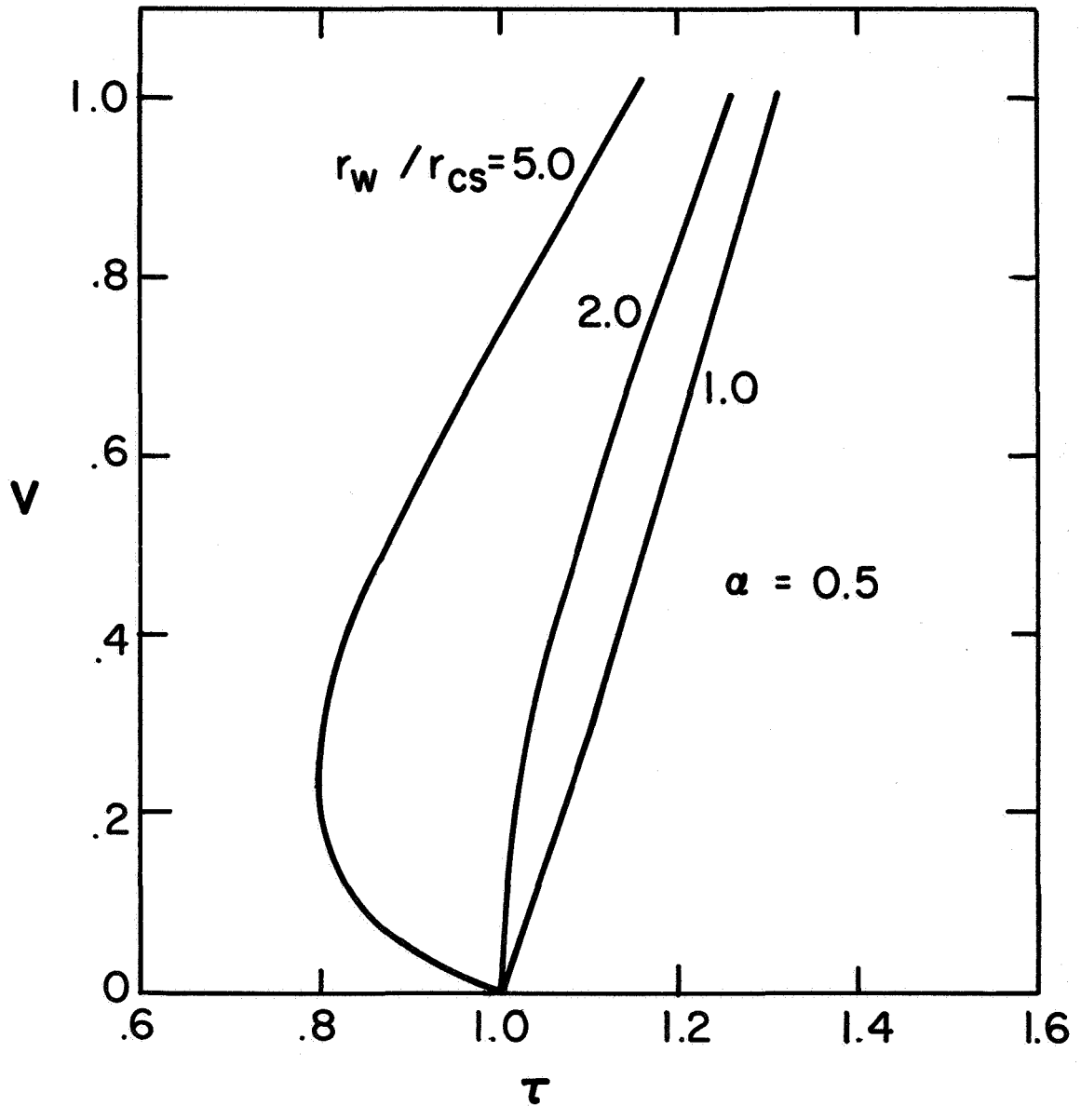

Fig. II-16 The voltage current characteristic as determined from Eq. (II-80) for the case $\alpha = 0.5$.

$T_{ch} - T_b = 2.5^{\circ}K$ (value for Nb - Ti at 50 kG)

$\rho = 2.5 \times 10^{-8} \Omega$ cm (resistivity of copper at 50 kG)

$h = 1 W/cm^2 {}^{\circ}K$

Using these values we calculate a value of

$$r_{cs} = .0254 \text{ cm} = .01 \text{ in.}$$

$$\alpha = \frac{\rho I_{ch}^2}{h PA(T_{ch} - T_b)} = .148$$

$$\frac{dV}{d\tau} = \frac{1}{1 - .148 - \frac{1}{8}\left(\frac{r_w}{.0254}\right)^2} = \frac{1}{.852 - .125\left(\frac{r_w}{.0254}\right)^2}$$

If we form the ratio of the slope to the slope that would exist if the superconductor size were zero (broken up into small filaments, assuming that size had no effect on the filament current density).

$$\frac{\left.\frac{dV}{d\tau}\right|_{r_w}}{\left.\frac{dV}{d\tau}\right|_{0}} = \frac{1}{1 - .147\left(\frac{r_w}{.0254}\right)^2}$$

where r_w is in centimeters.

For a single .010" dia (r_w = .0127 cm) the increase in slope over that without taking into account the conductor size is only 3.7%.

It can be concluded that, for the particular example considered, the steady state increase in temperature within the superconductor is not an important effect.

REFERENCE

1. Y.B. Kim, et al, Phys. Rev. Letters, 5, 26 (1964).

III. STEADY STATE STABILITY - ONE DIMENSION

A. Introduction

In the previous "zero" dimensional analysis we assumed no thermal gradients along the length of the composite conductor. To account for thermal disturbance we included a uniform heating per unit length. In engineering practice, however, the conductor is usually subjected to local heating which gives rise to thermal gradients. In effect, a long conductor will act as a cooling fin in the presence of a localized thermal disturbance.

B. Constant Heat Transfer Coefficient

We again consider a superconducting composite with the same thermal and magnetic properties as used in the zero-dimensional analysis. The first solution presented here will be for the case of constant heat transfer coefficient.

The composite conductor consists of a superconductor in good thermal and electrical contact with a normal conductor, and in which some or all of the conductor perimeter is in contact with a liquid helium bath at temperature T_b.

$$- \frac{\partial}{\partial x} \left(kA \frac{\partial T}{\partial x}\right) + hP (T - T_b) = v \cdot I \qquad \text{(III-1)}$$

where x is the direction along the conductor, A is the cross-sectional area, P is the wetted perimeter, k is the thermal conductivity of the normal material and h is the heat transfer coefficient between the conductor and the liquid helium bath.

The voltage per unit length v is given by:

$$v = \frac{\rho}{A} f I \quad 0 \leq f \leq 1.0 \qquad \text{(III-2)}$$

The amount of current the superconductor will carry is determined by its temperature and the magnetic field to which it is exposed. If we assume for simplicity that the superconductor current decreases linearly with increasing temperature then:

$$I_s = I_{ch}\left(1 - \frac{T - T_b}{T_{ch} - T_b}\right) \qquad \text{(III-3)}$$

where I_{ch} is the critical current at the external magnetic field at the bath temperature. The critical temperature T_c is the critical temperature with no current in the superconductor in the presence of the applied magnetic field. The quantity f is given by:

$$f = 1 - \frac{I_s}{I} = 1 - \frac{I_{ch}}{I}\left(1 - \frac{T - T_b}{T_{ch} - T_b}\right) \qquad \text{(III-4)}$$

making use of Eqs. (III-2) and (III-4), Eq. (III-1) can be put in the following forms:

$$\left.\begin{array}{l} f = 0 \\ v = 0 \end{array}\right\} \quad \frac{d^2\theta}{d\xi^2} - \theta = 0 \qquad \text{All current in the superconductor} \qquad \text{(III-5)}$$

$$\left.\begin{array}{l} 0 < f < 1.0 \\ v = \frac{\rho}{A} If \end{array}\right\} \quad \frac{d^2\theta}{d\xi^2} - \theta(1 - \alpha\tau) - \tau(1 - \tau) = 0 \qquad \text{Current shared between the superconductor and normal conductor} \qquad \text{(III-6)}$$

$$\left.\begin{array}{l} f = 1.0 \\ v = \frac{\rho}{A} If \end{array}\right\} \quad \frac{d^2\theta}{d\xi^2} - \theta + \alpha\tau^2 = 0 \qquad \text{All current in the normal conductor} \qquad \text{(III-7)}$$

where the following dimensionless variables have been introduced:

$$\theta = \frac{T - T_b}{T_{ch} - T_b}$$

$$\xi = \frac{x}{x_o}, \quad x_o = \sqrt{\frac{kA}{hP}}$$

$$\tau = \frac{I}{I_{ch}}$$

$$\alpha = \frac{\rho I_{ch}^2}{h\,PA\,(T_{ch} - T_b)}$$

These equations have the following solutions:

$$f = 0,\ v = 0 \qquad \theta = C_1 e^{\xi} + C_2 e^{-\xi} \qquad \text{(III-8)}$$

$$0 < f < 1.0 \quad v = \frac{\rho I f}{A}$$

$$\left.\begin{array}{l} c_3 \cosh \sqrt{1 - a\tau}\,\xi + C_4 \sinh \sqrt{1 - a\tau}\,\xi - \dfrac{a\tau(1-\tau)}{1 - a\tau} = \theta \\ \qquad\qquad \text{for } a\tau < 1.0 \\ c'_3 \cos \sqrt{a\tau - 1}\,\xi + c'_4 \sin \sqrt{1 - a\tau}\,\xi - \dfrac{a\tau(1-\tau)}{1 - a\tau} = \theta \\ \qquad\qquad \text{for } a\tau > 1.0 \end{array}\right\} \quad \text{(III-9)}$$

$$f = 1.0 \qquad \theta = c_5 e^{\xi} + c_6 e^{-\xi + a\tau^2} \qquad \text{(III-10)}$$

Equations (III-8), (III-9), and (III-10) can be solved for a variety of different conditions. In this report we shall consider the case of small localized heat source

1) Small Localized Heat Source

Consider the case of a conductor of infinite extent in both directions having a point heat source of power q_h at the origin. The temperature distribution will be symmetrical about the origin and therefore $q_h/2$ will flow in each direction. The boundary conditions at the origin is therefore:

$$q_h/2 = - k A \left.\frac{dT}{dx}\right]_{x = 0} \qquad \text{(III-11)}$$

in dimensionless form this reduces to:

$$\left.\frac{d\theta}{d\xi}\right]_{\xi = 0} = - \frac{q_h}{2\sqrt{hPkA}\ (T_{ch} - T_b)} = - Q_{h1} \qquad \text{(III-12)}$$

To understand the behavior of the superconductor and its normal substrate we need consider only those situations where $f > 0$, since for $f = 0$ all the current flows in the superconductor and we have only a simple steady state heat conduction problem.

We need two solutions - the first one for the case where only part of the current has been driven out of the superconductor at the origin, and the second one for the case where all the current is in the normal conductor at the origin.

2) Current Shared at the Origin

The solution for this case is broken down into two regions. A region of current sharing which extends a distance $\Delta\xi$ from the origin and a region in which the temperature decays but all the current is in the superconductor.

At the boundary of the two regions the temperature as well as its first derivative are continuous. The temperature at this boundary is such that f = 0, therefore the value of θ can be obtained from Eq. (III-4) as

$$\theta\Big]_{\xi = \Delta\xi} = 1 - \tau \qquad \text{(III-13)}$$

The boundary condition at $\xi \to \infty$ is $\theta \to 0$.

Using the above boundary conditions the solution is for $\alpha\tau < 1.0$:

$$0 \le \xi \le \Delta\xi$$

$$\theta = c_3 \cosh \sqrt{1 - \alpha\tau}\,\xi + c_4 \sinh \sqrt{1 - \alpha\tau}\,\xi - \frac{\alpha\tau\,(1 - \tau)}{1 - \alpha\tau} \qquad \text{(III-14)}$$

$$\Delta\xi \le \xi$$

$$\theta = (1 - \tau)\, e^{-(\xi - \Delta\xi)} \qquad \text{(III-15)}$$

where

$$c_3 = \left[\left(\frac{1-\tau}{1 - \alpha\tau}\right) + \frac{Q_{h1}}{\sqrt{1 - \alpha\tau}} \sinh \sqrt{1 - \alpha\tau}\,\Delta\xi\right]\left[\cosh \sqrt{1 - \alpha\tau}\,\Delta\xi\right]^{-1}$$

$$c_4 = -\frac{Q_{h1}}{\sqrt{1 - \alpha\tau}}$$

and the value of $\Delta\xi$ is obtained from:

$$\left(\frac{1 - \tau}{1 - \alpha\tau}\right) \tanh \sqrt{1 - \alpha\tau}\,\Delta\xi + \frac{1 - \tau}{\sqrt{1 - \alpha\tau}} = \frac{Q_{h1}}{\sqrt{1 - \alpha\tau}\,\cosh \sqrt{1 - \alpha\tau}\,\Delta\xi} \qquad \text{(III-16)}$$

The solution for $\alpha\tau > 1.0$ is:

$$0 \le \xi \le \Delta\xi$$

$$\theta = c_3' \cos \sqrt{\alpha\tau - 1}\,\xi + c_4' \sin \sqrt{\alpha\tau - 1}\,\xi - \frac{\alpha\tau(1-\tau)}{1 - \alpha\tau} \qquad \text{(III-17)}$$

$$\xi \ge \Delta\xi$$

$$\theta = (1 - \tau) e^{-(\xi - \Delta\xi)} \qquad \text{(III-18)}$$

where

$$c'_3 = \left[\left(\frac{1-\tau}{1-\alpha\tau}\right) + \frac{Q_{h1}}{\sqrt{\alpha\tau - 1}} \sin\sqrt{\alpha\tau - 1}\,\Delta\xi\right] \Big/ \cos\sqrt{\alpha\tau - 1}\,\Delta\xi \qquad \text{(III-19)}$$

$$c'_4 = -\frac{Q_h}{\sqrt{\alpha\tau - 1}}$$

and the value of $\Delta\xi$ is obtained from:

$$\frac{1-\tau}{1-\alpha\tau} \tan\sqrt{\alpha\tau - 1}\,\Delta\xi - \frac{1-\tau}{\sqrt{\alpha\tau - 1}} = -\frac{Q_{h1}}{\sqrt{\alpha\tau - 1}\,\cos\sqrt{\alpha\tau - 1}\,\Delta\xi} \qquad \text{(III-20)}$$

The voltage measured across the conductor from $-\infty$ to $+\infty$ is:

$$V = \int_{-\infty}^{+\infty} v\,dx = \frac{2\rho}{A} I x_o \int_0^{\Delta\xi} f\,d\xi$$

Using Eq. (III-4) to eliminate f in terms of θ, and performing the indicated integration results in:

$$V = \frac{vA}{2\rho I x_o} = \frac{Q_{h1} - (1 + \Delta\xi)(1 - \tau)}{\tau(1 - \alpha\tau)} \qquad \text{(III-21)}$$

This expression for V is good for all values of $\alpha\tau$.

3) Current all in the Normal Conductor at the Origin

If Q_{h1} is high enough, then all the current will be expelled from the superconductor at the origin, and the temperature distribution has three regions.

The only new boundary is that between region I and II and since f = 1.0 at this boundary, from Eq. (III-4) the value of θ = 1.0 is obtained.

The solution for $\alpha\tau < 1.0$ is:

$$0 \le \xi \le \xi_1$$

$$\theta \ge c_1 e^{\xi} + c_2 e^{-\xi} + \alpha\tau^2 \qquad \text{(III-22)}$$

$$\xi_1 \le \xi \le \xi_1 + \Delta\xi$$

$$\theta = c_3 \cosh\sqrt{1-\alpha\tau}\ (\xi - \xi_1) + c_4 \sinh\sqrt{1-\alpha\tau}\ (\xi - \xi_1) - \frac{\alpha\tau(1-\tau)}{1-\alpha\tau} \qquad \text{(III-23)}$$

$$\xi_1 + \Delta\xi \le \xi$$

$$\theta = (1-\tau)e^{-(\xi - \xi_1 - \Delta\xi)} \qquad \text{(III-24)}$$

where

$$c_1 = c_2 - Q_{h1}$$

$$c_2 = \frac{1 - \alpha\tau^2 + Q_{h1}e^{\xi_1}}{2\cosh\xi_1}$$

$$c_3 = \frac{1-\alpha\tau^2}{1-\alpha\tau}$$

$$c_4 = \left[(1-\alpha\tau^2)\tanh\xi_1 - \frac{Q_{h1}}{\cosh\xi_1}\right] \Big/ \sqrt{1-\alpha\tau}$$

and the value of ξ_1 and $\Delta\xi$ are obtained from:

$$\cosh\sqrt{1-\alpha\tau}\ \Delta\xi + \sqrt{1-\alpha\tau}\ \sinh\sqrt{1-\alpha\tau}\ \Delta\xi = \frac{1-\alpha\tau^2}{1-\tau} \qquad \text{(III-25)}$$

$$\frac{(1-\alpha\tau^2)\tanh\xi_1 - \frac{Q_{h1}}{\cosh\xi_1}}{\sqrt{1-\alpha\tau}} = -\frac{\frac{1-\tau}{\sqrt{1-\alpha\tau}} + \frac{1-\alpha\tau^2}{1-\alpha\tau}\sinh\sqrt{1-\alpha\tau}\,\Delta\xi}{\cosh\sqrt{1-\alpha\tau}\,\Delta\xi} \qquad \text{(III-26)}$$

Rather than solve explicitly for the solution for $\alpha\tau \ge 1.0$ it can be obtained directly from the solution for $\alpha\tau \le 1.0$ by substituting $i\sqrt{\alpha\tau - 1}$ for $\sqrt{1-\alpha\tau}$ and performing the necessary simplifications. The results for $\alpha\tau > 1.0$ are:

$$0 \le \xi \le \xi_1$$

$$\theta = c_1 e^{\xi} + c_2 e^{\xi} + \alpha\tau^2$$

$$\xi_1 \le \xi \le \xi_1 + \Delta\xi$$

$$\theta = c_3' \cos\sqrt{\alpha\tau - 1}\ (\xi - \xi_1) + c_4' \sin\sqrt{\alpha\tau - 1}\ (\xi - \xi_1) - \frac{\alpha\tau\,(1 - \tau)}{1 - \alpha\tau}$$

$$\xi + \Delta\xi \le \xi$$

$$\theta = (1 - \tau)e^{-(\xi - \xi_1 - \Delta\xi)}$$

where

$$c_1 = c_2 - Q_{h1}$$

$$c_2 = \frac{1 - \alpha\tau^2 + Q_{h1}e^{\xi_1}}{e^{\xi_1} + e^{-\xi_1}} = \frac{1 - \alpha\tau^2 + Q_{h1}e^{\xi_1}}{2\cosh\xi_1}$$

$$c_3' = \frac{1 - \alpha\tau^2}{1 - \alpha\tau}$$

$$c_4' = \left[(1 - \alpha\tau^2)\tanh\xi_1 - \frac{Q_{h1}}{\cosh\xi_1}\right] \Big/ \sqrt{\alpha\tau - 1}$$

and the value of ξ and $\Delta\xi$ are obtained from:

$$\cos\sqrt{\alpha\tau - 1}\,\Delta\xi - \sqrt{\alpha\tau - 1}\ \sin\sqrt{\alpha\tau - 1}\,\Delta\xi = \frac{1 - \alpha\tau^2}{1 - \tau} \qquad \text{(III-27)}$$

and:

$$\frac{(1 - \alpha\tau^2)\tanh\xi_1 - \dfrac{Q_{h1}}{\cosh\xi_1}}{\sqrt{\alpha\tau - 1}} = -\frac{\dfrac{1 - \tau}{\sqrt{\alpha\tau - 1}} - \dfrac{1 - \alpha\tau^2}{1 - \alpha\tau}\sin\sqrt{\alpha\tau - 1}\,\Delta\xi}{\cos\sqrt{\alpha\tau - 1}\,\Delta\xi} \qquad \text{(III-28)}$$

The voltage across the conductor from $-\infty$ to $+\infty$ is:

$$V = \int_{-\infty}^{+\infty} v\,dx = 2\int_0^{\xi_1 + \Delta\xi} \frac{\rho I f}{A}\,dx = \frac{2\rho I x_o}{A}\left[\int_0^{\xi_1} f\,d\xi + \int_{\xi_1}^{\xi_1 + \Delta\xi} f\,d\xi\right]$$

substituting for f from Eq. (III-4) and using the expression for θ the voltage is:

$$V = \frac{vA}{2\rho I x_o} = \tau\,\xi - \frac{(1-\tau)(1+\Delta\xi)}{\tau(1-\alpha\tau)} - \frac{(1-\alpha\tau^2)\tanh\xi - \dfrac{Q_{h1}}{\cosh\xi}}{\tau(1-\alpha\tau)} \qquad \text{(III-29)}$$

The dimensionless terminal voltage V is plotted as a function of Q_{h_1} in Fig. (III-1). Three classes of behavior are shown there:

(1) An uncontrolled quench ($\alpha = 10$)
(2) Hysteretic Behavior ($\alpha = 5$)
(3) Stable, single valued Behavior ($\alpha \leq 3$)

4) Stability Criteria

We now present the stability criteria for the one dimensional analysis. These will consist of determining the condition under which $\partial V/\partial Q_{h1} \to \infty$.

a. Case 1 - Current Shared at Origin.

It can be seen from equation (III-21) that the voltage will remain finite for $\alpha\tau<1$. For $\alpha\tau = 1$ the original differential equation, (III-6) breaks down and the voltage goes to ∞. For the case $\alpha\tau > 1$ the slope of the voltage-heater curve will go to infinity as $\partial\Delta\xi/\partial Q_h$ goes to infinity. Therefore we may find the critical length and critical heat input by finding the conditions for which $\partial\Delta\xi/\partial Q_h \to \infty$ or $\partial Q_h/\partial\Delta\xi \to 0$. This may be found from Eq. (III-20) by solving for $\partial Q_h/\partial\Delta\xi$ and setting it equal to zero.

$$\Delta\xi_{\text{take off}} = (\alpha\tau-1)^{-\frac{1}{2}} \arctan\left[(\alpha\tau-1)^{-\frac{1}{2}}\right] \qquad \text{(III-30)}$$

The critical heat input to the origin for take-off can be found by substituting this value for $\Delta\xi$ back into Eq. (III-4).

b. Case 2 - Current All in Normal Conductor at Origin

In this regime f = 1 at the origin. The stability criteria are determined by finding the conditions under which the (f = 1) region ($0 < \xi \leq \xi_1$), and hence the voltage, propagates to infinity.

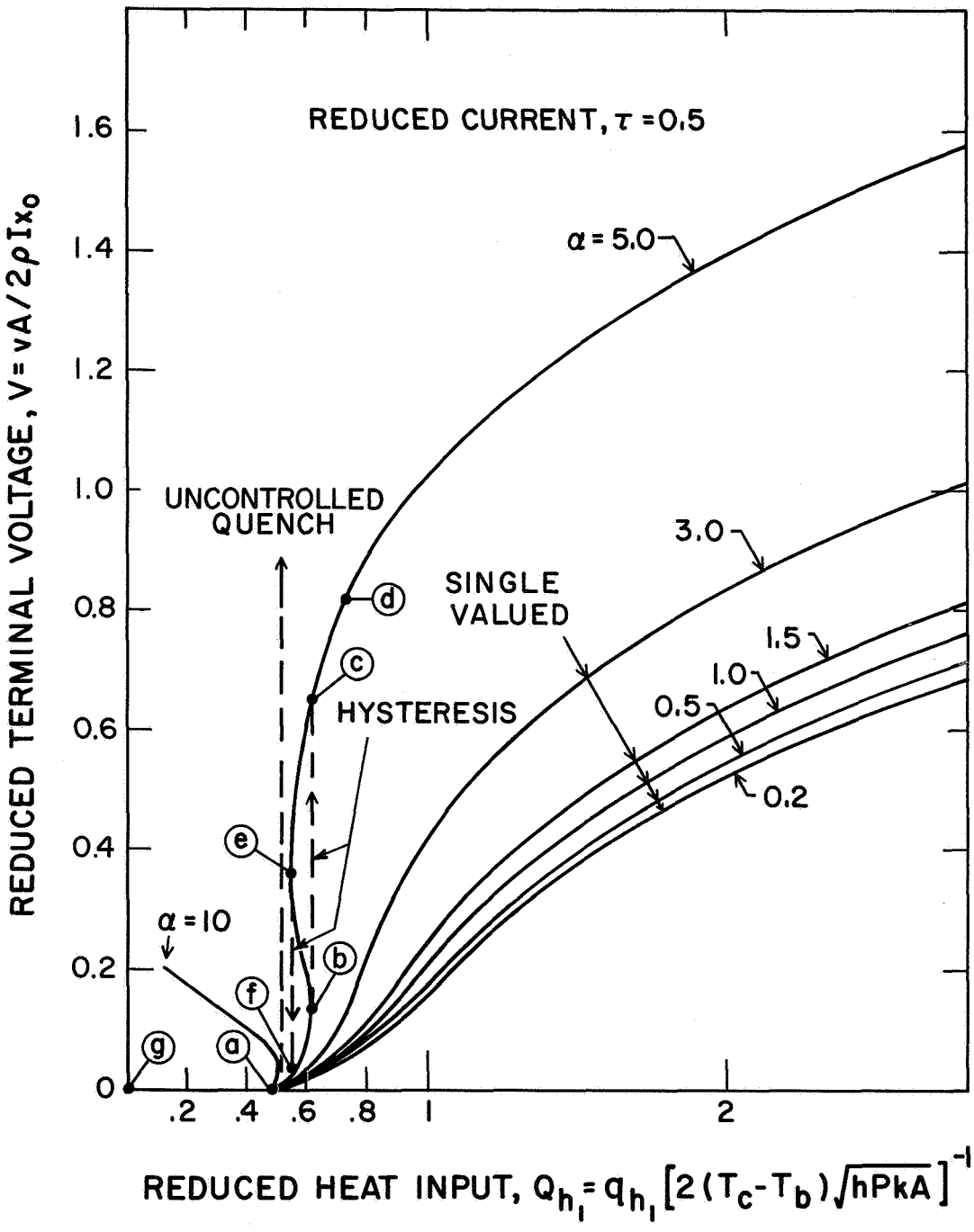

Fig. III-1 Terminal voltage as a function of heat input. Three classes of behavior are shown.

We find $(\partial V/\partial Q_{h1})$ from Eq. (III-29)

$$\frac{\partial V}{\partial Q_{h1}} = \frac{\cosh \xi_1}{1 - \alpha \tau^2 + Q_{h1} \sinh \xi_1}$$

This goes to infinity when

$$Q_{h1} = Q_{h1T} = \frac{\alpha \tau^2 - 1}{\sinh \xi_1} \qquad \text{(III-32)}$$

In addition it can also be shown that $\xi_1 \to \infty$ when $\alpha \tau^2 = (2 - \tau)$. This is the quench condition. The curve $\alpha \tau^2 = 2 - \tau$ as well as curves for constant Q_{hT} and $\Delta \xi_T$ are also plotted in Fig. III-2. This is interpreted as follows:

(1) For α, τ such that $\alpha \tau^2 < 1$, the behavior of the system is stable in the sense that $(\partial V/\partial Q_{h1})$ is always finite and positive.

(2) For α, τ such that $1 < \alpha \tau^2 < (2 - \tau)$, the behavior is hysteretic. The conductor will not regain its superconducting state until Q_{h1} is lowered through a recovery value.

(3) For α, τ such that $\alpha \tau^2 > (2 - \tau)$ the behavior is unstable since at Q_{h1T} the voltage rises to infinity.

Figure III-3 is a graph of Q_{h1} vs τ for $\alpha = 3$ and clearly represents the different regions of operation for different values of τ.

(1) For $\tau < \frac{1}{\sqrt{\alpha}}$, the stable range, no voltage is exhibited until $Q_{h1} = (1 - \tau)$ where the onset of resistance occurs. If Q_{h1} continues to increase, the voltage increases in a stable manner as shown in the insert.

(2) If the line of operation lies in the unstable range, $\alpha \tau^2 > 2 - \tau$ there is no voltage until $Q_{h1} = (1 - \tau)$, then the voltage increases controllably until the intersection with the Q_{h1T} curve at which time quench occurs (i.e., $V \to \infty$).

(3) The hysteretic range $1 < \alpha \tau^2 < 2 - \tau$ may be subdivided into two-regions.

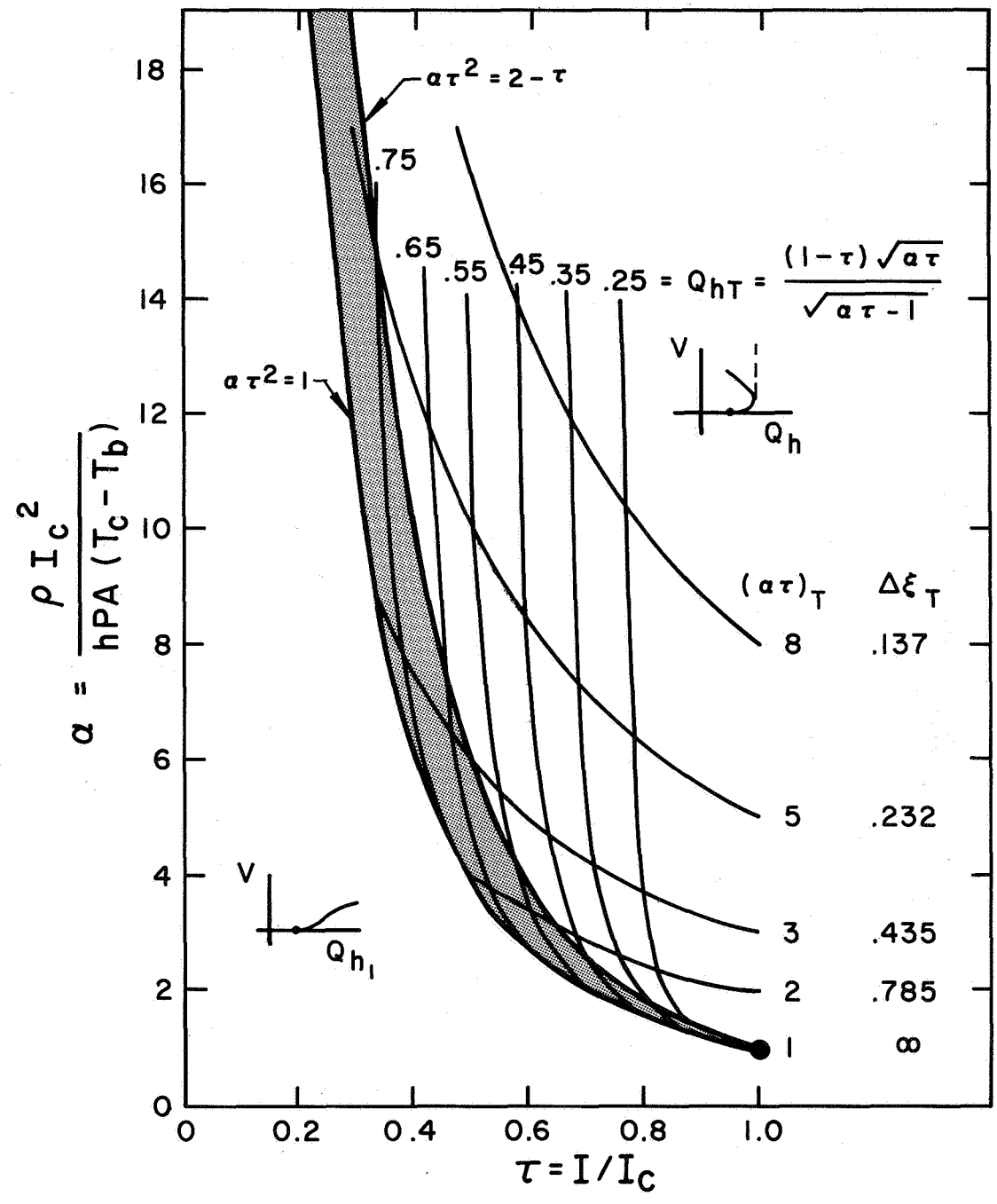

Fig. III-2 Stability diagram indicating range of α, τ over which stable, hysteretic, or unstable behavior occurs.

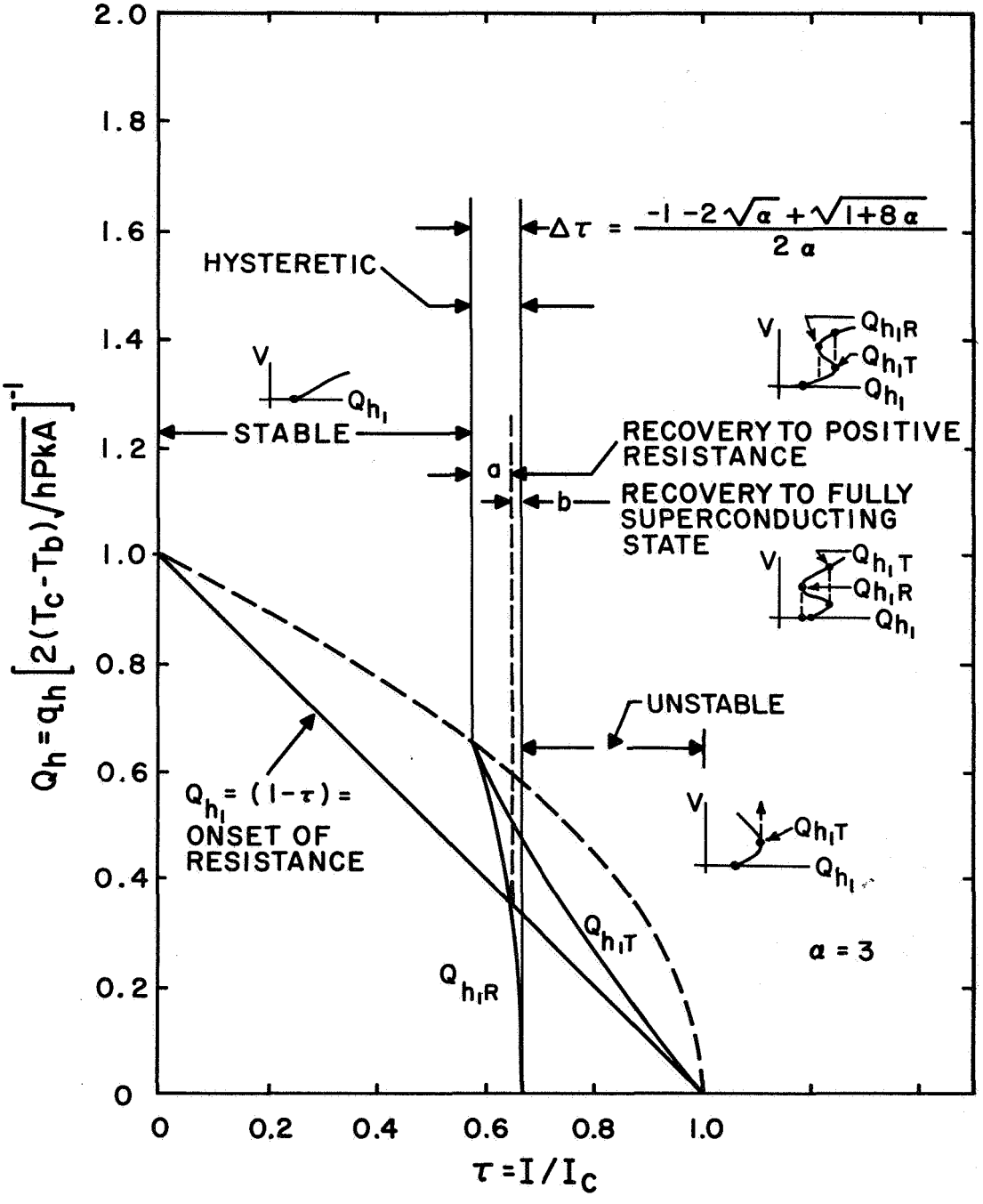

Fig. III-3 Heat input vs current: an indicator of the type of behavior for different τ as α is held fixed.

(a) For τ in region "a", there is again no voltage until $Q_{hl} = (1 - \tau)$. As Q_{hl} is increased, V increases until $Q_{hl} = Q_{hlT}$ when a discontinuous rise in voltage occurs. If Q_{hl} is then reduced to the value indicated by the intersection with the Q_{hlR} curve, V will decrease discontinuously, and a recovery will be made to a condition of positive resistance.

(b) Operation in this range is similar to that in region "a" with the important difference that recovery is made to a condition of zero voltage, that is, to the fully superconducting state. The relation between α and τ for the condition where Q_{hlR} is equal to $(1 - \tau)$ may be shown to be

$$\left(\frac{\alpha \tau^2 - 1}{1 - \tau} \right)^2 \alpha \tau = 1 \qquad \text{(III-33)}$$

A plot of the values of the critical voltages for the case of $\alpha = 5$ is shown in Fig. III-4.

(1) For τ in the region indicated, operation is stable.

(2) For τ in the unstable region, the voltage may increase as far as the curve labeled V_T at which point a quench will occur.

(a) In the hysteretic "a" region, the voltage may be increased to V_T where it will discontinuously rise to the value indicated by the V'' curve. If Q_{hl} is then decreased, the voltage will decrease to the value indicated by the V_R curve. At this point, it will decrease discontinuously to the value represented by the intersection of the line of operation with the V' curve. Further decrease in Q_{hl} leads to a continuous decrease in V to zero.

(b) In the hysteretic "b" region, operation is analogous to that in the "a" region except that the voltage drops discontinuously to zero at recovery.

Figure III-5 is similar to Fig. III-4 in that it shows the take-off and recovery voltages. This is done for a range of values of α. Several corresponding points are labeled in the two plots to aid interpretation of Fig. III-5.

C. Composite Superconductor Behavior Including Gradients Along the Conductor and Incorporating a Nonlinear Heat Transfer Characteristic

The configuration to be considered is essentially the same configuration analyzed under "One-Dimensional Effects" in the preceding section. In this section, however, the theoretical model is modified and improved by incorporating the nonlinear heat transfer characteristic illustrated in Fig. III-6.

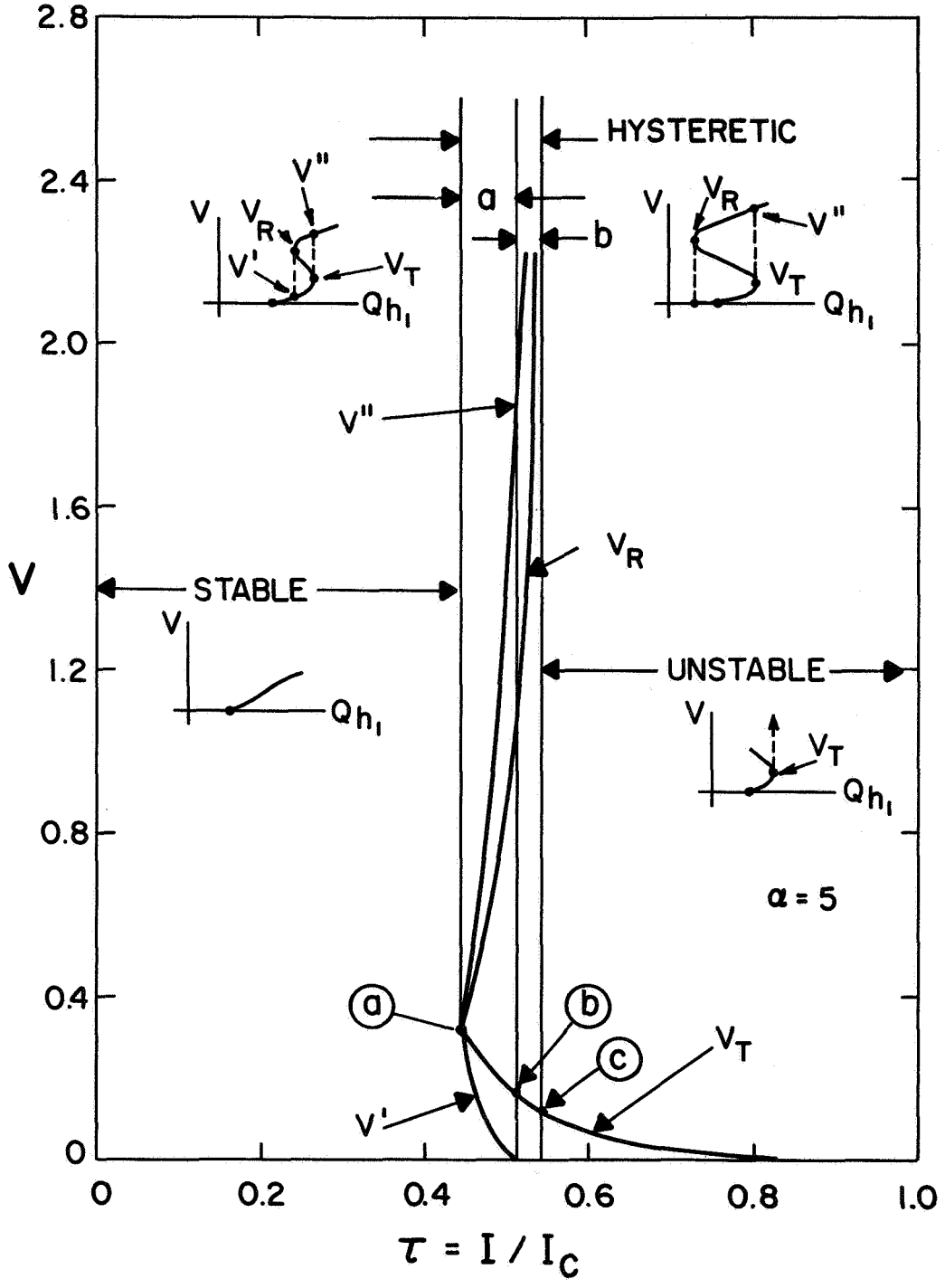

Fig. III-4 Terminal voltage vs current: the behavior of the voltage for various τ and for α fixed.

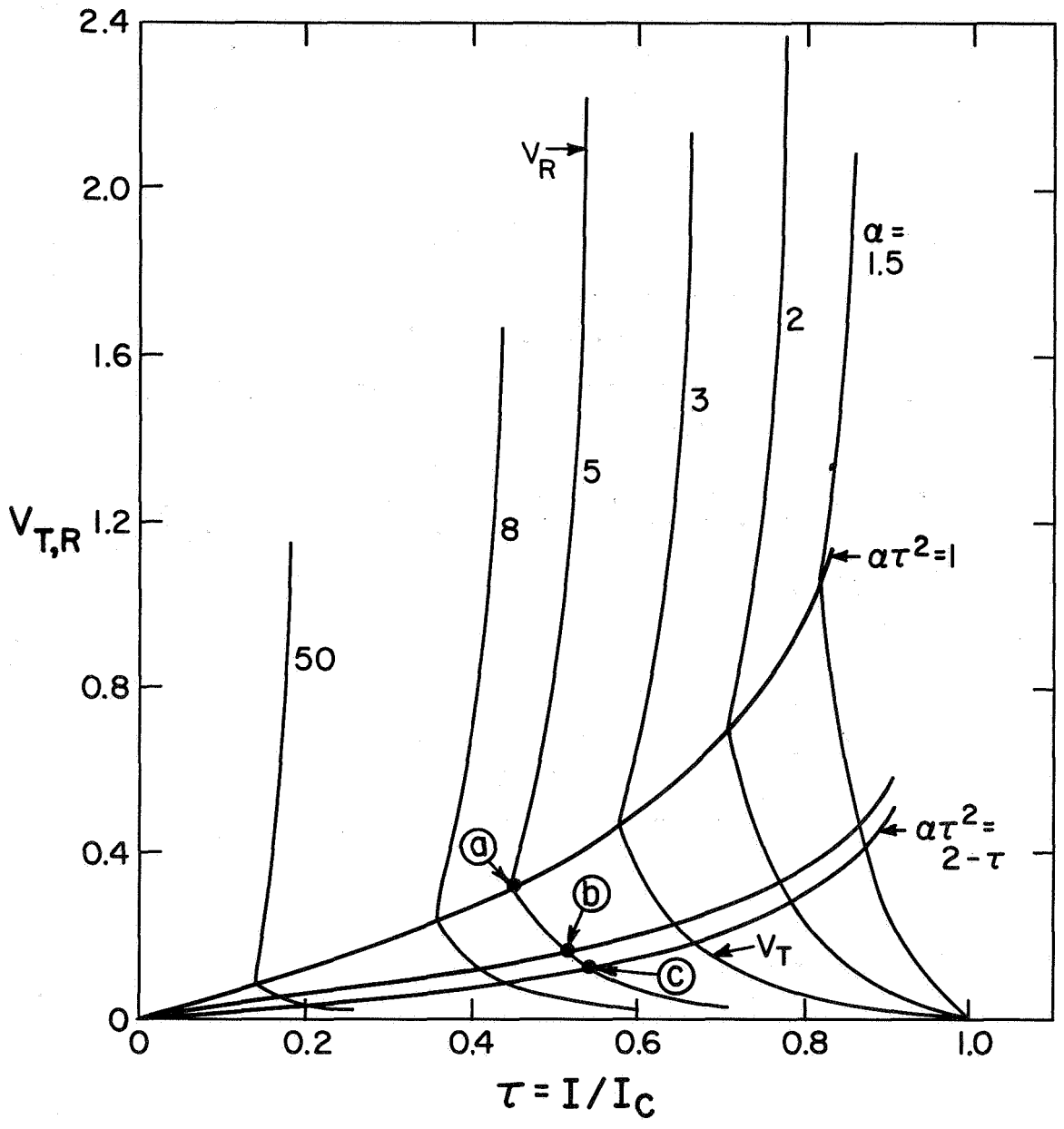

Fig. III-5 Takeoff and recovery voltages as a function of τ for various α.

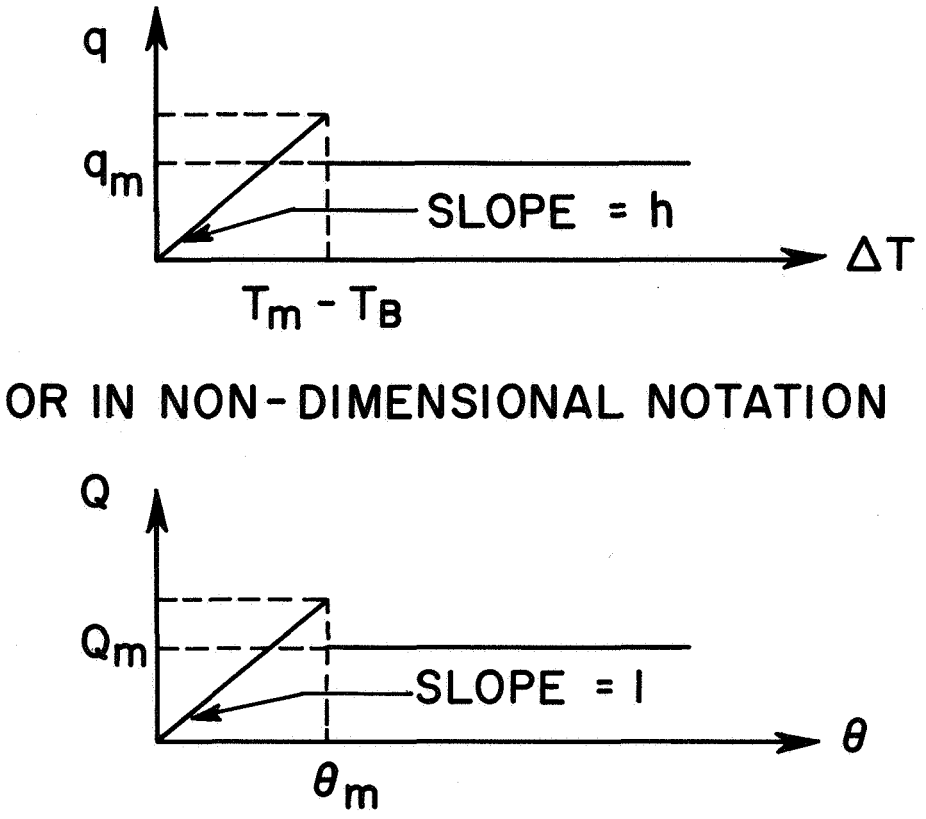

Fig. III-6 The first nonlinear model for the heat transfer characteristics of liquid helium

We assume that the current-carrying capacity of the superconductor is given by Eq. (III-3) and that the fraction of the total current carried by the substrate is given by Eq. (III-4). Remembering the characteristics of the constant heat transfer coefficient analysis, the sequence of events may be expected to be as shown in Fig. III-7. In Fig. III-7a, the heat input to the origin is small enough relative to the ability of the bath to cool the conductor through nucleate boiling (constant heat transfer coefficient) so that the dimensionless temperature at the origin, θ_o, is less than θ_m, the temperature corresponding to the transition from nucleate to film boiling, and also that $\theta_o < (1 - \tau)$ (the condition for onset of resistance or $f = 0^+$). Hence, the current will flow entirely in the superconductor. If the heat input is increased as in Fig. III-7b, until $\theta_m < \theta_o < (1 - \tau)$, the conductor will remain in a superconducting state, but for $0 < x < x_m$, it will be cooled by film boiling and for $x > x_m$ by nucleate boiling. In Fig. III-7c, the heat input is high enough so that $(1 - \tau) < \theta_o < 1$, hence, current is shared for $0 < x < \Delta x$ and joule heating becomes important. For $x > \Delta x$, all the current flows in the superconductor. Cooling is again by film boiling for $0 < x < x_m$ and by nucleate boiling for $x > x_m$. Increasing the heat at the origin until $\theta_o > 1$ is illustrated in Fig. III-7d, where all the current flows in the substrate for $0 < x < x_1$, the current transfers back into the superconductor for $x_1 < x < x_1 + \Delta x$ and all the current flows in the superconductor for $x > x_1 + \Delta x$.

If the bath can cool the conductor sufficiently, the transition from Fig. III-7 through Fig. III-7d and back again as q_{hl} is increased then decreased, may be expected to be controllable and reversible. If, on the other hand, cooling is sufficiently poor, q_{hl} may be increased to some point where the length of the non-superconducting section will suddenly propagate to infinity and recovery to a fully superconducting state is not possible even if q_{hl} is reduced to zero. Between these two extremes is the hysteretic behavior where the heat may be increased to a point where the resistive length increases suddenly but remains finite. A sudden recovery may then be obtained by reducing q_{hl} to some lower value.

In the previous section, conditions were found which bracket the above modes of behavior under the assumption of a constant heat transfer coefficient. This section presents results of an attempt to determine these same conditions for the case of a constant heat transfer coefficient for $0 < \theta < \theta_m$ and a maximum allowable heat flux per unit area, q_m, for $\theta > \theta_m$. The analysis is limited to $(1 - \tau) > \theta_m$. Since θ_m is relatively small, however, results will be applicable to one-dimensional situations where the current carried remains somewhat below the critical current at the bath temperature

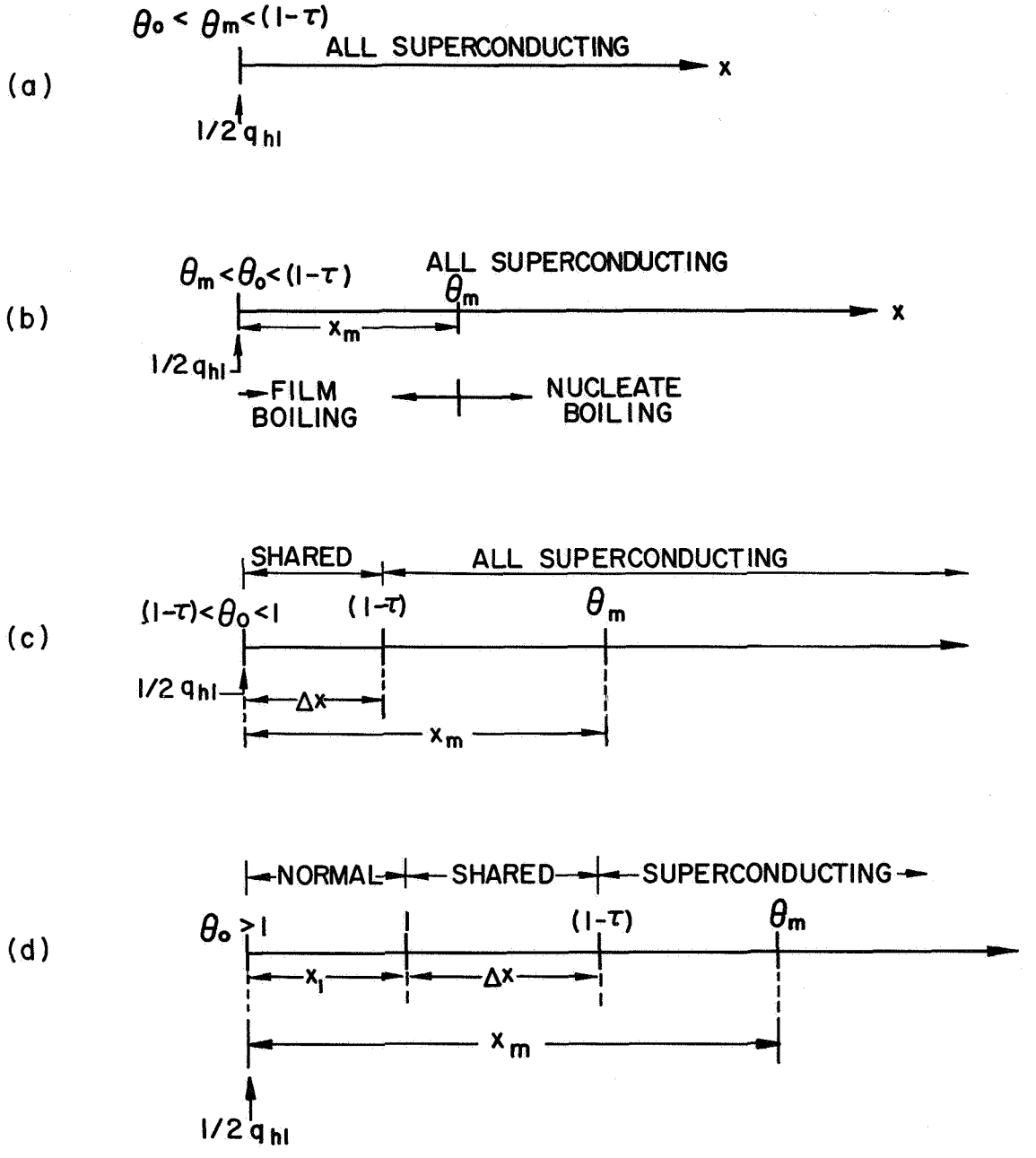

Fig. III-7a Conductor cooled entirely by nucleate boiling

b Conductor cooled partially by nucleate and partially by film boiling

c Cooling after the onset of resistance but before all of the current transfers into the substrate at the origin

d Configuration after $\theta_0 > 1$, provided $x_1 \neq \infty$

To determine a general governing equation, consider the element of length shown in Fig. III-8. The equation will be written including terms for both cooling by q_m and by constant h. This equation will then be applied to different sections of the wire shown in Fig. III-7. In each section, certain terms will not apply.

Begin by writing the steady-state energy equation for the element in Fig. III-8.

$$W_i A dx - q_m P dx - h P dx(T - T_b) + kA \frac{d^2T}{dx^2} = 0 \qquad \text{(III-34)}$$

where:

W_i = joule heat per unit volume (when $f \neq 0$)

q_m = maximum heat flux (when $\theta > \theta_m$)

and the other terms have been previously defined. Then Eq. (III-34) may be written in dimensionless form as:

$$\frac{d^2\theta}{d\xi^2} - \theta - Q_m + \alpha\tau^2\left(1 - \frac{1 - \theta}{\tau}\right) = 0 \qquad \text{(III-35)}$$

where

$$Q_m = \frac{q_m}{h(T_c - T_b)}$$

Earlier definitions of θ, α, τ, ξ, and f have been utilized.

The first term in Eq. (III-35) is due to conduction; the second to a constant heat transfer coefficient (nucleate boiling); the third to a maximum heat flux (transition to film boiling); the last to joule heating.

We will first solve Eq. (III-35) for the case where the nondimensional temperature at the origin is less than 1 and the sharing condition at the origin is ($0 \leq f < 1$). The following table shows the equations to be solved for each region.

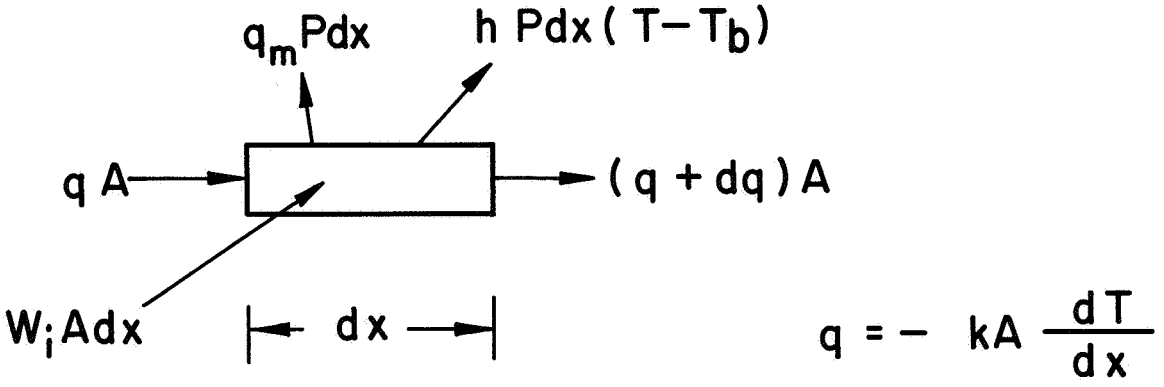

Fig. III-8 Element for determining general governing equation

Region	Sharing Condition	Equation
$0 < \xi < \Delta\xi$	$0 < f < 1$	$\frac{d^2\theta_1}{d\xi^2} - Q_m + \alpha\tau^2\left(1 - \frac{1-\theta_1}{\tau}\right) = 0$
$\Delta\xi < \xi < \xi_m$	$f = 0$	$\frac{d^2\theta_2}{d\xi^2} - Q_m = 0$
$\xi > \xi_m$	$f = 0$	$\frac{d^2\theta_3}{d\xi^2} - \theta_3 = 0$

The boundary conditions are that

$$\theta_3 \to 0 \text{ as } \xi \to \infty$$

$$\left.\frac{d\theta}{d\xi}\right|_{\xi=0} = -\frac{q_{h1}}{2\sqrt{hPkA}(T_{ch} - T_b)} \equiv -Q_{h1}$$

and that the temperature and its derivative be continuous at $\xi = \xi_m$ and $\xi = \Delta\xi$. The above equations, together with the boundary conditions, determine the problem and it may be shown that the solutions are:

$$0 < \xi < \Delta\xi \qquad \theta_1 = C_1 \sin(\sqrt{\alpha\tau}\,\xi) + C_2 \cos(\sqrt{\alpha\tau}\,\xi) + \frac{Q_m}{\alpha\tau} + (1 - \tau)$$

$$\Delta\xi < \xi < \xi_m \qquad \theta_2 = \frac{1}{2} Q_m(\xi^2 - \Delta\xi^2) - (\theta_m + Q_m\xi_m)(\xi - \Delta\xi) + (1 - \tau)$$

$$\xi > \xi_m \qquad \theta_3 = \theta_m e^{-(\xi - \xi_m)}$$

where

$$C_1 = \frac{-Q_{h1}}{\sqrt{\alpha\tau}}$$

$$C_2 = \frac{Q_{h1}}{\sqrt{\alpha\tau}} \tan(\sqrt{\alpha\tau}\,\Delta\xi) - \frac{Q_m}{\alpha\tau\cos(\sqrt{\alpha\tau}\,\Delta\xi)}$$

The lengths $\Delta\xi$ and ξ_m are determined by matching the solutions for θ at $\Delta\xi$ and ξ_m:

$$Q_{h1} = \frac{Q_m}{\sqrt{\alpha\tau}} \sin(\sqrt{\alpha\tau}\ \Delta\xi) + Q_m\sqrt{\left(\frac{\theta_m}{Q_m}\right)^2 + \frac{2}{Q_m}(1 - \tau - \theta_m)}\left[\cos(\sqrt{\alpha\tau}\ \Delta\xi)\right] \tag{III-36}$$

and

$$\xi_m = \Delta\xi - \frac{\theta_m}{Q_m} + \sqrt{\left(\frac{\theta_m}{Q_m}\right)^2 + \frac{2}{Q_m}(1 - \tau - \theta_m)} \tag{III-37}$$

The amount of heat required to cause the onset of resistance may be found using Eq. (III-36) with $\Delta\xi = 0$.

$$Q_{h_1}\Big|_{or} = Q_m\sqrt{\left(\frac{\theta_m}{Q_m}\right)^2 + \frac{2}{Q_m}(1 - \tau - \theta_m)} \tag{III-38}$$

which is restricted to $(1 - \tau) > \theta_m$. For $(1 - \tau) < \theta_m$, the constant h analysis presented in the preceding treatment is valid and this condition is:

$$Q_{h1}\Big|_{or} = (1 - \tau),\ (1 - \tau) < \theta_m \tag{III-39}$$

By taking $\frac{\partial Q_{h1}}{\partial \Delta\xi}$ using Eq. (III-36) and setting the result equal to zero, the length $\Delta\xi_T$ is found which determines the sudden takeoff in voltage, either as an uncontrolled quench or to another operating point as in hysteresis. Carrying out this process shows that the takeoff length is given by:

$$\tan(\sqrt{\alpha\tau}\ \Delta\xi_T) = \left\{\alpha\tau\left[\left(\frac{\theta_m}{Q_m}\right)^2 + \frac{2}{Q_m}(1 - \tau - \theta_m)\right]\right\}^{-\frac{1}{2}} \tag{III-40}$$

The heat input to the origin which corresponds to takeoff, Q_{h1T}, is determined by Eqs. (III-36) and (III-40).

$$Q_{h1T} = \sqrt{\frac{Q_m^2}{\alpha\tau} + \theta_m^2 + 2Q_m(1 - \tau - \theta_m)} \tag{III-41}$$

The above equations govern the situation depicted by Fig. III-7c, hence, it is necessary that $\theta \leq 1$ at the origin. This inequality, together with Eqs. (III-36), (III-40), and (III-41) yield the condition that:

$$\alpha \tau^2 > \theta_m \tag{III-42}$$

It is, therefore, necessary for Eq. (III-42) to be satisfied when $Q_{hl} \rightarrow Q_{hlT}$ (and in turn $\Delta \xi \rightarrow \Delta \xi_T$) in order for takeoff to occur from the configuration in Fig. III-7c. Hence,

$$\alpha \tau^2 < \theta_m \tag{III-43}$$

represents the limit of stability since takeoff is then not possible. This condition corresponds to the requirement that $\alpha \tau^2 < 1$ for stability to be satisfied when the conductor is cooled via a constant heat transfer coefficient throughout its length.

We will now find the solution for the case that $\theta_o > 1$ where all the current is in the substrate at the origin. This is the case shown in Fig. III-7d. The forms of Eq. (III-35) to be solved in the various regions are:

Region	Sharing Condition	Equation
$0 < \xi < \xi_1$	$f = 1$	$\frac{d^2\theta_1}{d\xi^2} - Q_m + \alpha \tau^2 = 0$
$\xi_1 < \xi < \xi_1 + \Delta\xi$	$0 < f < 1$	$\frac{d^2\theta_2}{d\xi^2} - Q_m + \alpha \tau^2 (1 - \frac{1 - \theta_2}{\tau}) = 0$
$\xi_1 + \Delta\xi < \xi < \xi_m$	$f = 0$	$\frac{d^2\theta_3}{d\xi^2} - Q_m = 0$
$\xi > \xi_m$	$f = 0$	$\frac{d^2\theta_4}{d\xi^2} - \theta = 0$

where we assume $1 - \tau > \theta_m$

The solutions to these equations are:

$$0 < \xi < \xi_1 \qquad \theta_1 = \frac{1}{2}(Q_m - \alpha \tau^2)\xi^2 + C_1 \xi + C_2 \xi$$

$$\xi_1 < \xi < \xi_1 + \Delta\xi \qquad \theta_2 = C_3 \sin(\sqrt{\alpha\tau}\ \xi) + C_4 \cos(\sqrt{\alpha\tau}\ \xi) + \frac{Q_m}{\alpha\tau} + (1 - \tau)$$

$$\xi_1 + \Delta\xi < \xi < \xi_m \qquad \theta_3 = \frac{1}{2} Q_m \xi^2 + C_5 \xi + C_6$$

$$\xi > \xi_m \qquad \theta_4 = C_7 e^{-\xi} + C_8 e^{-\xi}$$

The boundary conditions are:

(1) $\theta \to 0$ as $\xi \to \infty$

(2) $\left.\frac{d\theta}{d\xi}\right|_{\xi=0} = -Q_{h1}$

(3) θ and $\frac{d\theta}{d\xi}$ are continuous at $\xi = \xi_1,\ \xi_1 + \Delta\xi,\ \xi_m$.

The boundary conditions completely determine the constants C_1 through C_8 as well as the lengths ξ_1, $\Delta\xi$, and ξ_m.

The constants are determined to be:

$$C_1 = -Q_{h1}$$

$$C_2 = 1 + Q_{h1}\xi_1 - \frac{1}{2}(Q_m - \alpha\tau^2)\xi_1^2$$

$$C_3 = -\frac{Q_m}{\alpha\tau} \sin\left(\sqrt{\alpha\tau}\ (\xi_1 + \Delta\xi)\right) - \frac{Q_m}{\sqrt{\alpha\tau}} \sqrt{\left(\frac{\theta_m}{Q_m}\right)^2 + \frac{2}{Q_m}(1 - \tau - \theta_m)} \quad x$$

$$\cos(\sqrt{\alpha\tau}\ (\xi_1 + \Delta\xi)$$

$$C_4 = \frac{Q_m}{\alpha\tau} \sqrt{\left(\frac{\theta_m}{Q_m}\right)^2 + \frac{2}{Q_m}(1 - \tau - \theta_m)} \sin\left(\sqrt{\alpha\tau}\ (\xi_1 + \Delta\xi)\right) -$$

$$\frac{Q_m}{\alpha\tau} \cos\left(\sqrt{\alpha\tau}\ (\xi_1 + \Delta\xi)\right)$$

$$C_5 = -\theta_m - Q_m\xi_m$$

$$C_6 = \frac{1}{2} Q_m \xi_m^2 + \theta_m(1 + \xi_m)$$

$$C_7 = \theta_m e^{\xi_m}$$

$$C_8 = 0$$

The non-dimensional lengths are determined by the following equations:

$$\xi_m - \xi_1 - \Delta\xi = -\frac{\theta_m}{Q_m} + \sqrt{\frac{\theta_m}{Q_m}^2 + \frac{2}{Q_m}(1 - \tau - \theta_m)} \qquad \text{(III-44)}$$

$$\tau - \frac{Q_m}{\alpha\tau} = \frac{Q_m}{\sqrt{\alpha\tau}}\sqrt{\frac{\theta_m}{Q_m}^2 + \frac{2}{Q_m}(1 - \tau - \theta_m)}\,\sin\sqrt{\alpha\tau}\;\Delta\xi - \frac{Q_m}{\alpha\tau}\cos\sqrt{\alpha\tau}\;\Delta\xi \qquad \text{(III-45)}$$

$$Q_{h1} = (Q_m - \alpha\tau^2)\xi_1 + \frac{Q_m}{\sqrt{\alpha\tau}}\sin\sqrt{\alpha\tau}\;\Delta\xi + Q_m\sqrt{\frac{\theta_m}{Q_m}^2 + \frac{2}{Q_m}(1 - \tau - \theta_m)}\cos\sqrt{\alpha\tau}\,\Delta\xi \qquad \text{(III-46)}$$

Note from Eq. (III-44) that $(\xi_m - \xi_1 - \Delta\xi)$, the length of the fully superconducting region that is film boiling, and from Eq. (III-45) $\Delta\xi$, the length of the shared region, are <u>independent</u> of Q_{h1}, the non-dimensional heat input at the origin. From Eq. (III-46), only ξ_1, the length of the normal region is affected by Q_{h1}. Equation (III-45) has a solution only if the maximum value of the right hand side of the equation is greater than the left hand side of the equation. It is easily found that this condition is satisfied if:

$$\theta_m^2 + 2Q_m(1 - \theta_m) - \alpha\tau^3 > 0 \qquad \text{(III-47)}$$

It is easy to show that this condition always holds if $Q_m > \alpha\tau^2$ by replacing $\alpha\tau^3$ by τQ_m (which is larger than $\alpha\tau^3$ by the condition $Q_m > \alpha\tau^2$). Then Eq. (III-47) becomes:

$$\theta_m^2 + 2Q_m(1 - \frac{\tau}{2} - \theta_m) > 0 \qquad \text{(III-47a)}$$

But this is always true since we have found the solution for the assumption $1 - \tau > \theta_m$. It is obvious from the above method that Eq. (III-47) will also hold if $\alpha\tau^2$ is not too much greater than Q_m. If Eq. (III-47) is not satisfied, then a solution to the problem with the given boundary conditions ($\theta = 0$ as $\xi \to \infty$) is not possible.

If $\alpha\tau^2 > Q_m$ and condition of Eq. (III-47) is not satisfied; then the voltage takes off at a heat input of

$$Q_{hl\,T} = \sqrt{\frac{Q_m^2}{\alpha\tau} + \theta_m^2 + 2Q_m(1 - \tau - \theta_m)} \qquad \text{(III-48)}$$

which is obtained from the analysis presented previously for $\theta < 1$ at the origin. At take-off the voltage increases to infinity and the wire "quenches." Assuming that Eq. (III-47) is satisfied, we obtain from Eq. (III-46)

$$\frac{dQ_{hl}}{d\xi_1} = (Q_m - \alpha\tau^2)$$

since the length of the shared region $(\Delta\xi - \xi_1)$, is independent of the length of the normal region, ξ_1. Now $\frac{dV}{dQ_{hl}}$ (V is the conductor voltage) must be positive and finite for stable operation to occur and consequently positive and finite for stable operation to occur and consequently $\frac{dQ_{hl}}{dV} = \frac{dQ_{hl}}{d\xi_1} \cdot \frac{d\xi_1}{dV}$ must be positive. Then $\frac{dQ_{hl}}{d\xi_1}$ must be positive and finite since $d\xi_1/dV$ is always positive. Thus if

1) $Q_m > \alpha\tau^2$ stable operation always occurs independent of how much heat is added at the origin.

2) $Q_m < \alpha\tau^2$ the voltage takes off at a value given by Eq. (III-48) and it goes to infinity.

We conclude then, that with this model of the heat transfer characteristic, the wire is either stable or unstable with NO HYSTERESIS REGION between.

Experimentally a region of hysteresis is always observed; so we must choose a model for the heat transfer characteristic which corresponds more closely to the real case. We choose that characteristic to be as shown in Fig. III-9.

D. Composite Superconductor Behavior Including Temperature Gradients Along the Conductor and Incorporating a Modified Nonlinear Heat Transfer Characteristic

We will now use the heat transfer characteristic shown in Fig. III-9. This will be called the modified nonlinear characteristic. The one used

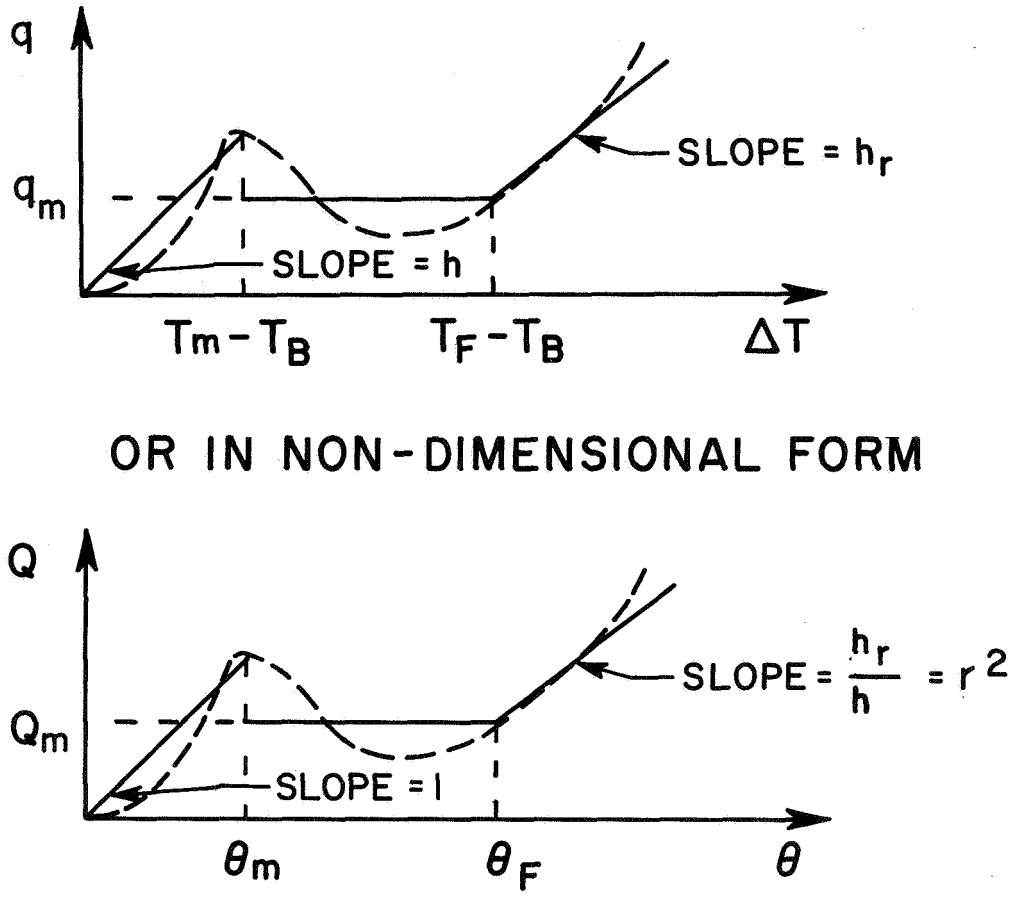

Fig. III-9 Second nonlinear model for the heat transfer characteristic of liquid helium.

previously will be called the first nonlinear characteristic. We have introduced some new parameters which are:

T_f = the temperature at which the heat transfer characteristic begins to rise again.

h_f = Slope of the second rise in the heat transfer characteristic.

r^2 = $\frac{h_r}{h}$ = ratio of the second slope to the initial slope.

From the actual measured heat transfer characteristics we find that $T_f > T_c$ for Nb - Ti or Nb - Zr and that $r^2 < 1$. For comparison an actual heat transfer characteristic is also shown in Fig. III-9 as a dotted line.

In the following analysis we will again use the same reduced variables as in the previous treatments. The only new variables introduced are:

$$\theta_f = \frac{T_f - T_b}{T_{ch} - T_b}$$

$$r^2 = \frac{h_f}{h} \text{ (defined above)}$$

and ξ_f = length of normal region whose temperature is greater than T_f

Again we find the solution for the case $1 - \tau > \theta_m$. Thus, we have that $\theta_m < 1 - \tau < 1 < \theta_f$.

In Fig. III-10, the sequence of events as the heat input to the origin is increased from zero is shown.

The case in Fig. III-10 that remains unsolved is that shown in III-10e. The solution follows. Note we have changed slightly the definitions of some of the lengths involved.

The equations for the non-dimensional temperature that need to be solved are:

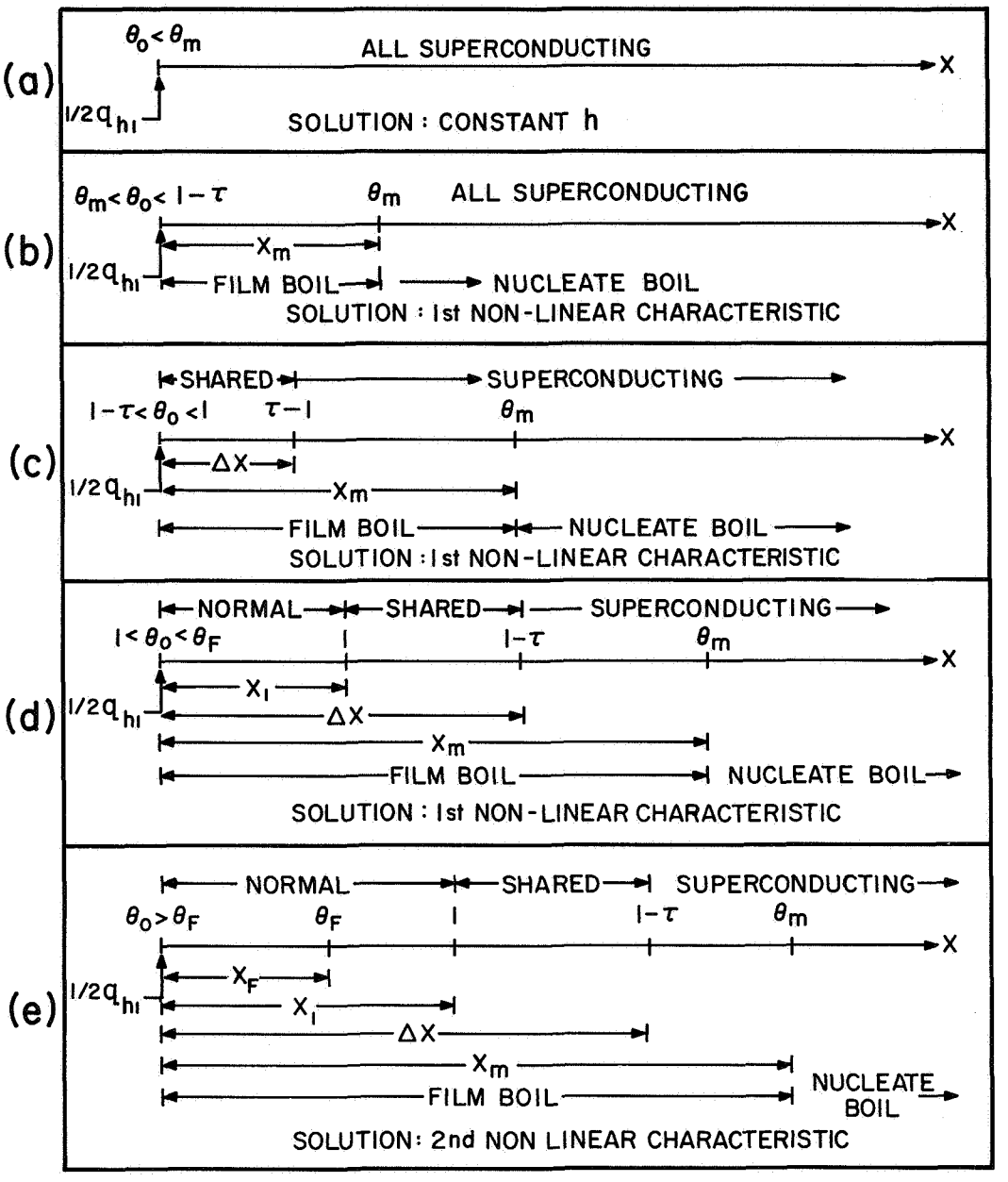

Fig. III-10a Conductor cooled entirely by nucleate boiling

b Conductor cooled partially by nucleate boiling and partially by film boiling

c Cooling after the onset of resistance but before all of the current transfers into the substrate at the origin

d Cooling when all the current is in the substrate at the origin but $\theta_0 < \theta_f$

e Cooling when $\theta_0 > \theta_f$

Region	Sharing Condition	Equation
$0 < \xi < \xi_f$	$f = 1$	$\frac{d^2\theta}{d\xi^2} + \alpha\tau^2 - r^2(\theta - \theta_f) - Q_m = 0$ (III-49)
$\xi_f < \xi < \xi_1$	$f = 1$	$\frac{d^2\theta}{d\xi^2} - Q_m + \alpha\tau^2 = 0$ (III-50)
$\xi_1 < \xi < \Delta\xi$	$0 < f < 1$	$\frac{d^2\theta}{d\xi^2} - Q_m + \alpha\tau(\tau - 1 + \theta) = 0$ (III-51)
$\Delta\xi < \xi < \xi_m$	$f = 0$	$\frac{d^2\theta}{d\xi^2} - Q_m = 0$ (III-52)
$\xi > \xi_m$	$f = 0$	$\frac{d^2\theta}{d\xi^2} - \theta = 0$ (III-53)

The solutions to these equations are:

$0 < \xi < \xi_f$, $\theta = C_1 \sinh r\xi + C_2 \cosh r\xi + \frac{\alpha\tau^2 - Q_m + r^2\theta_f}{r^2}$ (III-54)

$\xi_f < \xi < \xi_1$, $\theta = 1/2\ (Q_m - \alpha\tau^2)\xi^2 + C_3\xi + C_4$ (III-55)

$\xi_1 < \xi < \Delta\xi$, $\theta = C_5 \sin\sqrt{\alpha\tau}\ \xi + C_6 \cos\sqrt{\alpha\tau}\ \xi + \frac{Q_m}{\alpha\tau} + 1 - \tau$ (III-56)

$\Delta\xi < \xi < \xi_m$, $\theta = 1/2\ Q_m \xi^2 + C_7\xi + C_8$ (III-57)

$\xi > \xi_m$, $\theta = C_9 e^{-\xi} + C_{10} e^{\xi}$ (III-58)

Again the boundary conditions are:

(1) $\theta \to 0$ as $\xi \to \infty$

(2) $\left.\frac{d\theta}{d\xi}\right|_{\xi = 0} = -Q_{h\,1}$

(3) θ and $\frac{d\theta}{d\xi}$ are continuous at $\xi = \xi_f,\ \xi_1,\ \Delta\xi,\ \xi_m$.

These conditions are sufficient to determine all the constants in the solutions and the lengths ξ_f, ξ_1, $\Delta\xi$, and ξ_m.

The constants determined from the boundary conditions are:

$$C_1 = -\frac{Q_{h1}}{r}$$

$$C_2 = \frac{\frac{Q_{h1}}{r} \sinh r\,\xi_f + \frac{Q_m - a\tau^2}{r^2}}{\cosh r\,\xi_f}$$

$$C_3 = -\sqrt{{}^2_m + 2\,Q_m\,(1 - \theta_m) - a\tau^3} + (a\tau^2 - Q_m)\,\xi_1$$

$$C_4 = 1 + 1/2\,(Q_m - a\tau^2)\,\xi_1^2 + \sqrt{\theta_m^2 + 2\,Q_m\,(1 - \theta_m) - a\tau^3}\,\xi_1$$

$$C_5 = -\frac{Q_m}{a\tau} \sin\sqrt{a\tau}\,\Delta\xi - \frac{Q_m}{\sqrt{a\tau}} \sqrt{\frac{\theta_m^2}{Q_m^2} + \frac{2}{Q_m}(1 - \tau - \theta_m)} \cos\sqrt{a\tau}\,\Delta\xi$$

$$C_6 = \frac{Q_m}{\sqrt{a\tau}} \sqrt{\frac{\theta_m^2}{Q_m^2} + \frac{2}{Q_m}(1 - \tau - \theta_m)} \sin\sqrt{a\tau}\,\Delta\xi - \frac{Q_m}{a\tau} \cos\sqrt{a\tau}\,\Delta\xi$$

$$C_7 = -(\theta_m + Q_m\,\xi_m)$$

$$C_8 = (\theta_m + Q_m\,\xi_m)\,\xi_m - 1/2\,Q_m\,\xi_m^2 + \theta_m$$

$$C_9 = \theta_m\,e^{\xi_m}$$

$$C_{10} = 0$$

The lengths ξ_f, ξ_1, $\Delta\xi$, ξ_m are determined using the following equations:

$$\xi_m - \Delta\xi = -\frac{\theta_m}{Q_m} + \sqrt{\frac{\theta_m^2}{Q_m^2} + \frac{2}{Q_m}(1 - \tau - \theta_m)} \qquad \text{(III-59)}$$

$$\tau - \frac{Q_m}{\alpha\tau} = \frac{Q_m}{\sqrt{\alpha\tau}}\sqrt{\frac{\theta_m^2}{Q_m^2} + \frac{2}{Q_m}(1 - \tau - \theta_m)}\sin\sqrt{\alpha\tau}\,(\Delta\xi - \xi_1)$$

$$- \frac{Q_m}{\alpha\tau}\cos\sqrt{\alpha\tau}\,(\Delta\xi - \xi_1) \qquad \text{(III-60)}$$

$$\xi_1 - \xi_f = -\frac{\sqrt{\theta_m^2 + 2Q_m(1 - \theta_m) - \alpha\tau^3}}{Q_m - \alpha\tau^2}$$

$$+ \sqrt{\frac{\theta_m^2 + 2Q_m(\theta_f - \theta_m) - 2\alpha\tau^2(\theta_f - 1) - \alpha\tau^3}{(Q_m - \alpha\tau^2)^2}} \qquad \text{(III-61)}$$

$$Q_{h1}\cosh r\,\xi_f - \left(\frac{Q_{h1}}{r}\sinh r\,\xi_f + \frac{Q_m - \alpha\tau^2}{r^2}\right) r\tanh r\xi_f =$$

$$\sqrt{\theta_m^2 + 2Q_m(\theta_f - \theta_m) - 2\alpha\tau^2(\theta_f - 1) - \alpha\tau^3} \qquad \text{(III-62)}$$

Note that Eqs. (III-59), (III-60) are identical in form with (III-44) and (III-45) of this same report. Everything previously said about Eqs. (III-44) and (III-45) applies here also. The length $(\xi_1 - \xi_f)$ given by Eq. (III-61) does not depend on the heat input Q_{h1}. Only the length ξ_f depends on Q_{h1}. Equation (III-62) has a real solution only if the quantity under the radical is greater than zero. Thus the parameters must satisfy the condition:

$$\theta_m^2 + 2Q_m(\theta_f - \theta_m) - 2\alpha\tau^2(\theta_f - 1) - \alpha\tau^3 \geq 0 \qquad \text{(III-63)}$$

This condition is always satisfied if $Q_m > \alpha\tau^2$, and is satisfied if $\alpha\tau^2$ is not too much greater than Q_m.

If either Eq. (III-48) or (III-63) are not satisfied, then at take-off normal region grows to infinity. Assuming that both Eqs. (III-47) and (III-63) are satisfied, we must have for stability, as before:

$$\frac{dQ_{h1}}{d\xi_f} > 0 \text{ but finite}$$

From Eq. (III-62) we find:

$$\frac{dQ_{h\,1}}{d\xi_f} = \frac{Q_m - \alpha\tau^2 + r\,Q_{h\,1}\sinh r\,\xi_f}{\cosh r\,\xi_f} \qquad \text{(III-64)}$$

Using Eq. (III-60) again to eliminate $Q_{h\,1}$ from Eq. (III-62):

$$\frac{dQ_{h\,1}}{d\xi_f} = (Q_m - \alpha\tau^2)\cosh r\,\xi_f + r\sqrt{\theta_m^2 + 2Q_m(\theta_f - \theta_m) - 2\alpha\tau^2(\theta_f - 1) - \alpha\tau^3}\,\sinh r\,\xi_f \qquad \text{(III-65)}$$

In order to understand the behavior of the conductor, it is helpful to plot $Q_{h\,1}$ vs ξ_f as in Fig. III-11. The heat input at the origin when $\xi_f = 0$ is determined from Eq. (III-60) to be:

$$Q_{h\,1}(\xi_f = 0) = \sqrt{\theta_m^2 + 2Q_m(\theta_f - \theta_m) - 2\alpha\tau^2(\theta_f - 1) - \alpha\tau^3} \qquad \text{(III-66)}$$

which decreases for increasing τ. If $Q_m > \alpha\tau^2$, $\frac{dQ_{h\,1}}{d\xi_f} > 0$ for all ξ_f and the operation is stable (curve #1 - Fig. III-11). If $Q_m < \alpha\tau^2$, there are two modes of behavior:

1) $\alpha\tau^2$ not much larger than Q_m (see curve #3 - Fig. III-11) the slope $\frac{dQ_{h\,1}}{d\xi_f}$ is negative at $\xi_f = 0$, but the curve reaches a minimum and from then on the slope is positive. This change in slope must occur at a point where $Q_{h1} > 0$ (see Eq. (III-64)).

2) $\frac{dQ_{h\,1}}{d\xi_f} < 0$ always (curve #4 - Fig. III-11)

From Eq. (III-65) we see that the plot may have minimum (if $Q_m < \alpha\tau^2$) but never has a maximum for finite ξ_f. Thus take-off never occurs in this region because take-off occurs at a maximum (recovery occurs at a minimum). We have shown, then, that the conductor may only take-off when in the state shown in Fig. III-10c, and if $\alpha\tau^2 > Q_m$. Thus, if $Q_m > \alpha\tau^2$, the conductor voltage vs heater power is continuous and reversible for all values of heat input at the origin.

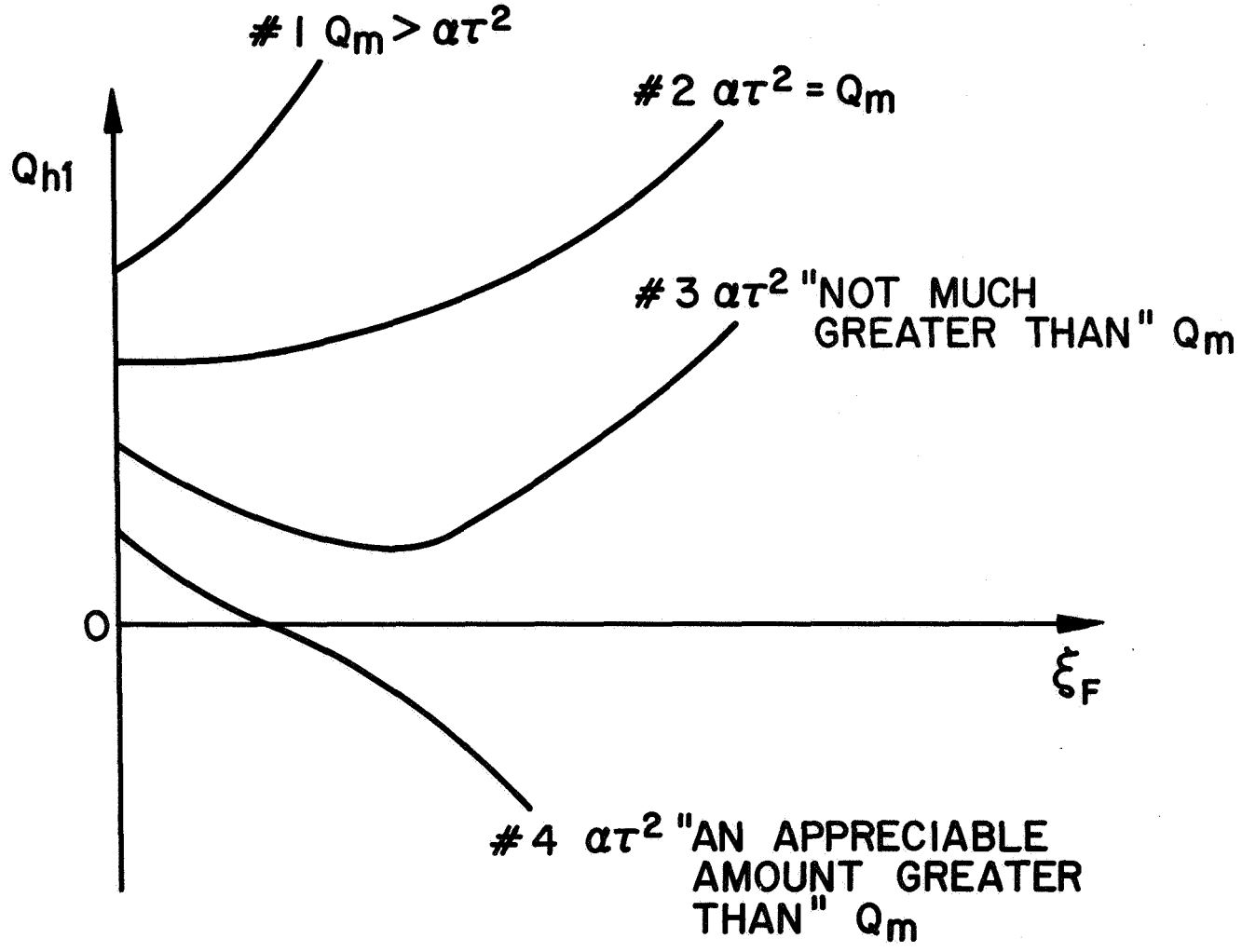

Fig. III-11 A schematic of the behavior of the reduced heat input at the origin Q_{h1}, vs the reduced length ξ_f at constant α and Q_m for different τ

It is easy to show that the heat input at take-off

$$Q_{h\,1\,T} > Q_{h\,1}(\xi_f = 0) \text{ if } \alpha\tau^2 > Q_m, \text{ where } Q_{h\,1\,T}$$

is given in Eq. (III-48). At take-off, if $\alpha\tau^2$ is not much larger than Q_m (curve #3 - Fig. III-11) the normal region will grow spontaneously until ξ_f is large enough so that $Q_{h\,1\,T} = Q_{h\,1}(\xi_f)$. A further increase in heat input results in a controllable voltage increase. If the heat input is reduced, recovery will occur at the minimum in the Q_{h1} vs ξ_f curve. The situation described above is called hysteresis, and the range of τ for which this occurs is called the hysteresis region.

If τ is such that the situation shown by curve #4 - Fig. III-11 exists, or if Eq. (III-47) or (III-63) is not satisfied, the wire will "quench" (develop an infinite voltage) at take-off. A schematic of typical V-Q plots (conductor voltage vs heat input) for the same α and different τ is shown in Fig. III-12.

The hysteresis region is determined using the fact that $\frac{dQ_{h\,1}}{d\,\xi_f}$ goes to zero only in this region. The slope is zero when (from Eq. (III-65)

$$\tanh r\,\xi_f = \frac{\alpha\tau^2 - Q_m}{r\sqrt{\theta_m^2 + 2Q_m(\theta_f - \theta_m) - 2\alpha\tau^2(\theta_f - 1) - \alpha\tau^3}} \quad \text{(III-67)}$$

For a solution to Eq. (III-67) to exist with $\xi_f > 0$ we must have:

$$\alpha\tau^2 \geq Q_m$$

and

$$\frac{\alpha\tau^2 - Q_m}{r\sqrt{\theta_m^2 + 2Q_m(\theta_f - \theta_m) - 2\alpha\tau^2(\theta_f - 1) - \alpha\tau^3}} \leq 1$$

thus the region of hysteresis is defined by:

$$Q_m < \alpha\tau^2 < Q_m + r\sqrt{\theta_m^2 + 2Q_m(\theta_f - \theta_m) - 2\alpha\tau^2(\theta_f - 1) - \alpha\tau^3} \quad \text{(III-68)}$$

The last detail of the V-Q plot to be determined is the slope $\frac{dV}{dQ_{h\,1}}$ at the onset of voltage (resistance). This may be determined using the analysis

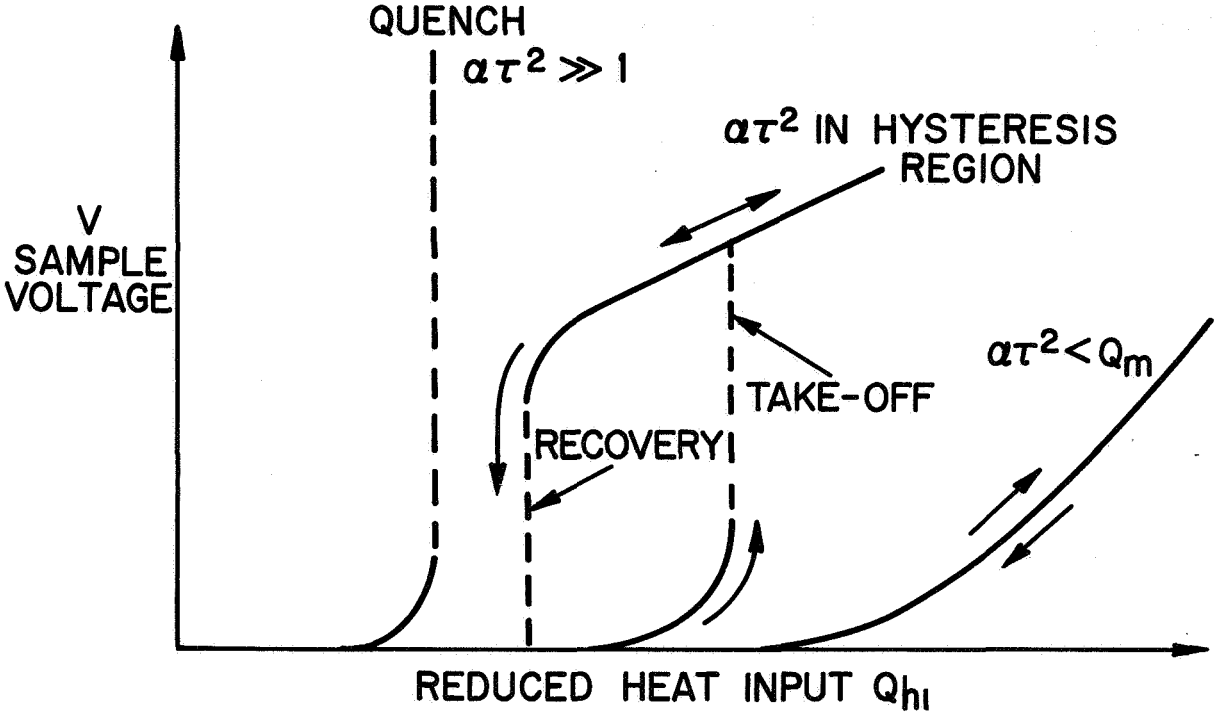

Fig. III-12 Types of V-Q plots expected for a one dimensional composite superconductor at constant applied magnetic fields for different τ

presented in the previous treatment since at the onset of resistance $\theta_0 = 1 - \tau < 1$. The voltage per unit length in the shared state is:

$$v = \frac{\rho I}{A} f = \frac{\rho I_c}{A} (\tau - 1 + \theta) \qquad \text{(III-69)}$$

Since we wish to find the solution as $\Delta\xi \to 0$ we have the lowest order in ξ and $\Delta\xi$ from Eq. (III-61)

$$\theta \simeq Q_{h\,1}(\Delta\xi - \xi) + 1 - \tau \qquad \text{(III-70)}$$

The total voltage across the conductor is:

$$V = 2\int_0^{\Delta x} v\, dx = 2\, x_o \int_0^{\Delta\xi} v\, d\xi \qquad \text{(III-71)}$$

Using Eqs. (III-69) and (III-70), Eq. (III-71) becomes:

$$V = \frac{\rho I_c\, x_o}{A} Q_{h\,1} \Delta\xi^2 \qquad \text{(III-72)}$$

At the onset of resistance $Q_{h\,1} = Q_{h\,1}\big|_{or}$ and $\Delta\xi = 0$. Thus the slope $\frac{dV}{dQ_{h\,1}}$, obtained from Eq. (III-72) is:

$$\frac{dV}{dQ_{h\,1}}\Big]_{Q_{h1}\big|or} = \frac{\rho I_c\, x_o}{A}\left[\Delta\xi^2 + 2Q_{h\,1}\Delta\xi \frac{d\Delta\xi}{dQ_{h\,1}}\right]$$

But, $d\Delta\xi/dQ_{h\,1}$ is finite at this point and we have:

$$\left.\frac{dV}{dQ_{h\,1}}\right|_{Q_{h1}\big|or} = 0 \qquad \text{(III-73)}$$

The slope $\frac{dV}{dQ_{h\,1}}$ is always zero at the onset of resistance.

Recapitulating the results for the one dimensional model, with our assumption that $\theta_m \le 1 - \tau \le 1 \le \theta_f$, we have found the heater characteristics to be:

1) the onset of resistance (or voltage) occurs at a heat input of

$$Q_{h\,1}\big|_{or} = \sqrt{\theta_m\left[2(1 - \tau) - \theta_m\right]}$$

2) the slope $\frac{dV}{dQ_{h\,1}}$ at the onset is zero.

3) If $Q_m > \alpha\tau^2$, increasing the heat input from $Q_{h\,1}\big|_{or}$ causes a controllable and reversible increase in voltage across the conductor.

4) If $Q_m < \alpha\tau^2 < Q_m + r\sqrt{\theta_m^2 + 2Q_m(\theta_f - \theta_m) - 2\alpha\tau^2(\theta_f - 1) - \alpha\tau^3}$ (hysteresis region),

Increasing the heat input from $Q_{h\,1}\big|_{or}$ causes the voltage to increase. This increase is controllable and reversible up to a heat input of $Q_{h\,1\,T}$ (Eq. (III-48)) at which point $\frac{dV}{dQ_{h\,1}}$ has become infinite and the voltage increases spontaneously ("take-off") to some finite value. Just before take-off the reduced temperature at the origin $\theta_0 < 1$, thus at the origin the current is shared. Just after take-off $\theta_0 > \theta_f$, thus the region around the origin is completely normal.

If the heat input is increased beyond $Q_{h\,1\,T}$ no other take-off is produced, the voltage is again controllable and reversible. If the heat input is decreased from $Q_{h\,1\,T}$, the voltage decreases continuously until the heat reaches $Q_{h\,1\,R}$, at which point the voltage drops spontaneously ("Recovery") to a relatively small value or zero.

Recovery always occurs from a state such that $\theta_0 > \theta_f$ to a state such that $\theta_0 < 1$. According to this model, recovery always occurs before $Q_{h\,1\,R}$ is zero.

5) If $\alpha\tau^2 > Q_m + r\sqrt{\theta_m^2 + 2Q_m(\theta_f - \theta_m) - 2\alpha\tau^2(\theta_f - 1) - \alpha\tau^3}$ increasing the heat input from $Q_{h\,1\,or}$ causes the voltage to increase controllably and reversibly until the heat input reaches $Q_{h\,1\,T}$. At this value of heat input the slope $\frac{dV}{dQ_{h\,1}}$ is infinite and the voltage increases spontaneously to infinity ("quenches"). This region is called the unstable region. Just before take-off $\theta_0 < 1$ so the current is shared at the origin. Note, however, that a "precursor" (a controllable voltage) always appears before the quench.

Typical values of the parameters θ_m, Q_m, θ_f, and r depend upon the applied magnetic field and on the preparation and orientation of the conductor

surface. In a superconducting magnet the range of values of these parameters is approximately:

$$.05 < \theta_m < .4$$

$$.05 < Q_m < .3$$

$$.5 < \theta_f < 5$$

$$.1 < r < .3$$

The solutions for the cases $\theta_m > 1 - \tau$ or $\theta_f < 1$ have not been worked out. The solutions, however, ought to contain the same type of behavior as the case we have considered. Some of the equations obtained will of course change; for example, the size of the hysteresis region will be different than that obtained if $\theta_f < 1$.

It is interesting to note that the constant h analysis also predicts the same kinds of behavior as that obtained from the modified nonlinear heat transfer characteristic. However, numerical values obtained by the constant h analysis are much different than those obtained using the latter model. It is shown in the experimental section of this report the modified nonlinear model predicts correctly pertinent experimental quantities.

IV. THREE-DIMENSIONAL STEADY STATE STABILITY

A. Introduction

It may be expected that the effects exhibited by a multi-dimensional treatment of the stabilization problem would be qualitatively similar to those which are indicated by the zero and one-dimensional analyses. However, when attempting to obtain experimental correlation, it is well to have an indication of any changes in the stability criterion which may occur as a result of the actual three-dimensional nature of the heat transfer problem.

B. The Case of $\alpha \to \infty$ -- Conduction Cooled

This section deals with the limiting case where there is no cooling provided by helium within the coil. A point heat source is assumed at the origin. This injection of a finite amount of heat requires an infinite temperature gradient at the origin and leads to a condition where only a three-region solution is possible:

1) A region $0 \leq \zeta \leq \zeta_o$ in which all the current flows in the substrate,

2) A region $\zeta_o \leq \zeta \leq \zeta_1$ in which the current is shared, and

3) A region $\zeta > \zeta_1$ where all the current flows in the superconductor.

In its three-dimensional form the heat conduction equation is:

$$0 = W_i + \frac{k}{r^2} \frac{\partial}{\partial r} \left(r^2 \frac{\partial T}{\partial r} \right) \qquad \text{(IV-1)}$$

We now specify the ohmic dissipation per unit volume to be

$$W_i = \lambda \frac{\rho f I^2}{A^2} \qquad \text{(IV-2)}$$

where

$\frac{\rho f I}{A}$ = voltage per unit length

λ = $\frac{\text{wire volume}}{\text{total volume}}$

λ thus allows for the packing factor or any volume not producing heat (e.g., insulation). If we now use Eq. (IV-1) and

$$\theta = \frac{T - T_b}{T_{ch} - T_b} \tag{IV-3}$$

$$\tau = \frac{I}{I_{ch}} \tag{IV-4}$$

$$\zeta = \frac{r}{r_o} \tag{IV-5}$$

$$r_o^2 = \frac{kA^2 (T_{ch} - T_b)}{\lambda \rho I_{ch}^2} \tag{IV-6}$$

then the governing equation in region 1 where f = 1, may be shown to be

$$\frac{1}{\zeta^2} \frac{\partial}{\partial \zeta} \left(\zeta^2 \frac{\partial \theta_1}{\partial \zeta}\right) + \tau^2 = 0, \quad 0 < \zeta < \zeta_o \tag{IV-7}$$

In region 2 ($0 < f < 1$) the current is shared and the situation is governed by

$$\frac{1}{\zeta^2} \frac{\partial}{\partial \zeta} \left(\zeta^2 \frac{\partial \theta_2}{\partial \zeta}\right) + \tau \theta_2 - \tau (1 - \tau) = 0, \quad \zeta_o < \zeta < \zeta_1 \tag{IV-8}$$

The proper equation for region 3 (f = 0), in which all the current is in the superconductor, is

$$\frac{1}{\zeta^2} \frac{\partial}{\partial \zeta} \left(\zeta^2 \frac{\partial \theta_3}{\partial \zeta}\right) = 0, \quad \zeta > \zeta_1 \tag{IV-9}$$

The boundary conditions for this configuration which are found by matching points and slopes at the boundaries to each region, are:

$$\theta_3 \to 0 \quad \text{as} \quad \zeta \to \infty \tag{IV-10}$$

$$\theta_2 = \theta_3 = (1 - \tau) \quad \text{and} \quad \frac{d\theta_2}{d\zeta} = \frac{d\theta_3}{d\zeta} \quad \text{at} \quad \zeta = \zeta_1 \tag{IV-11}$$

$$\theta_1 = \theta_2 = 1 \quad \text{and} \quad \frac{d\theta_1}{d\zeta} = \frac{d\theta_2}{d\zeta} \quad \text{at} \quad \zeta = \zeta_o \tag{IV-12}$$

$$\zeta^2 \frac{d\theta_1}{d\zeta} \rightarrow -Q'_{h3} \equiv -\frac{q_{h3}}{4\pi k r_o (T_{ch} - T_b)} \text{ as } \zeta \rightarrow 0 \quad \text{(IV-13)}$$

It may be shown that the solutions to these three differential Eqs. (IV-7) through (IV-9), subject to the given boundary conditions, are

$$\theta_1 = \frac{\tau^2}{6}(\zeta_o^2 - \zeta^2) - Q'_{h3}\left(\frac{1}{\zeta_o} - \frac{1}{\zeta}\right) + 1 \quad \text{(IV-14)}$$

$$\theta_2 = \zeta^{-1}\left[C \sin(\sqrt{\tau}\,\zeta) + D \cos(\sqrt{\tau}\,\zeta)\right] + (1 - \tau) \quad \text{(IV-15)}$$

$$\theta_3 = (1 - \tau)\,\zeta_1\,\zeta^{-1} \quad \text{(IV-16)}$$

where:

$$C = -\frac{(1 - \tau)}{\sqrt{\tau}} \cos(\sqrt{\tau}\,\zeta_1)$$

$$D = \frac{(1 - \tau)}{\sqrt{\tau}} \sin(\sqrt{\tau}\,\zeta_1)$$

The lengths ζ_1 and ζ_o are determined by substituting the boundary conditions on θ into Eqs. (IV-14) through (IV-16)

$$\sin\left[\sqrt{\tau}(\zeta_1 - \zeta_o)\right] = \frac{\zeta_o \tau^{3/2}}{1 - \tau} \quad \text{(IV-17)}$$

and

$$\cos\left[\sqrt{\tau}(\zeta_1 - \zeta_o)\right] = -(1 - \tau)^{-1}\left[\tau - \frac{(\zeta_o \tau)^2}{3} - \frac{Q'_{h3}}{\zeta_o}\right] \quad \text{(IV-18)}$$

Equations (IV-17) and (IV-18) may be manipulated, to show that

$$Q'_{h3} = \zeta_o\left[\tau - \frac{(\zeta_o \tau)^2}{3} \pm \sqrt{(1 - \tau)^2 - \zeta_o^2\,\tau^3}\right] \quad \text{(IV-19)}$$

The condition for which $\frac{\partial V}{\partial Q'_{h3}} \rightarrow \infty$ is of particular interest since it represents instability. V is closely related to ζ_o, however, so that it is only necessary to determine the "take-off" heat Q_{h3T} or "take-off", length, ζ_{oT}, for which $\frac{\partial \zeta_o}{\partial Q'_{h3}} \rightarrow \infty$. By equating $\partial Q'_{h3} / \partial \zeta_o$ to zero, ζ_{oT} may be found to be given by:

$$\zeta_{oT}^6 + (\tau^2 + 2\tau - 1)\tau^{-3} \zeta_{oT}^4 - (\tau^2 - 4\tau + 2)\tau^{-4} \zeta_{oT}^2 + (1-\tau)^2 (1-2\tau)\tau^{-7} = 0 \qquad \text{(IV-20)}$$

Equation (IV-20) may now be used together with Eq. (IV-19) to find $Q'_{h3T} = Q'_{h3T}(\tau)$, which is plotted in Fig. IV-1. A process of curve fitting may then be used to show that the curve is closely approximated by

$$Q'_{h3T} \approx (0.72) \frac{(1-\tau)^{0.88}}{\tau^{0.97}} \qquad \text{(IV-21)}$$

in the range of interest. For constant current operation, Q'_{h3} may be increased up to the value of Q'_{h3T} indicated by the intersection of the line of operation with the Q'_{h3T} curve. At that time $\zeta_o \rightarrow \infty$ and, in turn, $V \rightarrow \infty$. This behavior is illustrated in Fig. IV-2 which is a plot of Eq. (IV-19) for selected values of τ. Operation on the dashed portion of the curves is not possible. Note that ζ_o remains finite as $\tau \rightarrow 0$. This results from the boundary condition at the origin which requires an infinite temperature gradient to "drive" a finite Q'_{h3}.

C. The Case of Arbitrary α

A study has been initiated concerning a configuration similar to that in the previous section with the important difference that the convection of heat to helium is retained. We, therefore, begin by writing

$$0 = W_i + \frac{k}{r^2} \frac{\partial}{\partial r} \left(r^2 \frac{\partial T}{\partial r}\right) - \frac{h}{P'} (T - T_b) \qquad \text{(IV-22)}$$

where P' is a characteristic length related to the cooling by the helium within the winding. It is the ratio of the coil volume to the internal heat transfer surface area. Using Eqs. (IV-2), (IV-3), (IV-4), and the definition of f, together with

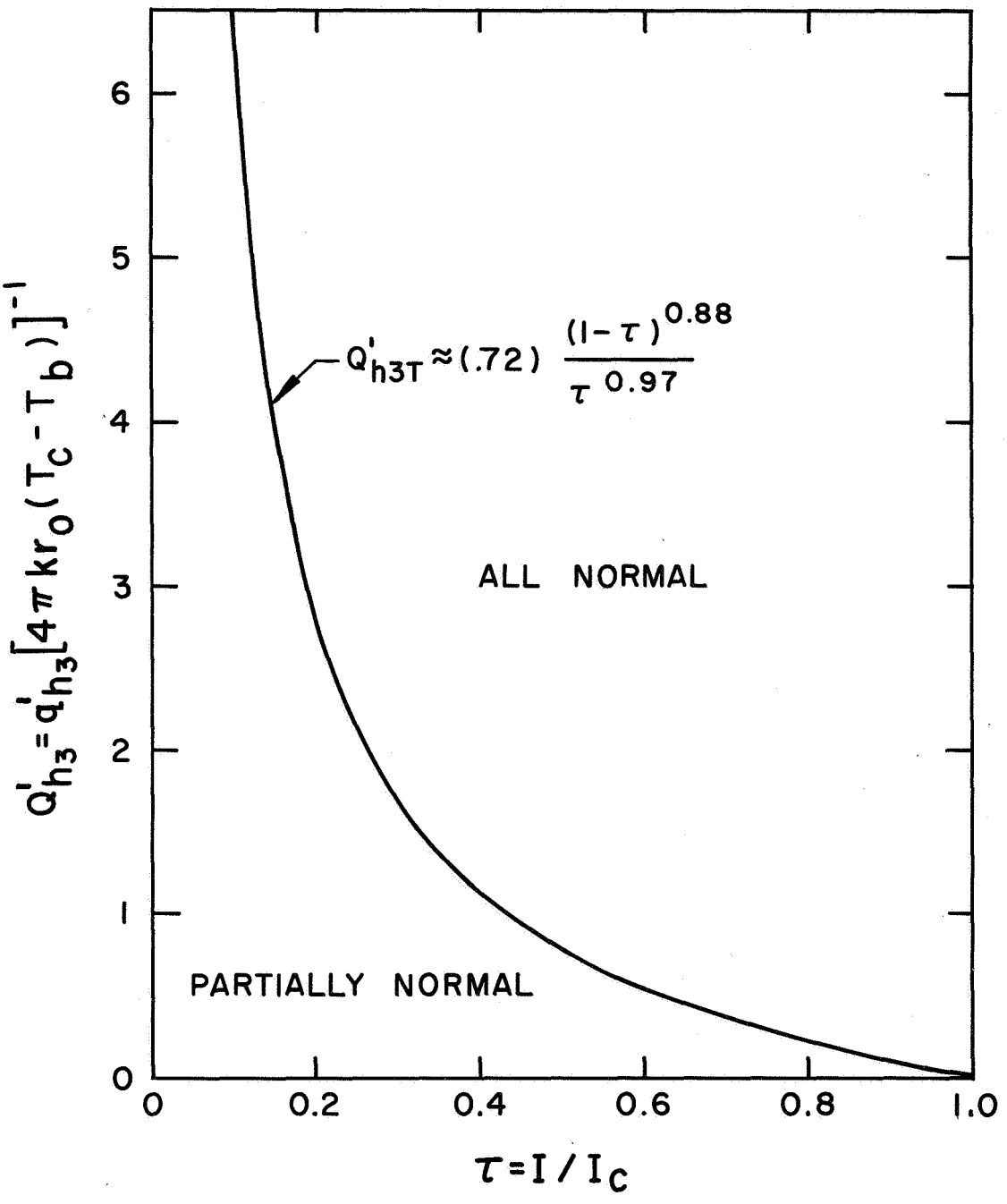

Fig. IV-1 Heat input as a function of current; Q_{h3T} is that value of Q_{h3} at which quench occurs.

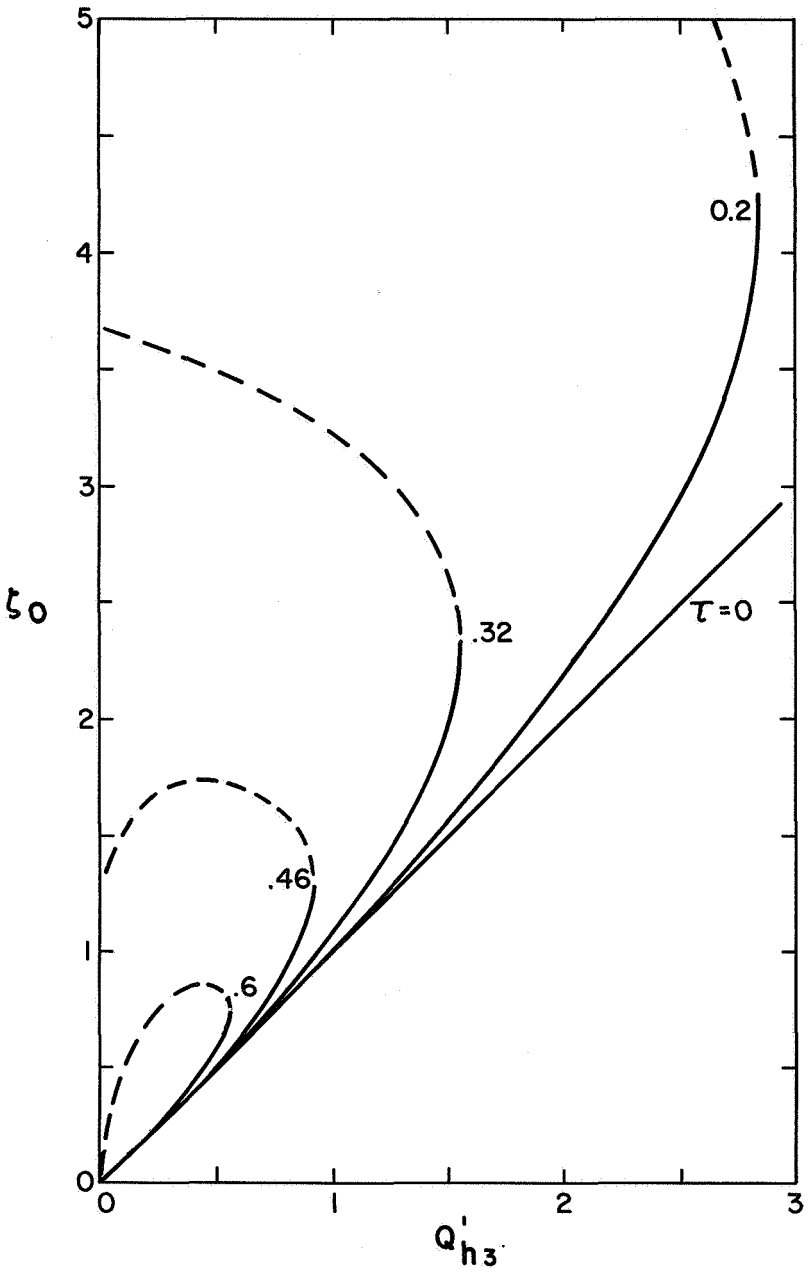

Fig. IV-2 Dimensionless radius over which the coil is normal versus heat input at the origin. Quench occurs when $\partial \zeta_0 / \partial Q'_{h3} \rightarrow \infty$.

$$\zeta = \frac{r}{r_o}$$

$$\alpha = \frac{\lambda \rho \, I_{ch}^2 \, P'}{h \, A^2 \, (T_{ch} - T_b)} ,$$

and

$$r_o^2 = \frac{k x_o}{h} ,$$

it may be shown that the governing equation for:

1) The region where all the current is carried by the substrate (f = 1) is:

$$\frac{1}{\zeta^2} \frac{\partial}{\partial \zeta} \left(\zeta^2 \frac{\partial \theta_1}{\partial \zeta} \right) - \theta_1 + \alpha \tau^2 = 0, \quad 0 < \zeta < \zeta_o \qquad \text{(IV-23)}$$

2) The region where current is shared ($0 < f < 1$) is

$$\frac{1}{\zeta^2} \frac{\partial}{\partial \zeta} \left(\zeta^2 \frac{\partial \theta_2}{\partial \zeta} \right) - \theta_2 (1 - \alpha \tau) - \alpha \tau (1 - \tau) = 0, \quad \zeta_o < \zeta < \zeta_1 \qquad \text{(IV-24)}$$

3) The region where all the current is in the superconductor (f = 0) is

$$\frac{1}{\zeta^2} \frac{\partial}{\partial \zeta} \left(\zeta^2 \frac{\partial \theta_3}{\partial \zeta} \right) - \theta_3 = 0, \quad \zeta > \zeta_1 \qquad \text{(IV-25)}$$

The boundary conditions are Eqs. (IV-10), (IV-11), (IV-12) and

$$\zeta^2 \left(\frac{d \theta_1}{d \zeta} \right) \rightarrow - Q_{h3} \equiv - \frac{q_{h3}}{4 \pi k r_o (T_c - T_b)} \quad \text{as } \zeta \rightarrow 0 \qquad \text{(IV-26)}$$

It may be shown that the solution to the three differential equations subject to the stated boundary conditions is:

$$\theta_1 = (\zeta \sinh \zeta_o)^{-1} \left[Q_{h3} \sinh (\zeta_o - \zeta) + \zeta_o (1 - \alpha \tau^2) \sinh \zeta \right] + \alpha \tau^2 \qquad \text{(IV-27)}$$

$$\theta_2 = \zeta^{-1}\left[C_1 \sin\left(\sqrt{\alpha\tau - 1}\,\zeta\right) + C_2 \cos\left(\sqrt{\alpha\tau - 1}\,\zeta\right)\right] - \frac{\alpha\tau(1-\tau)}{1-\alpha\tau}, \quad \text{for } \alpha\tau > 1$$

(IV-28)

$$\theta_2 = \zeta^{-1}\left[C_3 \sinh\left(\sqrt{1-\alpha\tau}\,\zeta\right) + C_4 \cosh\left(\sqrt{1-\alpha\tau}\,\zeta\right)\right] - \frac{\alpha\tau(1-\tau)}{(1-\alpha\tau)} \text{ for } \alpha\tau < 1$$

(IV-29)

$$\theta_3 = (1-\tau)\,\zeta^{-1}\,\zeta_1\,\, e^{(\xi_1 - \xi)} \qquad \text{(IV-30)}$$

where:

$$C_1 = \frac{\zeta_1(1-\tau)}{1-\alpha\tau}\sin\left(\sqrt{\alpha\tau - 1}\,\zeta_1\right) + \frac{(1-\tau)}{\sqrt{\alpha\tau - 1}}\left[\frac{\alpha\tau}{1-\alpha\tau} - \zeta_1\right]\cos\left(\sqrt{\alpha\tau - 1}\,\zeta_1\right)$$

(IV-31)

$$C_2 = \frac{\zeta_1(1-\tau)}{1-\alpha\tau}\cos\left(\sqrt{\alpha\tau - 1}\,\zeta_1\right) - \frac{(1-\tau)}{\sqrt{\alpha\tau - 1}}\left[\frac{\alpha\tau}{1-\alpha\tau} - \zeta_1\right]\sin\left(\sqrt{\alpha\tau - 1}\,\zeta_1\right)$$

(IV-32)

$$C_3 = -\frac{\zeta_1(1-\tau)}{1-\alpha\tau}\sinh\left(\sqrt{1-\alpha\tau}\,\zeta_1\right) + \frac{(1-\tau)}{\sqrt{1-\alpha\tau}}\left[\frac{\alpha\tau}{1-\alpha\tau} - \zeta_1\right]\cosh\left(\sqrt{1-\alpha\tau}\,\zeta_1\right)$$

(IV-33)

$$C_4 = \frac{\zeta_1(1-\tau)}{(1-\alpha\tau)}\cosh\left(\sqrt{1-\alpha\tau}\,\zeta_1\right) - \frac{(1-\tau)}{\sqrt{1-\alpha\tau}}\left[\frac{\alpha\tau}{1-\alpha\tau} - \zeta_1\right]\sinh\left(\sqrt{1-\alpha\tau}\,\zeta_1\right)$$

(IV-34)

When $\alpha\tau > 1$, the lengths ζ_o and ζ_1 are determined by

$$\cos\left[\sqrt{\alpha\tau - 1}\,(\zeta_1 - \zeta_o)\right] - \frac{(1-\alpha\tau)}{\sqrt{\alpha\tau - 1}}\left[\frac{\alpha\tau}{\zeta_1(1-\alpha\tau)} - 1\right]\sin\left[\sqrt{\alpha\tau - 1}\,(\zeta_1 - \zeta_o)\right] = \frac{\zeta_o(1-\alpha\tau^2)}{\zeta_1(1-\tau)}$$

(IV-35)

and

$$\sin\left[\sqrt{\alpha\tau - 1}\,(\zeta_1 - \zeta_o)\right] + \frac{1 - \alpha\tau}{\sqrt{\alpha\tau - 1}}\left[\frac{\alpha\tau}{\zeta_1(1 - \alpha\tau)} - 1\right]\cos\left[\sqrt{\alpha\tau - 1}\,(\zeta_1 - \zeta_o)\right]$$

$$= \frac{\sqrt{\alpha\tau - 1}}{\zeta_1(1 - \tau)}\left[\frac{Q_{h3}}{\sinh\zeta_o} - (1 - \alpha\tau^2)(\cosh\zeta_o - 1) + \frac{1 - \alpha\tau^2}{\alpha\tau - 1}\right] \quad \text{(IV-36)}$$

When $\alpha\tau < 1$, the lengths $\zeta_o + \zeta_1$ are determined by

$$\zeta_1\,\frac{(1 - \tau)}{(1 - \alpha\tau)}\cosh\left[\sqrt{1 - \alpha\tau}\,(\zeta_1 - \zeta_o)\right] - \frac{(1 - \tau)}{\sqrt{1 - \alpha\tau}}\left[\frac{\alpha\tau}{1 - \alpha\tau} - \zeta_1\right]$$

$$\sinh\left[\sqrt{1 - \alpha\tau}\,(\zeta_1 - \zeta_o)\right] = \zeta_o\,\frac{(1 - \alpha\tau^2)}{(1 - \alpha\tau)} \quad \text{(IV-37)}$$

and

$$-\zeta_1\,\frac{(1 - \tau)}{(1 - \alpha\tau)}\sinh\left[\sqrt{1 - \alpha\tau}\,(\zeta_1 - \zeta_o)\right] + \frac{(1 - \tau)}{\sqrt{1 - \alpha\tau}}\left[\frac{\alpha\tau}{1 - \alpha\tau} - \frac{\alpha\tau}{1 - \alpha\tau} - \zeta_1\right]$$

$$\cosh\left[\sqrt{1 - \alpha\tau}\,(\zeta_1 - \zeta_o)\right] = (1 - \alpha\tau)^{-1/2}\left[-\frac{Q_{h3}}{\sinh\zeta_o} + (1 - \alpha\tau^2)(\coth\zeta_o - 1)\right.$$

$$\left. + \frac{(1 - \alpha\tau^2)}{1 - \alpha\tau}\right] \quad \text{(IV-38)}$$

It may now be shown that $\zeta_o \to \infty$ when $\alpha\tau^3 = 1$. This is done by using Eqs. (IV-35) and (IV-36) and using the trigonometric relationship $\sin^2 + \cos^2 = 1$. This will yield a relationship between the coefficients and arguments of Eqs. (IV-35) and (IV-36). The condition $\zeta_o \to \infty$ may now be applied resulting in a quadratic equation yielding the root $\alpha\tau^3 = 1$. This is analogous to the condition that $V \to \infty$ when $\alpha\tau^2 = (2 - \tau)$ in the one-dimensional situation. This implies that for α, τ such that $\alpha\tau^3 > 1$, quench will occur ($\zeta_o \to \infty$) when Q_{h3} approaches a take-off value. These conditions for Q_{h3T} have not been determined, and need to be investigated. Other conditions which are needed are those corresponding to the limits of stability and those indicating hysteretic performance.

V. TWO-DIMENSIONAL ANALYSIS OF THE CHARACTERISTICS OF A COMPOSITE SUPERCONDUCTOR INCLUDING THE EFFECTS OF ANISOTROPIC CONDUCTIVITY AND OF A NONLINEAR HEAT TRANSFER COEFFICIENT

This particular case is of interest when considering relatively large coil systems in which long lengths of conductor are subjected to essentially the same field and cooling environment, but where, because of constructional detail, the effective thermal conductivity is anisotropic in the plane perpendicular to the winding direction. The treatment here is incomplete since one and three dimensional effects have yielded more significant results.

The analysis will model the nonlinear heat transfer character of the bath in the manner utilized in the previous sections and illustrated in Fig. III-6. A general equation including all the terms in the energy equation will be developed at the outset then applied to different sections of the conductor with cancellation of appropriate terms. An additional external point heat source will be assumed to be located at the origin for the purpose of determining limits of stability. The combination of the two-dimensional geometry together with a point heat source immediately implies that a normal region will always exist about the source since an infinite temperature gradient and, in turn, a mathematically infinite source temperature, will be required to drive a finite amount of heat, q_{h2}.

With reference to Fig. V-1, the following steady state energy equation may be written.

$$-k_x \frac{\partial^2 T}{\partial x^2} dy\, dx - k_y \frac{\partial^2 T}{\partial y^2} dy\, dx + \frac{q_m}{P'} dx\, dy + \frac{h}{P'} (T - T_b)\, dx\, dy - W_i\, dx\, dy = 0 \qquad (V-1)$$

where:

k_x = effective thermal conductivity in the x - direction

k_y = effective thermal conductivity in the y - direction

q_m = maximum heat flux per unit area as indicated in Fig. III-6

P' = ratio of volume to internal heat transfer surface area

W_i = joule heating per unit volume

h = heat transfer coefficient

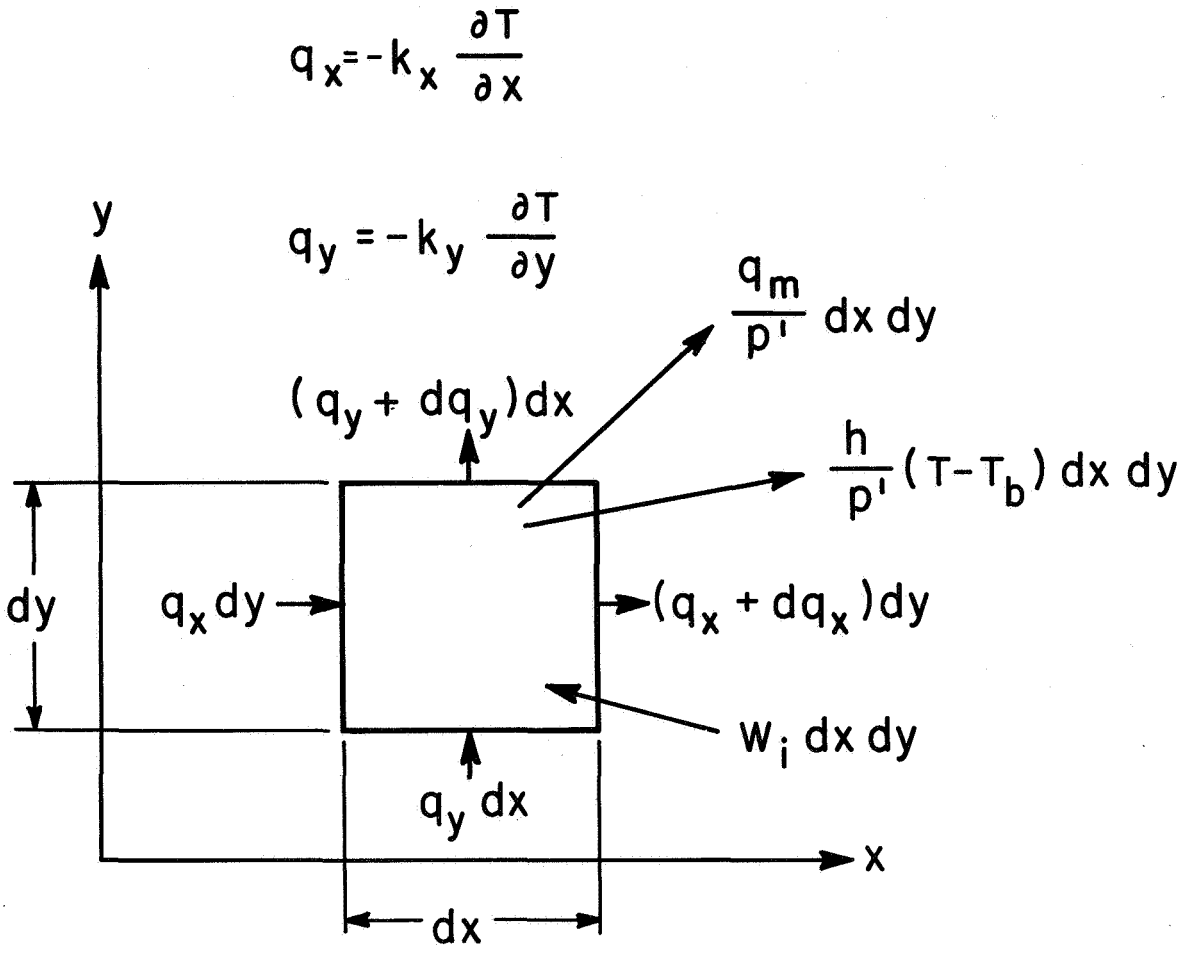

Fig. V-1 Energy balance for determining the general equation for the two-dimensional case with anisotropic conductivity and non-linear heat transfer coefficient

Define:

$$x'^2 = \frac{k}{k_x} x^2$$

$$y'^2 = \frac{k}{k_y} y^2$$

$$r^2 = x'^2 + y'^2$$

and assume $dxdy = dx' dy'$

then $k = \sqrt{k_x k_y}$

and Eq. (V-1) becomes

$$\frac{k}{r} \frac{\partial}{\partial r} \left(r \frac{\partial T}{\partial r}\right) - \frac{q_m}{P'} - \frac{h}{P'} (T - T_b) + W_i = 0 \qquad \text{(V-2)}$$

As in the previous section, let

$$W_i = \frac{\rho f I^2}{A^2}$$

where: ρ = resistivity of the substrate

f = fraction of the current carried by the substrate

I = total current carried by the conductor

A = cross-sectional area of the conductor

and

$$\frac{I_s}{I_c} = 1 - \frac{T - T_b}{T_c - T_b} = 1 - \theta$$

where: I_s = current carrying capacity of the superconductor at temperature T

I_c = critical current at the applied field and the bath temperature, T_b

T_c = critical temperature at the applied field and zero current

Also, let $\tau = I/I_c$

$$\xi = \frac{r}{r_o}$$

$$r_o^2 = \frac{kP'}{h}$$

$$Q_m = \frac{q_m}{h\,(T_c - T_b)}$$

$$\alpha = \frac{\rho\, I_c^2\, P'}{hA^2\,(T_c - T_b)}$$

then Eq. (V-2) becomes:

$$\frac{1}{\xi}\frac{\partial}{\partial \xi}\left(\xi \frac{\partial \theta}{\partial \xi}\right) - Q_m - \theta + \alpha\tau^2 \left[1 - \frac{1-\theta}{\tau}\right] = 0 \qquad \text{(V-3)}$$

The first term in Eq. (V-3) arises from the conduction of heat into the volume element; the second from cooling via a maximum heat flux corresponding to the transition from nucleate to film boiling; the third from cooling by nucleate boiling; the fourth from joule heating.

With reference to Fig. V-2, this equation may now be applied to the different regions of the superconductor.

for $0 < \xi < \xi_1$,

$$\frac{1}{\xi}\frac{\partial}{\partial \xi}\left(\xi \frac{\partial \theta_1}{\partial \xi}\right) - Q_m + \alpha\tau^2 = 0 \qquad \text{(V-4)}$$

for $\xi_1 < \xi < \xi_1 + \Delta\xi$

$$\frac{1}{\xi}\frac{\partial}{\partial \xi}\left(\xi \frac{\partial \theta_2}{\partial \xi}\right) + \alpha\tau\,\theta_2 - Q_m - \alpha\tau\,(1-\tau) = 0 \qquad \text{(V-5)}$$

for $\xi_1 + \Delta\xi < \xi < \xi_m$,

$$\frac{1}{\xi}\frac{\partial}{\partial \xi}\left(\xi \frac{\partial \theta_3}{\partial \xi}\right) - Q_m = 0 \qquad \text{(V-6)}$$

for $\xi_m < \xi$,

$$\frac{1}{\xi}\frac{\partial}{\partial \xi}\left(\xi \frac{\partial \theta_4}{\partial \xi}\right) - \theta_4 = 0 \qquad \text{(V-7)}$$

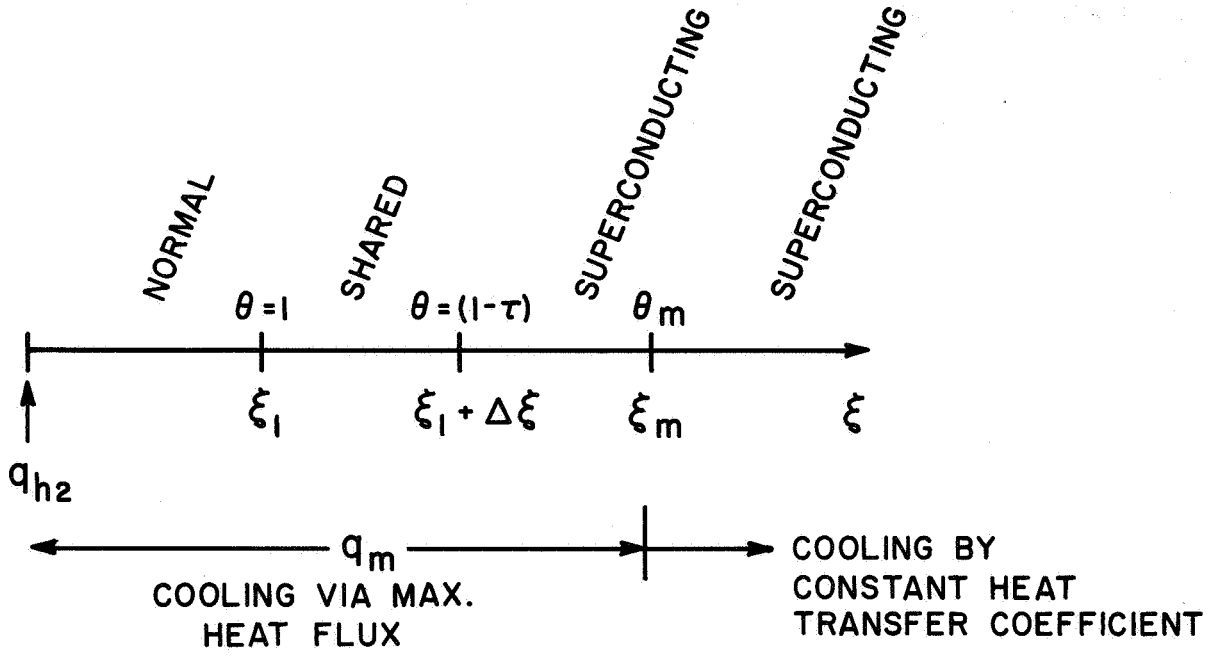

Fig. V-2 Regions denoting current distribution for the two-dimensional analysis

In region I, all the current flows in the substrate; in region II, the current is shared between the substrate and superconductor; in regions III and IV, all the current is carried by the superconductor. The temperature in regions I, II, and III is above, θ_m, the temperature corresponding to the transition from nucleate to film boiling; therefore, these regions are constrained by the model (Fig. III-6) to be cooled by a given heat flux per unit area. The temperature in region IV is below the transition temperature and is cooled via a constant heat transfer coefficient. A source of heat, q_{h2}, is located at the origin. The analysis is limited to cases where $\theta_m < (1 - \tau)$.

The boundary conditions are that:

$$\theta_4 \rightarrow 0 \text{ as } \xi \rightarrow \infty \tag{V-8}$$

$$\lim_{\xi \rightarrow 0} \xi \frac{d\theta_1}{d\xi} = - \frac{q_{h2}}{2\pi k (T_c - T_b)} \equiv - Q_{h2} \tag{V-9}$$

and that the temperature and its derivatives must be continuous at $\xi = \xi_1$, $\xi = \xi_1 + \Delta\xi$ and at $\xi = \xi_m$.

Using Eqs (V-4) to (V-7), together with the above boundary conditions, it may be shown that:

$$\theta_1 = \frac{1}{4} (Q_m - \alpha \tau^2) \xi^2 - Q_{h2} \ln \xi + C_2, \text{ for } 0 < \xi < \xi_1 \tag{V-10}$$

$$\theta_2 = C_3 J_o (\sqrt{\alpha\tau}\, \xi) + C_4 Y_o (\sqrt{\alpha\tau}\, \xi) + (1-\tau) + \frac{Q_m}{\alpha\tau}, \quad \text{for } \xi_1 < \xi < \xi_1 + \Delta\xi \tag{V-11}$$

$$\theta_3 = \frac{Q_m}{4} \xi^2 + C_5 \ln \xi + C_6, \text{ for } \xi_1 + \Delta\xi < \xi < \xi_m \tag{V-12}$$

$$\theta_4 = \theta_m \frac{K_o(\xi)}{K_o(\xi_m)} \text{ for } \xi > \xi_m \tag{V-13}$$

where:

$J_\nu(x)$ = Bessel function of the first kind of order ν and argument x

$Y_\nu(x)$ = Bessel function of the second kind of order ν and argument x

$K_\nu(x)$ = modified Bessel function of the second kind of order ν and argument x

$$C_2 = 1 + Q_{h2} \ln \xi_1 - \frac{1}{4} (Q_m - \alpha\tau^2) \xi_1^2$$

$$C_3 = \frac{\pi b}{2} \left[B\, Y_o(b) - C\, Y_1(b) \right]$$

$$C_4 = \frac{\pi a}{2} \left[D\, J_1(a) - A\, J_o(a) \right]$$

$$a = \sqrt{\alpha\tau}\ \xi_1$$

$$b = \sqrt{\alpha\tau}\ (\xi_1 + \Delta\xi)$$

$$A = \frac{1}{\sqrt{\alpha\tau}} \left[\frac{Q_{h2}}{\xi_1} - \frac{1}{2} \xi_1 (Q_m - \alpha\tau^2) \right]$$

$$B = -\frac{1}{\sqrt{\alpha\tau}} \left[\frac{Q_m}{2} (\xi_1 + \Delta\xi) + \frac{C_5}{(\xi_1 + \Delta\xi)} \right]$$

$$C = \frac{Q_m}{\alpha\tau}$$

$$D = \tau - \frac{Q_m}{\alpha\tau}$$

$$C_5 = \left\{ 1 - \tau - \theta_m + \frac{Q_m}{4} \left[\xi_m^2 - (\xi_1 + \Delta\xi)^2 \right] \right\} \left(\ln \frac{\xi_1 + \Delta\xi}{\xi_m} \right)^{-1}$$

$$C_6 = 1 - \tau - \frac{Q_m}{4} (\xi_1 + \Delta\xi)^2 - C_5 \ln (\xi_1 + \Delta\xi)$$

The unknown lengths ξ_1, $\xi_1 + \Delta\xi$ and ξ_m are determined by:

$$\frac{\pi b}{2} \left[B\, Y_o(b) - C\, Y_1(b) \right] J_o(a) + \frac{\pi a}{2} \left[D\, J_1(a) - A\, J_o(a) \right] Y_o(a) = \tau - \frac{Q_m}{\alpha\tau} \qquad \text{(V-14a)}$$

$$\frac{\pi b}{2} \left[B\, Y_o(b) - C\, Y_1(b) \right] J_o(b) + \frac{\pi a}{2} \left[D\, J_1(a) - A\, J_o(a) \right] Y_o(b) = \frac{Q_m}{\alpha\tau} \qquad \text{(V-15a)}$$

$$\frac{Q_m}{2}\,\xi_m + \frac{C_5}{\xi_m} = -\theta_m \frac{K_1(\xi_m)}{K_o(\xi_m)} \qquad \text{(V-16a)}$$

For clarity, these equations may be written in a corresponding functional representation which indicates the dependence of ξ_1, $\xi_1 + \Delta\xi$, and ξ_m on α, τ, Q_m, θ_m, and Q_{h2}.

$$f_1\,(\xi_1,\ \xi_1 + \Delta\xi,\ \xi_m,\ \alpha,\ \tau,\ Q_m,\ \theta_m,\ Q_{h2}) = 0 \qquad \text{(V-14b)}$$

$$f_2\,(\xi_1,\ \xi_1 + \Delta\xi,\ \xi_m,\ \alpha,\ \tau,\ Q_m,\ \theta_m,\ Q_{h2}) = 0 \qquad \text{(V-15b)}$$

$$f_3\,(\xi_1 + \Delta\xi,\ \xi_m,\ \tau,\ \theta_m,\ Q_m) = 0 \qquad \text{(V-16b)}$$

These three equations may now, in principle, be used in a manner similar to that utilized in earlier analyses for a determination of the conditions limiting stability. This was not carried to completion.

VI. EXPERIMENTAL INVESTIGATIONS OF COIL STABILITY

A. Coil Operation at Supercritical Pressures

A series of tests were conducted to gain an insight into any change in the operating characteristics of superconducting coils when cooled with supercritical helium rather than the usual method of cooling with liquid helium at 1 atm. This involved a facility which allowed small coils to be excited and driven to quench while immersed in helium at 4.2°K and pressures from 0 to 45 psig. Since the magnitude of the quench current is dependent on the ability of the heat transfer environment to cool and, in turn, prevent the propagation of a localized normal region (4, 5), these tests provided an indication of the cooling efficiency at elevated pressures relative to that at 0 psig for particular coil constructions.

To create a pressurized coil environment, a vessel was constructed, as shown in Fig. VI-1, from a short length of brass pipe and caps. The vessel was pressurized through a stainless steel tube which also served as a conduit for the instrumentation leads to the two carbon resistors and for the leads to the coil voltage taps. Three superconducting power leads entered the vessel via three ceramic feed-throughs and were solder-joined to the leads on the coil.

The procedure was to mount a coil on the coil support, connect the power and instrumentation leads, assemble the vessel, purge the system with a helium flow from the bottle and out the purge hole, seal the purge hole, leak test the system, pre-cool and immerse the entire assembly in liquid helium. Initially, a great deal of boil-off was observed as the helium from the gas supply was being condensed by the cold walls of the vessel. In each case, it was evident when the liquid level in the vessel rose and covered first the lower temperature probe and then the higher. A short time after the higher probe was covered, boil-off was no longer evident.

Each coil was tested under various initial conditions on pressure. This was controlled via the regulator on the gas bottle and the test began after the upper probe indicated a temperature of 4.2°K, the temperature of the bath. In each case, as coil current was increased, no change in initial pressure or temperature was observed until the coil developed a resistance. After quench, the pressure and temperature rise were dependent on the magnitude of the quench current itself, since this determines the amount of energy dumped into the confined vessel.

Figure VI-2 indicates typical test results. In each case, quench current decreased somewhat as pressure was increased above 0 psig. For coil B, the change in performance was much more pronounced. This coil

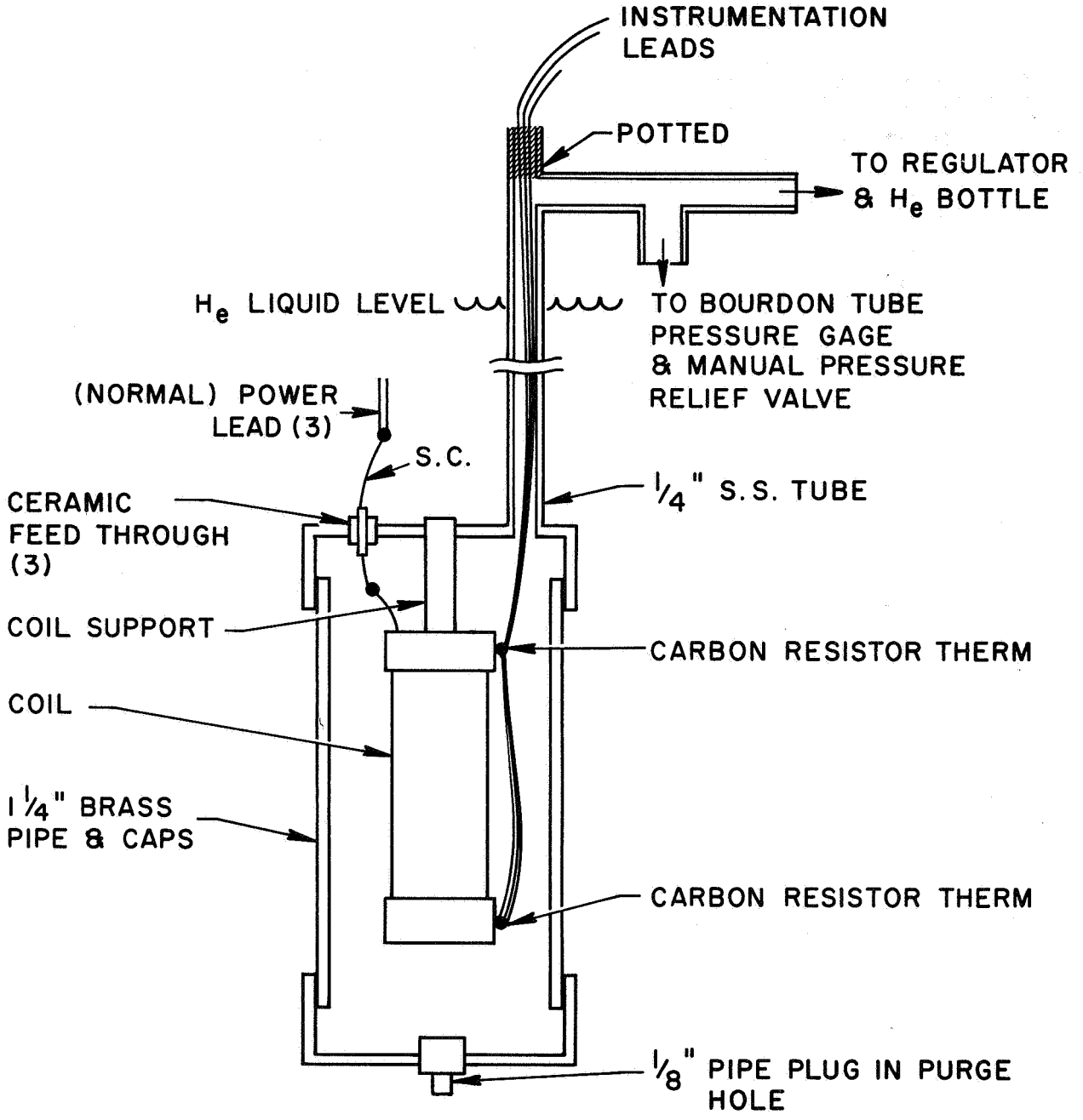

Fig. VI-1 Experimental apparatus to test coil operation in a supercritical pressure environment

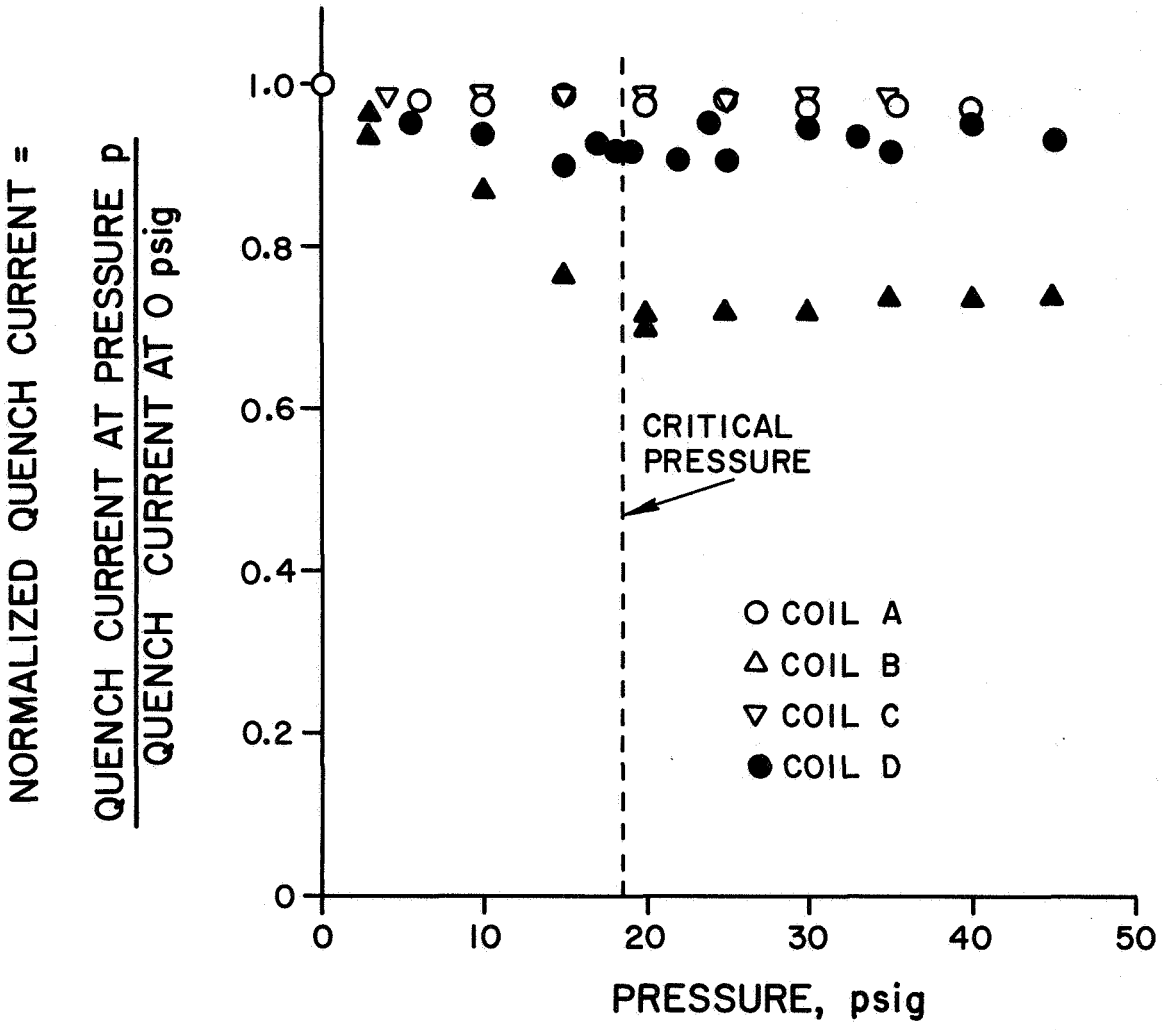

Fig. VI-2 Normalized quench current vs environmental pressure

exhibited a relatively large voltage prior to quench, hence, the rate of energy deposition to the environment before quench was much larger and the decrease in the ability of the environment to cool the coil at increased pressure is more evident . The coils were a number of small Nb-Zr composite solenoids that were available. Exact construction is not known at this time. We were only looking for gross effects.

Further tests at high pressures for a larger coil are described below.

B. Experimental One-Dimensional Stability Characteristics

A series of experiments have been conducted in an effort to exhibit the stability characteristics predicted by the one-dimensional theory. In the following, the test facility is described and typical test results are included. The qualitative agreement with the predictions of the theory is obvious.

1) Experimental Apparatus

A test facility which closely approximates the model underlying the one-dimensional analyses must necessarily incorporate a relatively long composite conductor immersed in a magnetic field and heat transfer environment which are invariant with length. It should also include a small heat source which can introduce a perturbation of known size into the system. An experiment which fulfilled these requirements was carried out with the apparatus illustrated in Fig. VI-3.

Tests were conducted on two different composite conductor samples: (1) a 0.02" OD - 0.01" core, copper clad Nb Ti and (2) a 0.016" OD - 0.01" copper clad Nb Ti. Each sample was approximately 40" long and wound on a grooved phenolic sample holder as shown in Fig. VI-3. The ends of the sample were soldered to copper end plates which were the terminals of the sample current leads. A 0.003" D. nichrome wire was wound bifilar with the sample as shown in the insert. Voltage was measured across the sample utilizing the nichrome wire as the voltage tap to the lower end of the superconductor. Induced voltages arising from any high frequency fluctuation of the essentially steady applied magnetic field were thus cancelled. Voltage taps were located two inches from the sample ends, well away from the joint to the sample current leads. A uniform field was provided during the tests by a relatively long three inch bore superconducting solenoid.

2) Test Results

Typical data is shown in Fig. VI-4. The heat input Q_{hl} is proportional to the heater current squared, thus:

$$\frac{dV}{dQ_{hl}} \sim \frac{dV}{dI_h^2} = \frac{1}{2I_h} \cdot \frac{dV}{dI_h}$$

At the onset of resistance (marked with an x on the figures), we see $\frac{dV}{dI_h} = 0$.

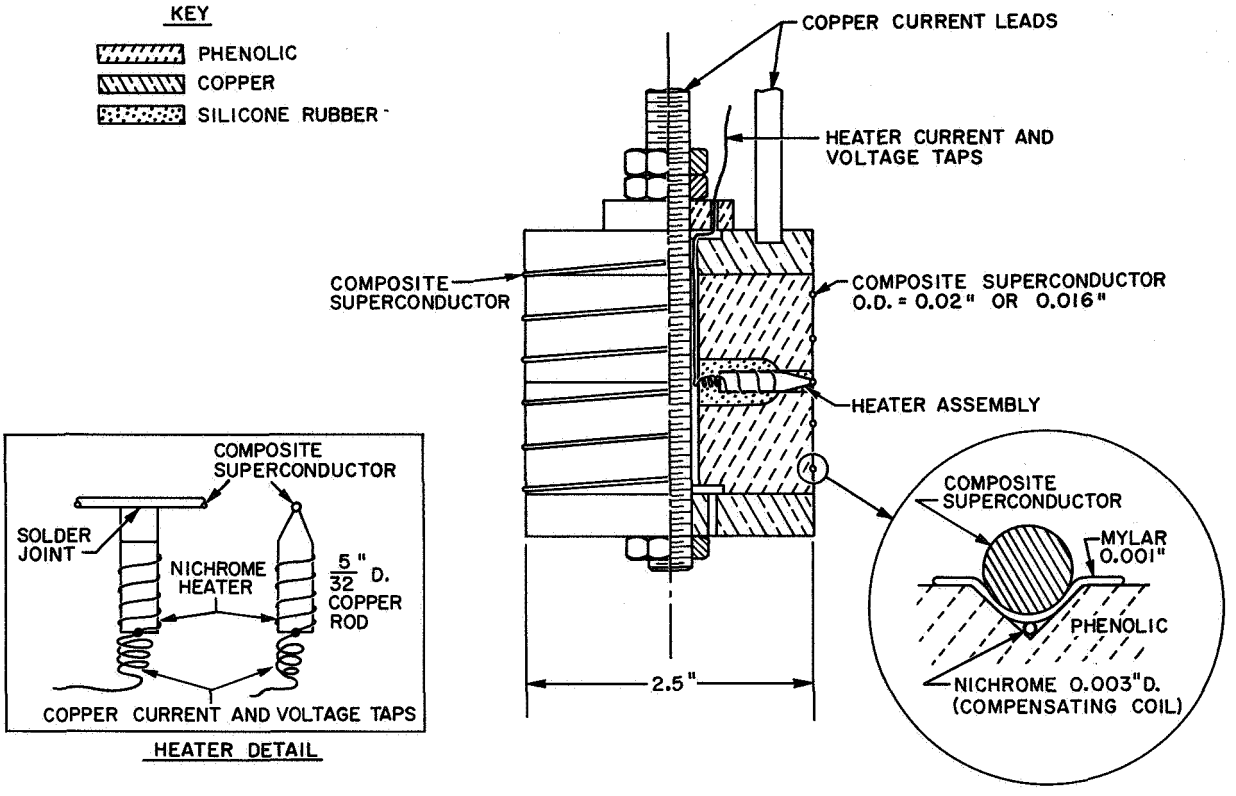

Fig. VI-3 Test apparatus for correlation of one-dimensional effects

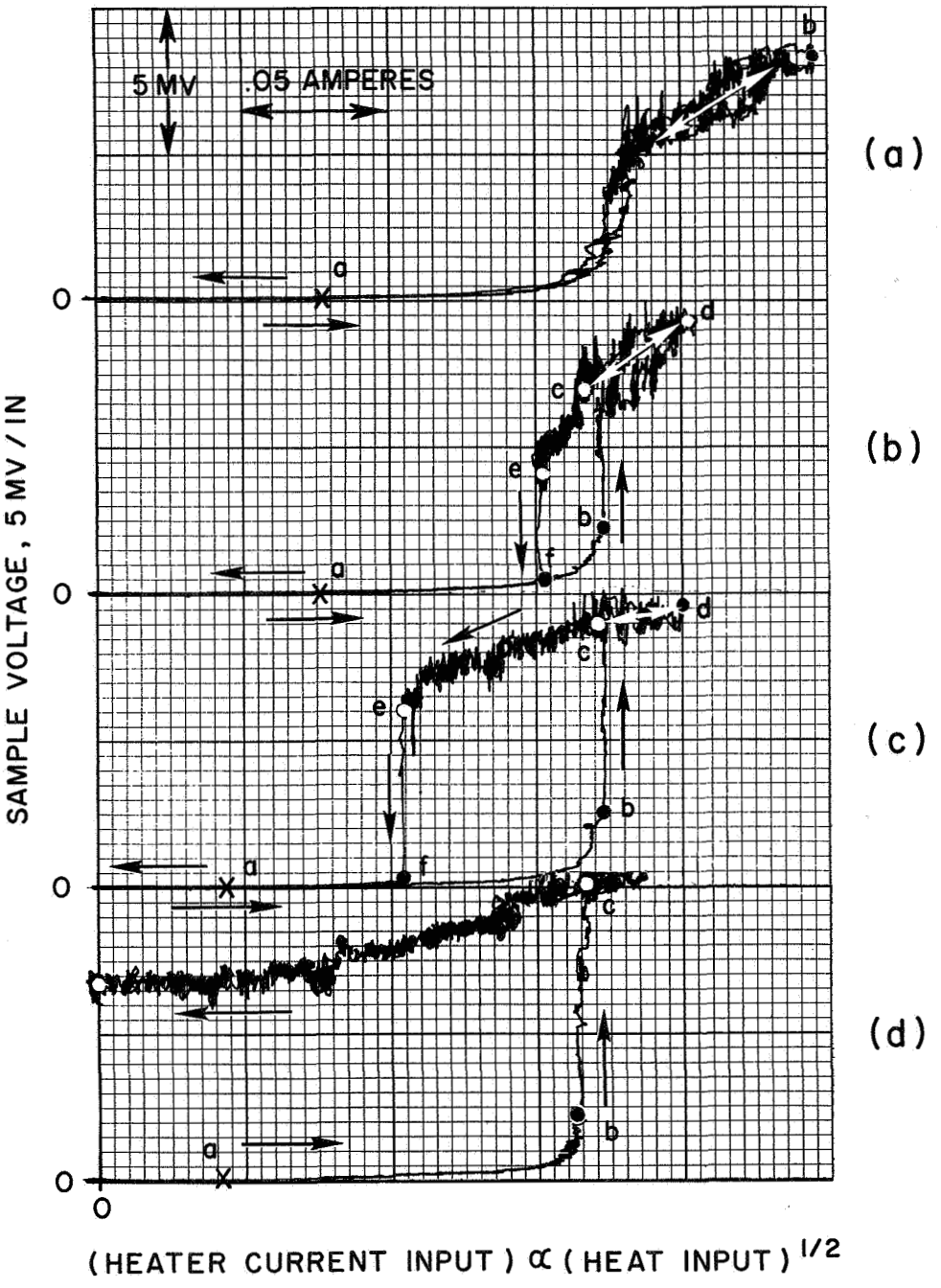

Fig. VI-4 Typical test results regarding one-dimensional stability

a) $I/I_c = .88$, stable operation

b) $I/I_c = .91$, hysteretic behavior

c) $I/I_c = .93$, hysteretic behavior

d) $I/I_c = .94$, unstable operation

For non infinite sample current, $\left.\frac{dV}{dQ_{hl}}\right|_{Qhl}$ = 0 as predicted. At take-off (Fig. VI-4b, c, d, marked as point b) $\frac{dV}{dQ_{hl}}$ has become quite large, if not infinite, again as predicted. The reversibility of the voltage after take-off is also illustrated in Fig. VI-4b, c.

It should be noted that the behavior shown in Fig. VI-4d is not predicted using the modified non-linear heat transfer characteristic. Our model predicts that, in the hysteresis region, the sample will be fully superconducting when the heat input is reduced to zero. If the entire sample were normal, the voltage measured would be about 100 millivolts. It is obvious from Fig. VI-4d that the voltage observed is an order of magnitude too low. Once triggered (by a heat input of Q_{hlT}), a stable normal region exists at this conductor current when the heat input is reduced to zero. It does not propagate nor does it collapse. This behavior, as can be seen from the data, occurs near the end of the hysteresis region. Since this behavior occurs close to the fully unstable region (where quench occurs at take-off), it does not seem profitable, at this time, to use a more detailed heat transfer characteristic to fully determine this behavior.

Quantitative agreement with the theory is also good, considering the uncertainties involved in determining some of the parameters. From Fig. III-9 it is seen that h is somewhat undetermined. Also the value of h depends on the orientation and preparation of the sample surface. We have chosen a value of $h = 1 \frac{watt}{cm^2 - {}^oK}$ as representative -- this may be in error by as much as a factor of 2. The thermal conductivity k, which appears in determining the reduced length ξ and Q_{hl}, is a function of temperature and copper purity.[1] We chose a value of k = 40 watts/cm - ^oK as representative of our sample by extrapolating from the data given by Johnson.[1] It is estimated that this could be in error by as much as 20%. The cooled perimeter P of the conductor is approximately half the total conductor perimeter, as can be seen from the schematic of the experimental setup (Fig. VI-3). It is also estimated that $.15 < \theta_m < .20$ and $.1 < Q_m < .15$, for this sample at the given applied field (40 kG). In this particular experiment, most of the heat generated by the heater flows into the sample. The heater resistance R is 4.45 ohms.

Using the above values for h and k, and choosing $\theta_m = .17$, a curve of heater power at the onset of resistance vs $\tau = I/I_c$ may be generated from Eqs. (III-38) and (III-39). Figure VI-5 shows the comparison between this theoretical curve and the experimental data. This choice of parameters ($h = 1$, $k = 40$, $\theta_m = .18$) fits the data well. However, with the quoted uncertainty in these same parameters, the calculated range of heater power at the onset of resistance is also shown in Fig. VI-5 by broken lines.

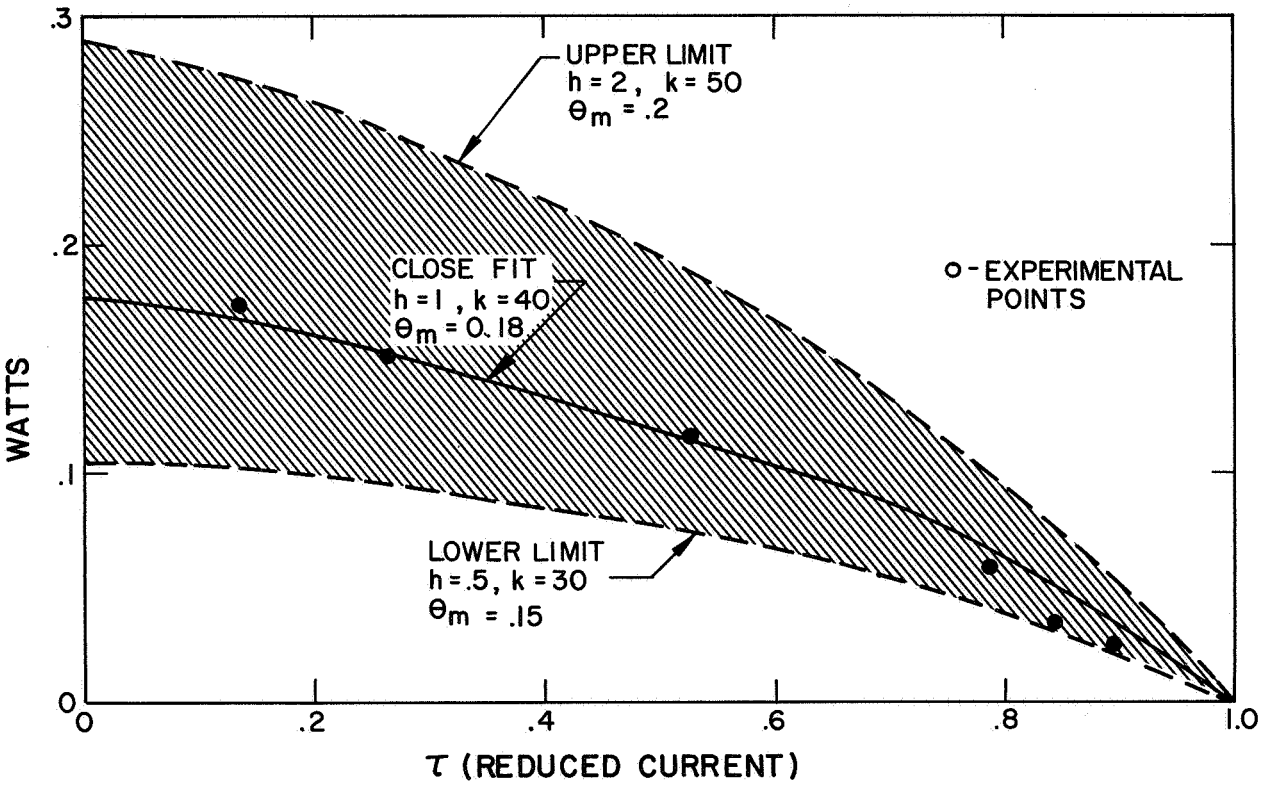

Fig. VI-5 Heater power at the onset of resistance vs reduced sample current τ

A8733

From Fig. VI-4 it is obvious that the onset of the hysteresis region occurs at about $\tau = .90$. The calculated α for this sample is .175, which could be in error by as much as a factor of 2. Thus, $\alpha\tau^2$ at the beginning of the hysteresis region is approximately (within a factor of two) 0.155. This obviously does not agree with $\alpha\tau^2 = 1$ at the beginning of the hysteresis region as obtained by the constant h solution. In fact, the constant h model predicts that for this α there is no hysteresis. This agrees quite well, however, with $\alpha\tau^2 = Q_m$, where Q_m is in the range quoted previously in this report.

It seems that the one-dimensional theory is quite complete. However, further experimental work should be undertaken to determine more precisely the numerical values of the parameters h, k, θ_m, Q_m.

3) Tests on 6-Inch i.d. Nb-Ti Coil

We have made use of a 6 inch i.d. superconducting solenoid* to examine the steady state stability characteristics. Specifically, information was sought on the ability of the coil to recover from distrubance at various temperatures and pressures, the maximum current before quench, and the quench time.

The coil was wound with stabilized niobium-titanium composite superconductor. The wire consisted of fifteen 0.010 in. diameter Nb-Ti cores in a copper matrix 0.086 in. square. The ratio of copper to superconductor was approximately 2.7:1.

This conductor was layer wound onto the coil as shown in Fig. VI-6. Each turn is separated from the adjacent turn by intermittent mylar insulation 0.006 in. thick. The adjacent layers were separated by G-10 epoxy fiberglass slats 0.015 in. thick. This configuration allowed cooling passages and liquid Helium convection.

To provide localized thermal disturbance four small Nichrome heaters were wound into the coil. These were constructed so that the path of least thermal resistance would be from the Nichrome wire to the conductor. Only heater number 2 which is located five layers from the inside of the coil was used extensively in the testing program.

*The design and construction of this coil was performed under contract NAS 3-9684 for NASA - Lewis Research Center, Cleveland, Ohio.

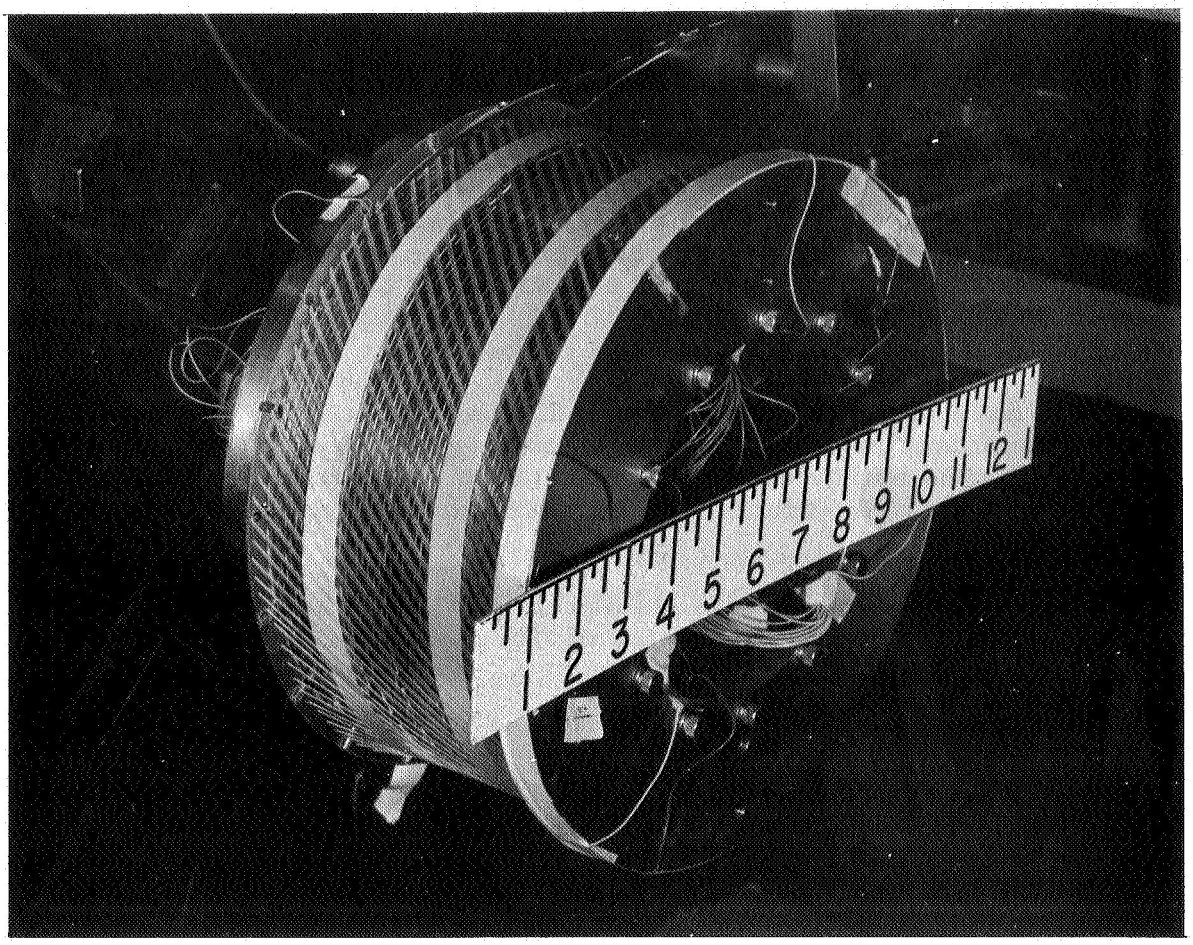

Fig. VI-6 A view of the magnet being wound

A8722

A summary of the coil parameters is given in the table below

TABLE VI-1

Nb-Ti COIL PARAMETERS

Inside Winding Dia	6.030	in.
Outside Winding Dia	8.780	in.
Winding Length	4.00	in.
Length of Conductor	1136	ft.
FIELD TO CURRENT RATIO		
CENTRAL	34.5	G/A
MAXIMUM	46.5	G/A
HEATER	26.25	G/A
Number of Turns	582	
Inductance	0.052	H
Room Temp Resistance	1.6Ω	
Fraction of Conductor		
Surface Exposed to Helium	50%	

Information regarding stability against thermal disturbances was obtained by using the heaters within the windings. At a fixed coil current, the heater was energized, and the voltage across the heated section was monitored. Once a voltage appeared across the terminals of the heated section, the heater power was reduced to observe the behavior of the voltage.

Typical data of this type are presented in Fig. VI-7 for various values of coil current.

At low coil currents (Fig. VI-7a and VI-7b) the appearance and disappearance of voltage is gradual and the voltage retraces the same curve on decreasing heater current that it traced on increasing heater current. Notice here that the initial slope of the voltage is zero. At 640 amperes coil current a hysteresis exists where the onset of voltage is sudden, and a recovery back to the superconducting state occurs at a lower heater power than the onset. At 660 amperes it takes a finite heater power before onset occurs; however no recovery back to the superconducting state occurs even when the heater current is reduced to zero. At higher currents (800 A) it takes a finite heater current before onset of resistance occurs; however once voltage appears it grows in an uncontrolled manner. Note also that at the sensitivity used (5 mv/in.) no detectable voltage appeared prior to the rapid increase of voltage at the onset of resistance.

The onset of resistance and recovery was determined for the whole operating range of the coil, and in addition at low coil currents heater power was increased considerably beyond that required for the appearance of resistance. A typical trace is shown in Fig. VI-7b, which exhibits a sudden change in slope of the coil voltage at a heater current above the onset value. These changes

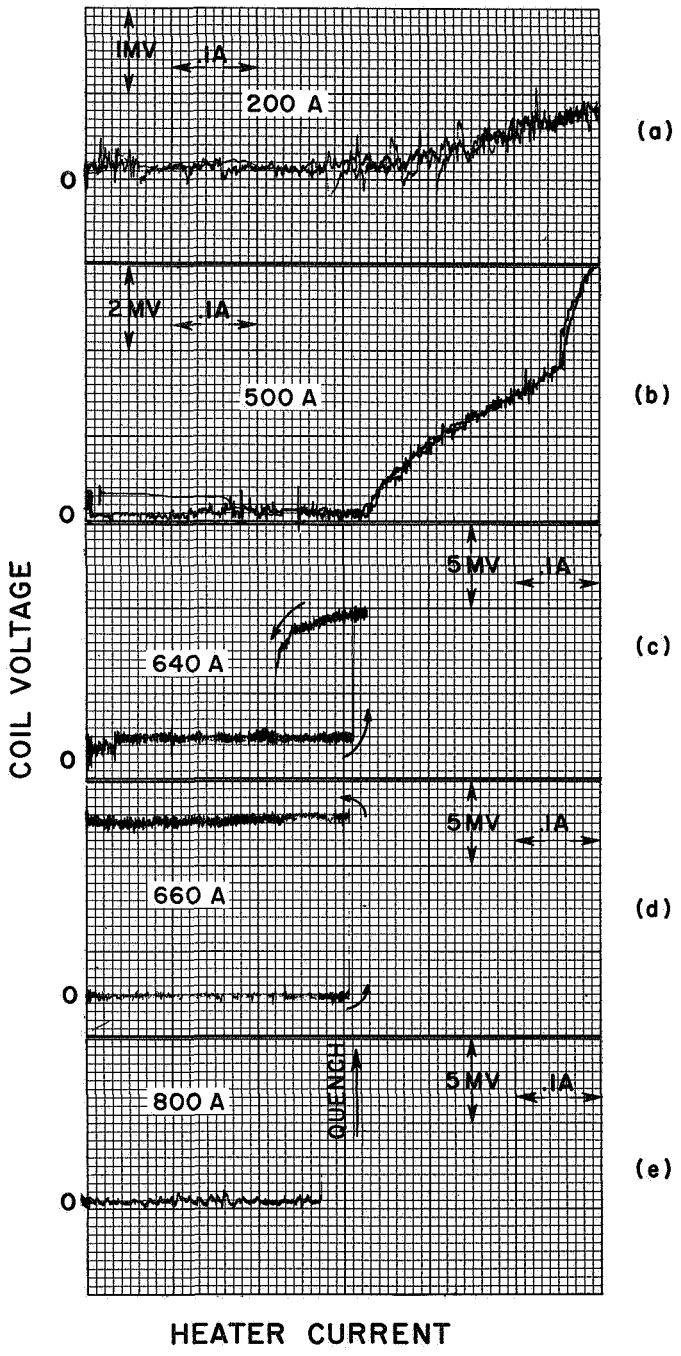

Fig. VI-7 Typical heater characteristics for the coil shown in Fig. VI-6 (Htr. #2)

a) At a magnet current of 200 amperes
b) At a magnet current of 500 amperes
c) At a magnet current of 640 amperes
d) At a magnet current of 660 amperes
e) At a magnet current of 800 amperes

in slope are due to the propagation of resistance to the adjacent turns. This is due to the fact that one turn acts as a heater to the adjacent one. It was found that for low currents resistance appeared first in the heated turn, then propagated to one adjacent turn, then the other adjacent turn, and then to the next layer.

The complete heater data for 4.2 ^{o}K is summarized in Fig. VI-8. At low currents (within the range tested) the onset of resistance is gradual and quench occurs when resistance propagates to the adjacent layer. At higher currents the onset of resistance is still gradual, and quench occurs when resistance propagates to the adjacent turns. At slightly higher currents, onset of resistance occurs at higher heater power than the heater power at recovery from the resistive state and a quench occurs on propagation of resistance to the adjacent turn. At currents above 660 A the onset of resistance in the heated turn coincides with a quench. As expected the heater power required for onset of resistance decreases with increasing coil current.

The conclusions that can be reached are that for currents above 660 A, the coil (in the vicinity of the heater) is unstable to thermal disturbances large enough to produce a measurable voltage. At lower currents a detectable voltage exists before uncontrolled propagation of the normal region results. Also the slope of the quench line is very steep; consequently the degree of stability (at the heater) increases very rapidly below 660 A.

The onset of resistance was determined for the entire operating range of the coil at different values of the bath temperature. Figure VI-9 shows the heater power at onset and recovery for different values of pressure of Helium gas above the bath. There is a degradation as one goes from atmosphere (4.2^{o}K) to 15 psig. However there is some improvement in the stability characteristics as one increases the pressure above the critical point. Figure VI-10 shows the power at onset and recovery for 4.2^{o}K and for a number of lower temperatures. Figure VI-11 shows take-off and recovery points at 620 A for the pressures above atmosphere, while Fig. VI-12 summarizes the results of the experiments at reduced temperatures at a magnet current of 620 A. In these plots the heater current at take-off and recovery are shown at different temperatures. Note the increase in stability below the λ-point and above the critical pressure.

4) Charge Rate Dependence

The coil was energized without the heater and the current at quench was measured as a function of charge rate. The results are summarized in Fig. VI-13.

At charge rates lower than 2.5 A/second the coil operated up to its short sample current carrying capacity. At higher charge rates quench occured at progressively lower currents, but always above the predicted recovery current.

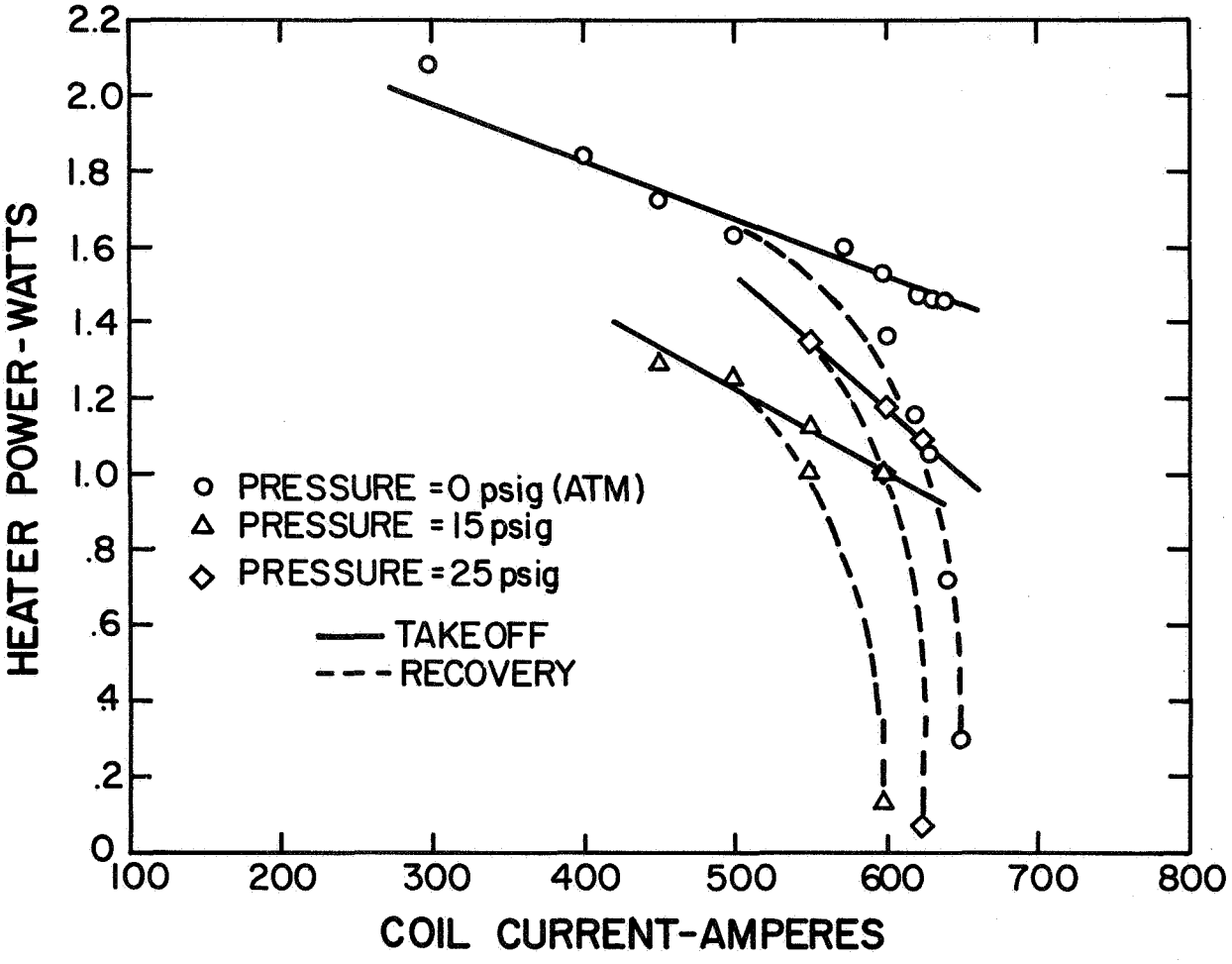

Fig. VI-8 Heater power at takeoff and recovery for several pressures of helium gas above the bath

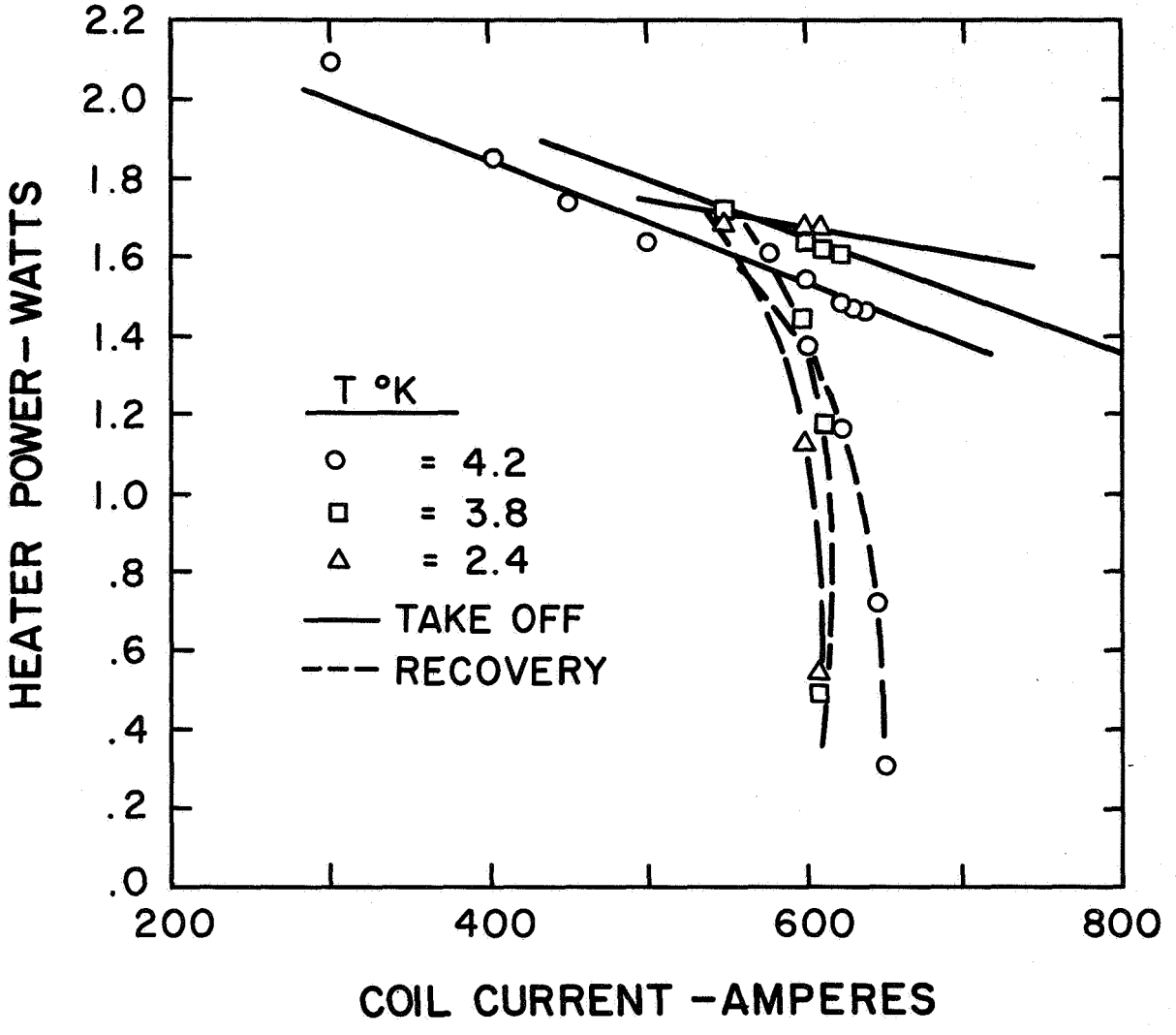

Fig. VI-9 Heater power at takeoff and recovery for several bath temperatures

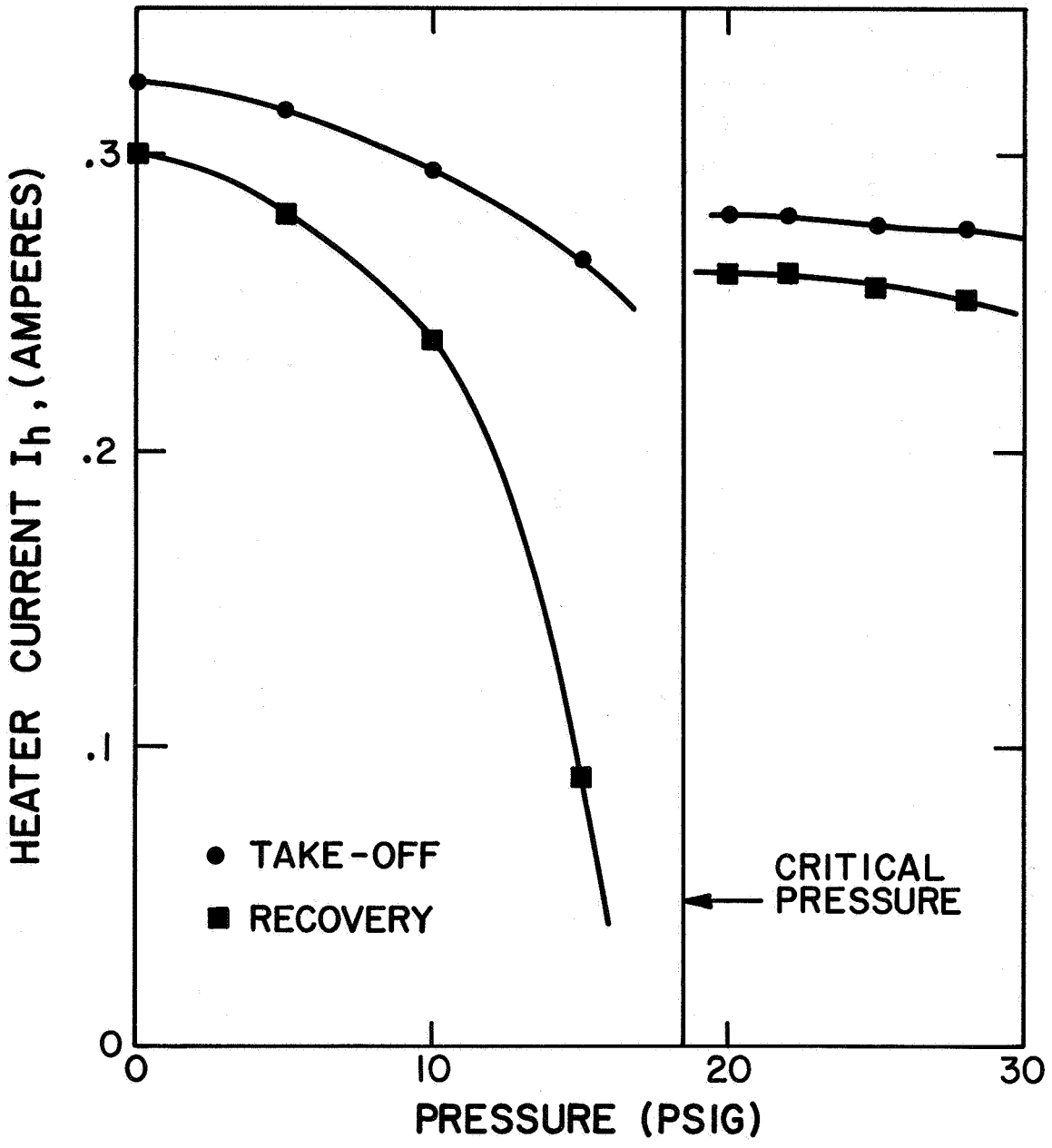

Fig. VI-10 Heater current at takeoff and recovery vs helium pressure at a magnet current of 620 amperes

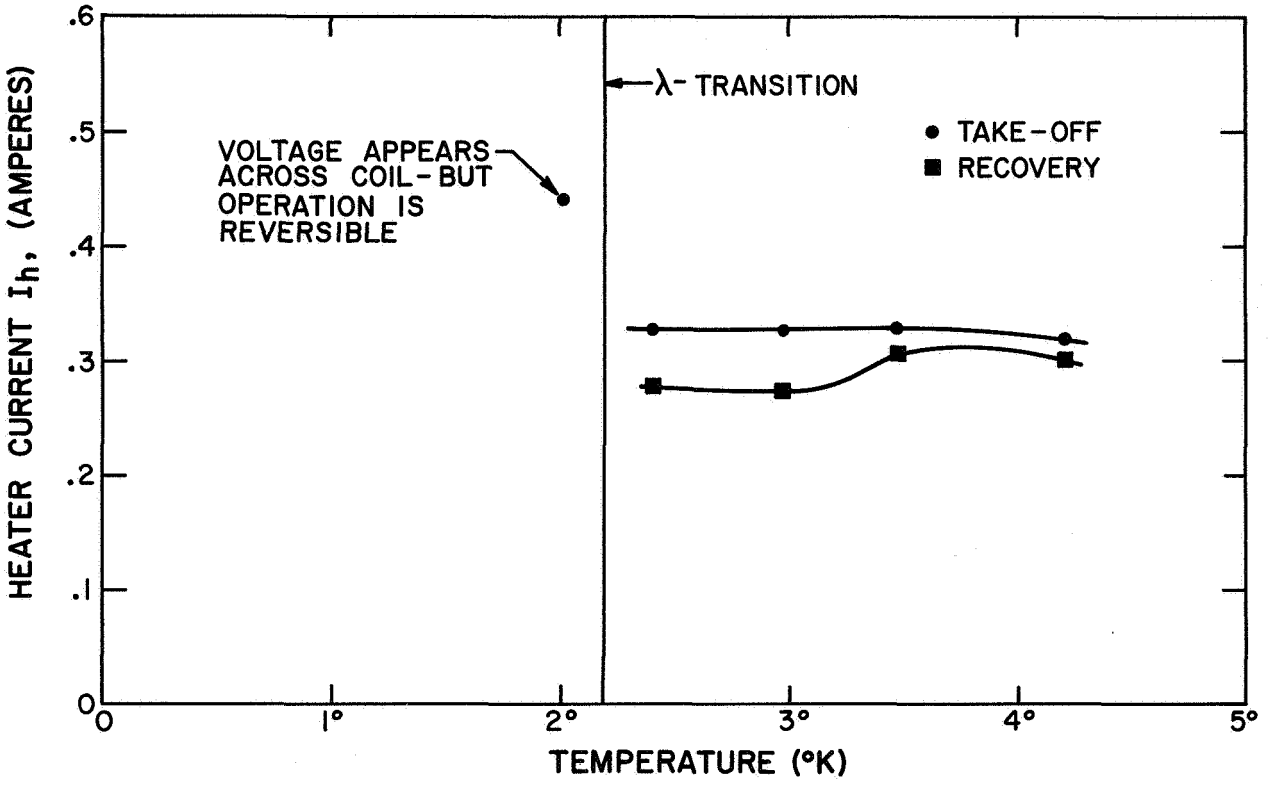

Fig. VI-11 Heater current at takeoff and recovery vs bath temperature at a magnet current of 620 amperes

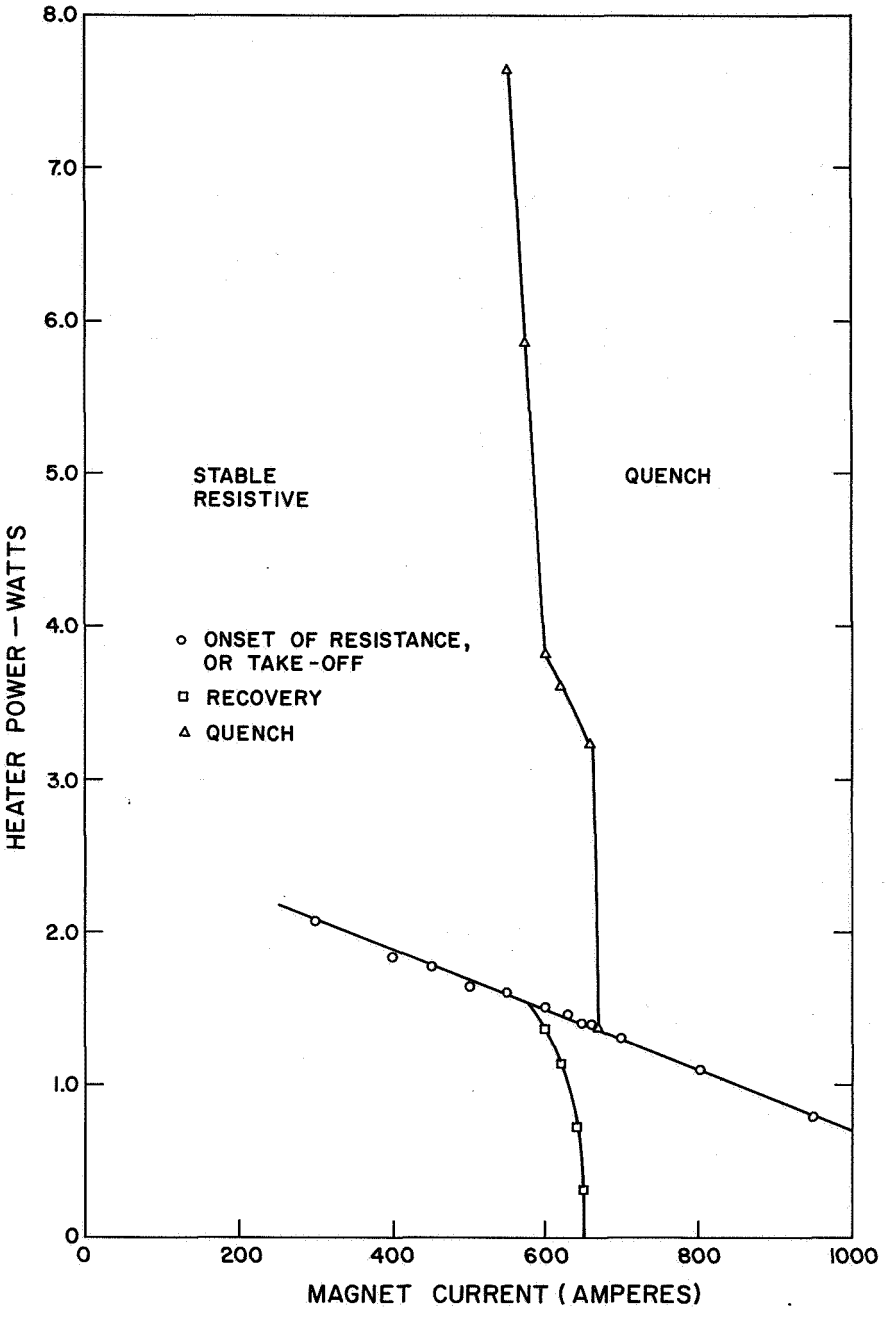

Fig. VI-12 Summary of heater data for NbTi coil

5) Quench Characteristics

One of the important design considerations in a large coil with a sizeable amount of magnetic energy is the question of what happens if a quench is initiated. The stability or lack of it determines under what conditions a quench might be initiated. The quench characteristics are important mainly from the point of view of preventing damage to the coil or coil system during uncontrolled propagation of a resistive region.

Damage during quench can occur from two causes -- excessive voltage and excessive temperature. An estimate of both the voltage and maximum temperature rise is possible if the quench time can be estimated.

The quench characteristics of each coil were obtained by charging the coil up to a fixed current, then shorting the coil with a room temperature shorting switch. This resulted in a relatively long decay time constant. The heater was then energized to a power level high enough to initiate a quench. The coil current during the quench was measured by a shunt in the circuit, and the rate of change of field was measured by a pickup coil. A typical set of quench data for the coil is shown in Fig. VI-14.

The data for a coil is summarized in Fig. VI-15, which shows the quench time as a function of coil current. The quench time is defined as the initial coil current divided by the maximum rate of current decay with time.

In Ref. 2 it is predicted theoretically that the characteristic time, τ, should be proportional to $I_o^{-3/4}$. Our results find $\tau \sim I^{-1.35}$. The analysis assumes a constant value for the normal state resistivity, a reasonable assumption if the local temperature remains under about 10°K. However, the resistivity rises rapidly above this temperature. Because of the high energy storage in the coil, we expect considerable local heating at the quench point. This local heating brings the resistivity to a point where it is strongly temperature dependent, thus yielding the observed dependence of τ on the quench current. This is confirmed by our data measuring the rise in coil resistance with time (Fig. VI-16).

Here we find an increasing rate of rise in coil resistance with quench current. In addition the maximum resistance is almost three times higher than the normal state resistance of the coil at 4.2°K. This indicates that there are high local temperatures in the coil.

Appendix C is a copy of a paper to be published in the Journal of Applied Physics on the stability characteristics of this coil and a Nb_3Sn pancake coil.

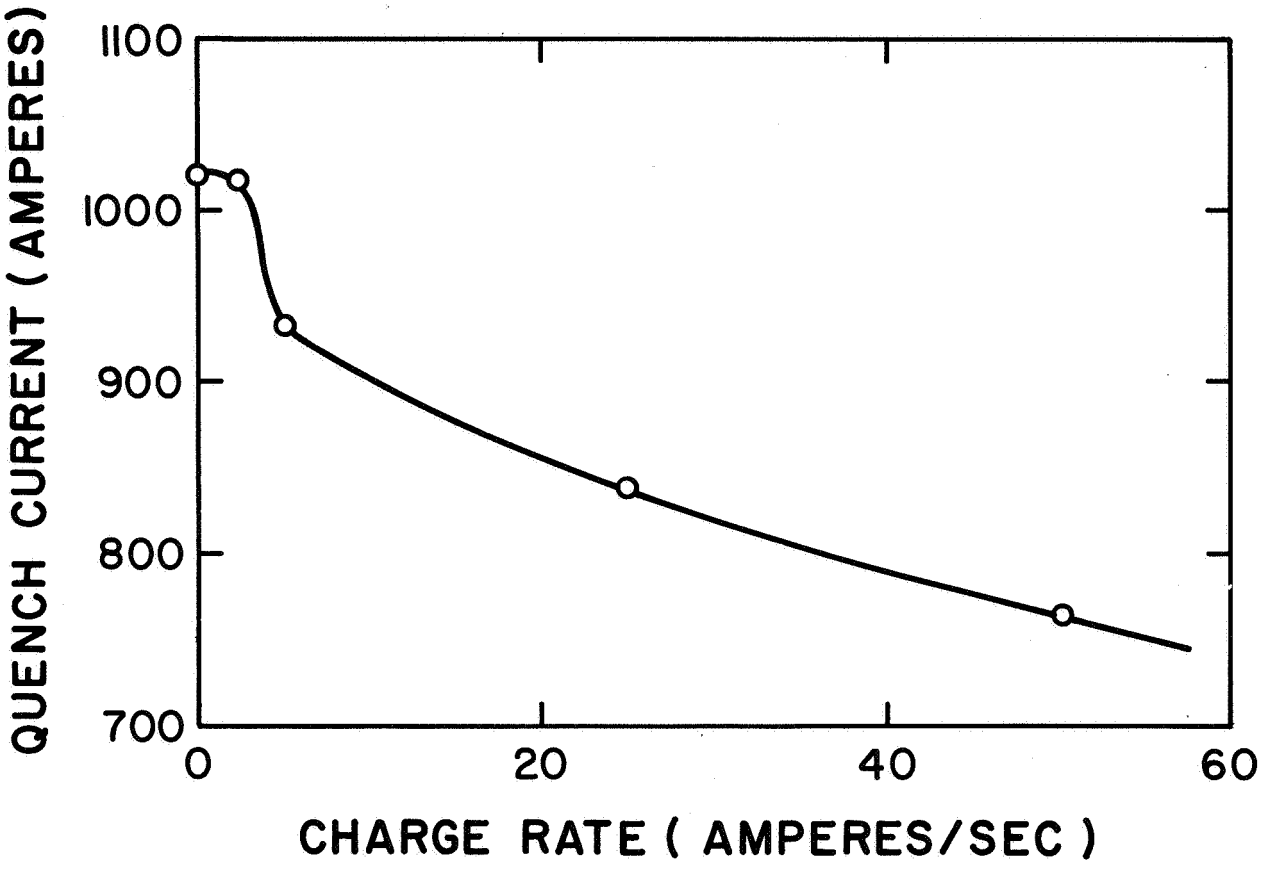

Fig. VI-13 Quench current vs charge rate for the coil

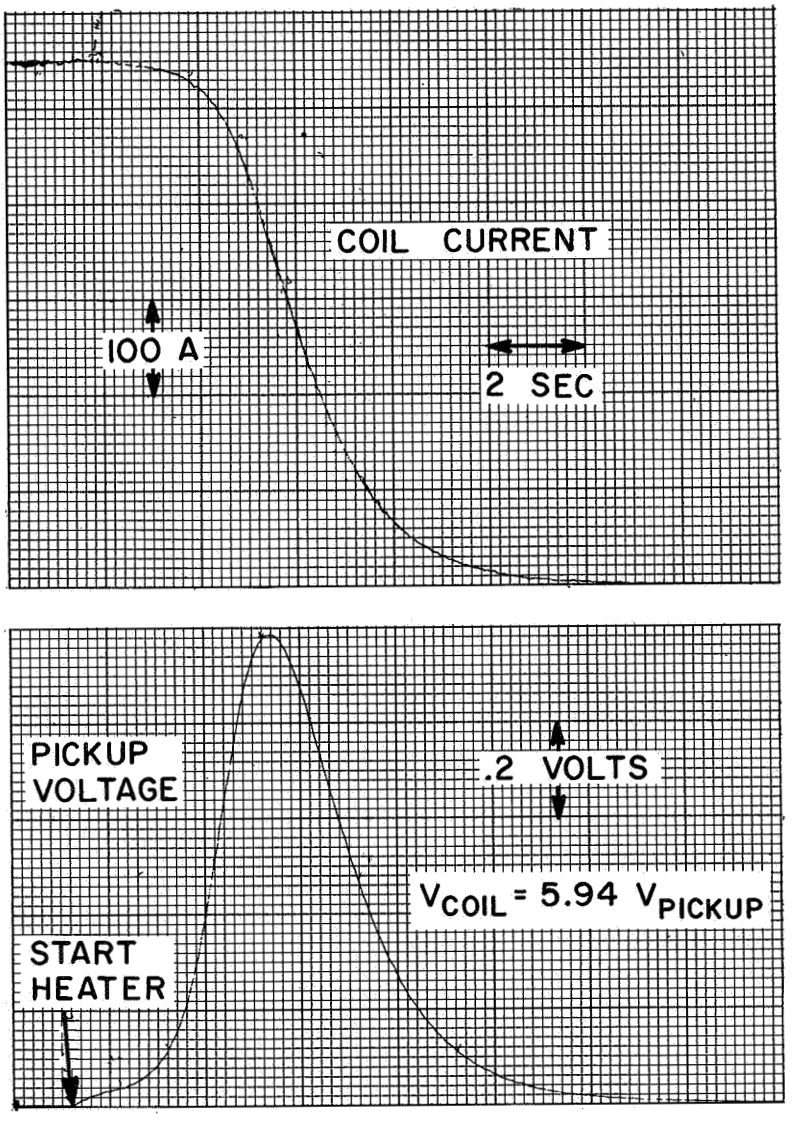

Fig. VI-14 Quench characteristics: The upper curve is a recording of current in the coil, while the lower curve is the voltage output of a pickup coil

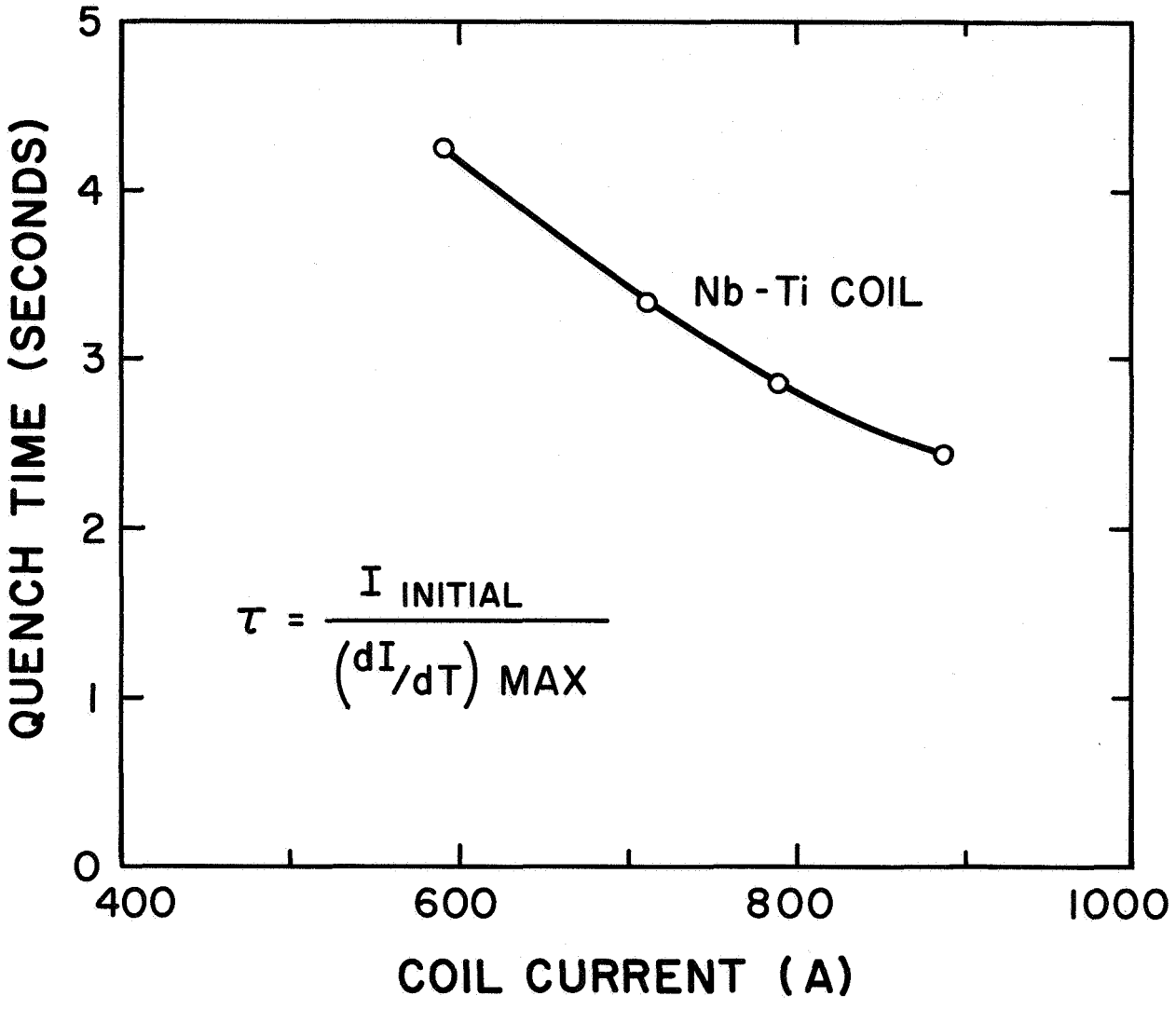

Fig. VI-15 Quench time as a function of coil current

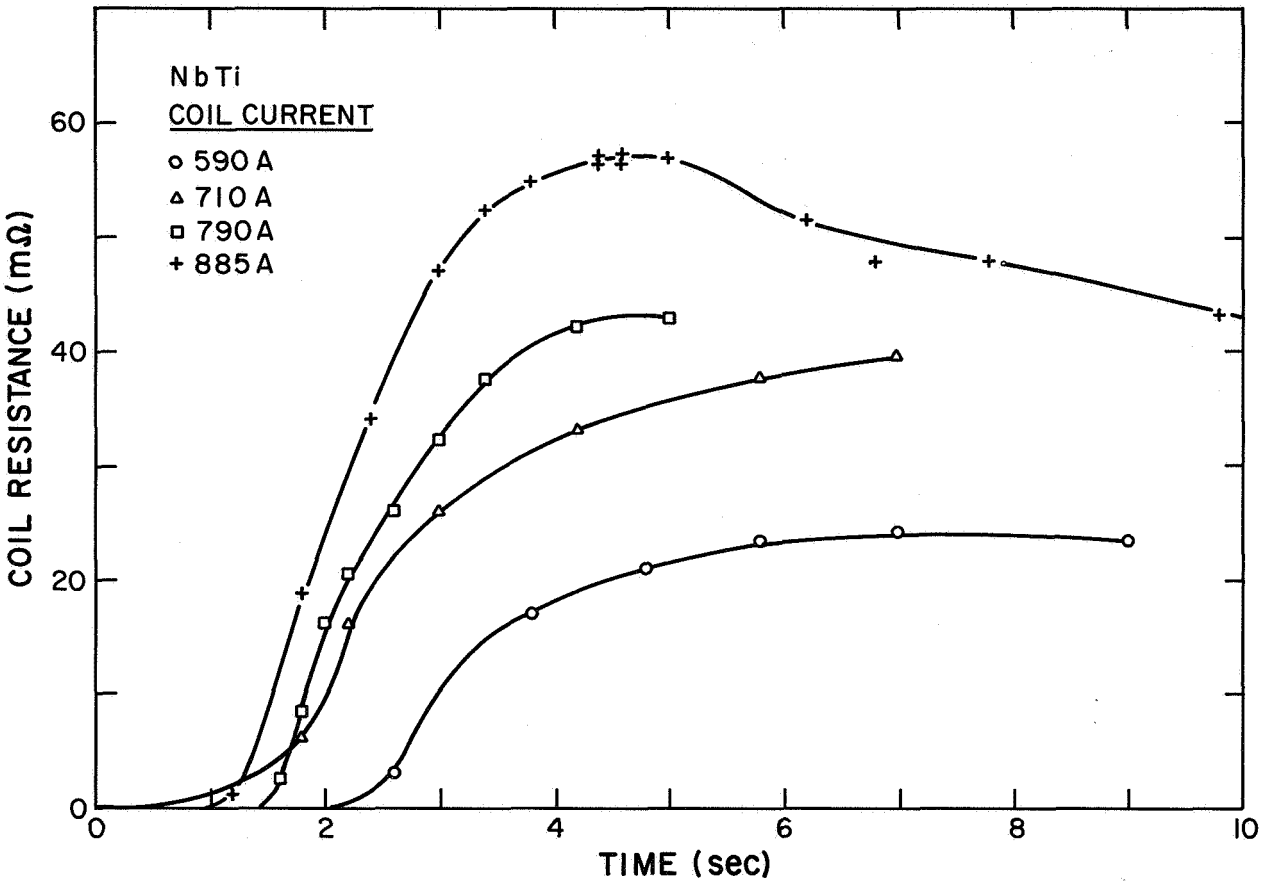

Fig. VI-16 Coil resistance vs time from start of quench for a number of quench currents

REFERENCES

1. WADD Technical Report 60-56, "A Compendium of the Properties of Materials at Low Temperatures (Phase I)," Part II, V. J. Johnson, Ed.

2. Stekly, Z. J. J., published in Advances in Cryogenic Engineering, Vol. 8, N. Y. Plenum Press 1963, pp. 585-600.

APPENDIX A

THERMAL CONDUCTIVITY OF Cu

The average value of the thermal conductivity of annealed OFHC copper (99.99% pure) has been measured. The method of measurement is to immerse one end of the sample in liquid helium, heat the other end and measure the temperature at the heated end. A schematic of the experimental setup is shown in Fig. A-1. The sample was a piece of copper stabilized composite conductor .086" square. The copper matrix has a thermal conductivity several orders of magnitude larger than the Nb-Ti so the thermal conduction is due completely to the copper. A calibrated carbon thermometer is used to measure the temperature. The entire sample is insulated with mylar tape down to the liquid helium level, so that the heat flow is one dimensional.

The average thermal conductivity k is determined from the following equation:

$$k = \frac{qL}{\Delta T A}$$

where

q = heat input from heater

L = distance from heater to the liquid helium bath

ΔT = Temperature of conductor at the heater minus the bath temperature (4.2°K)

A = cross sectional area of the copper

For this sample L = 10 cm, $A = 3.5 \times 10^{-2}$ cm^2. The value of k obtained is (perhaps 10%) in error, because the temperature of the conductor at the helium level is slightly higher than 4.2°K when the heater is on. The thermal conductivity of pure copper rises as the temperature is increased up to 15°K. Thus we expect that the average thermal conductivity will rise with ΔT (up to $\Delta T = 10^{\circ}$K). The measured value of k (average thermal conductivity) vs ΔT is shown in Fig. A-2.

The value of $k = 20 \frac{\text{watts}}{\text{cm} - {}^{0}\text{K}}$ was chosen for the calculation of Q_{hT} for the coil discussed in Section VI because the ΔT was small. These values of k agree well with the extrapolated values obtained from the data by Johnson (Ref. 1 of Section VI).

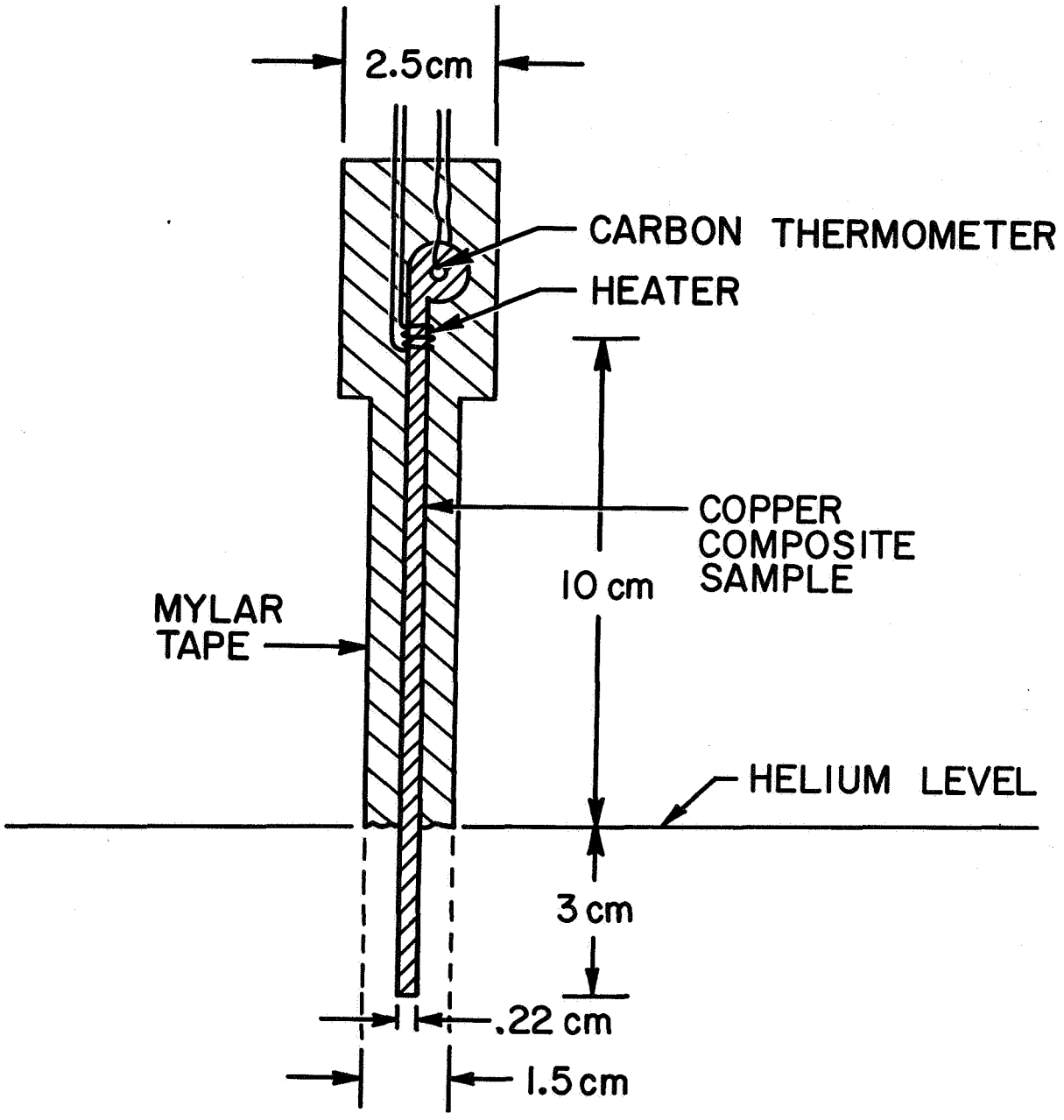

Fig. A-1 Experimental setup to determine the average thermal conductivity of copper

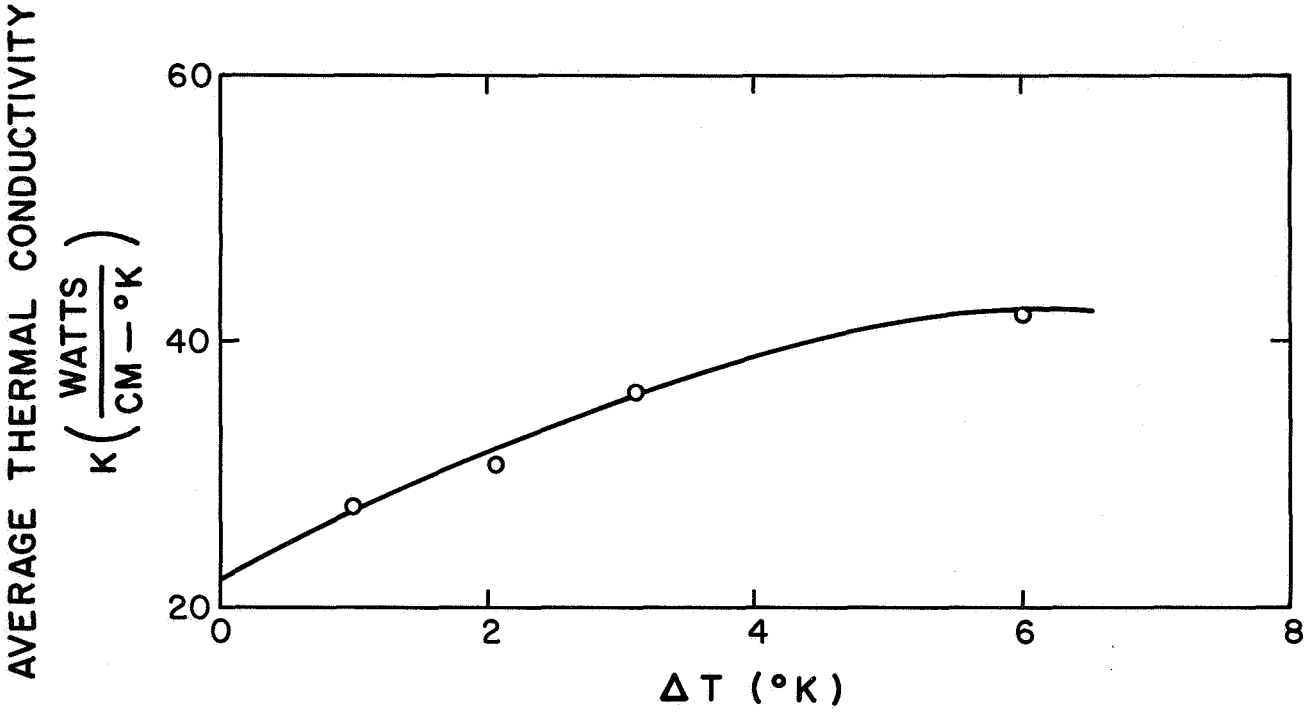

Fig. A-2 Measured average thermal conductivity vs ΔT

APPENDIX B

THERMAL CONDUCTIVITY OF Nb-Ti

The average thermal conductivity of Nb-Ti alloy rod has been measured. Standard measurement techniques were used. One end of the sample was held at liquid helium temperature. The other end had a heater and measurement thermometers. The rod was placed in a vacuum can and during the period of measurement the pressure of gas was held below 1 Torr.

The vacuum can served as a thermal shield for the NbTi rod. This was necessary due to the extremely low values of thermal conductivity for the NbTi material. The whole can was held below the helium level as can be seen in Fig. B-1.

The following equation was used to calculate the average thermal conductivity:

$$k = \frac{q}{A} \frac{L}{\Delta T}$$

where

q = heat input from heater

L = distance from heater to bath. (6.35 cm in this case)

ΔT = temperature of conductor at the heater minus the bath temperature

A = cross sectional area of Nb-Ti rod ($0.495\ cm^2$)

The results are shown in Fig. B-2. These values of the thermal conductivity are about three orders of magnitude below those of copper reported in Appendix A.

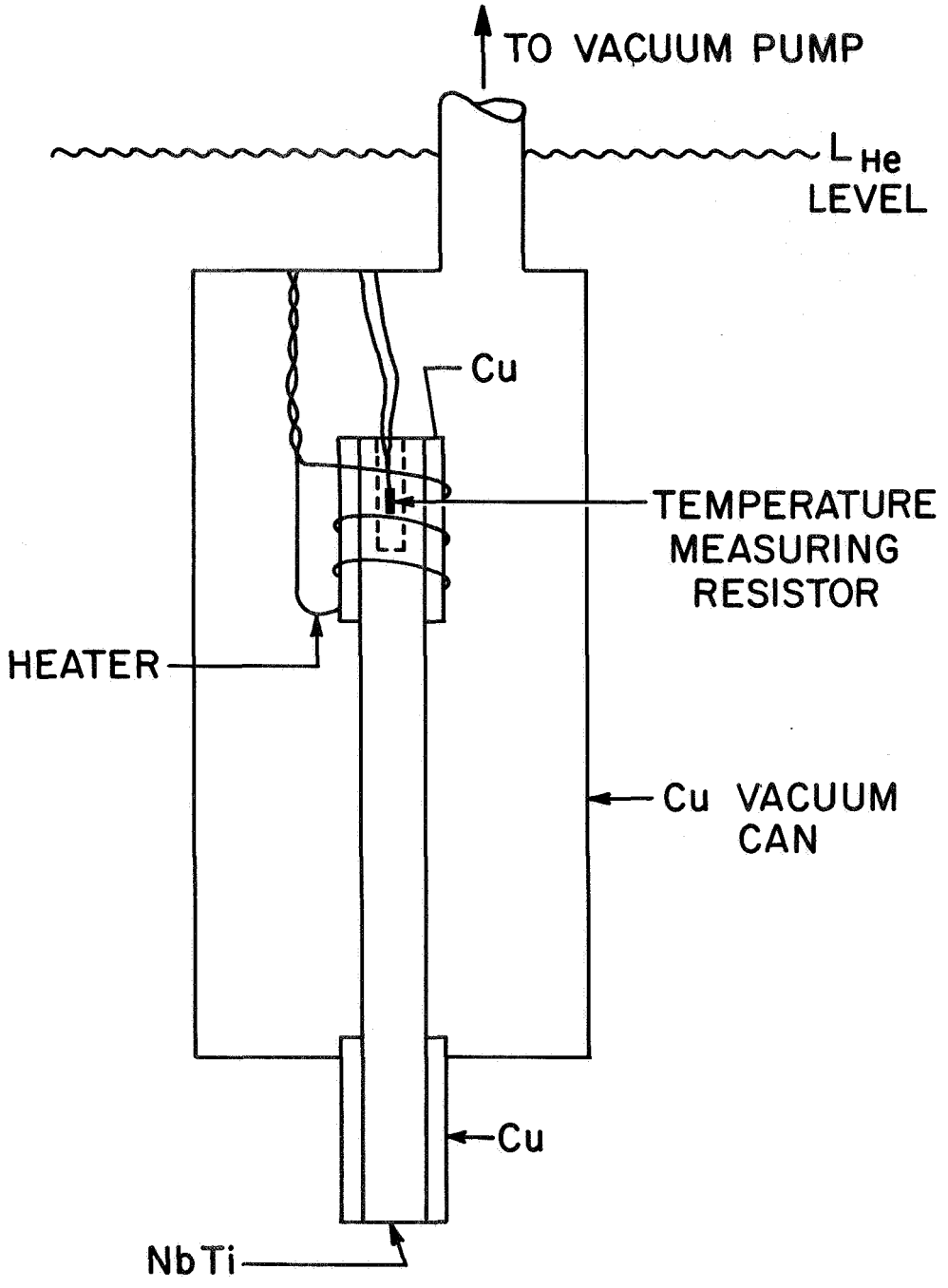

Fig. B-1 Experimental apparatus used for determining the thermal conductivity of NbTi

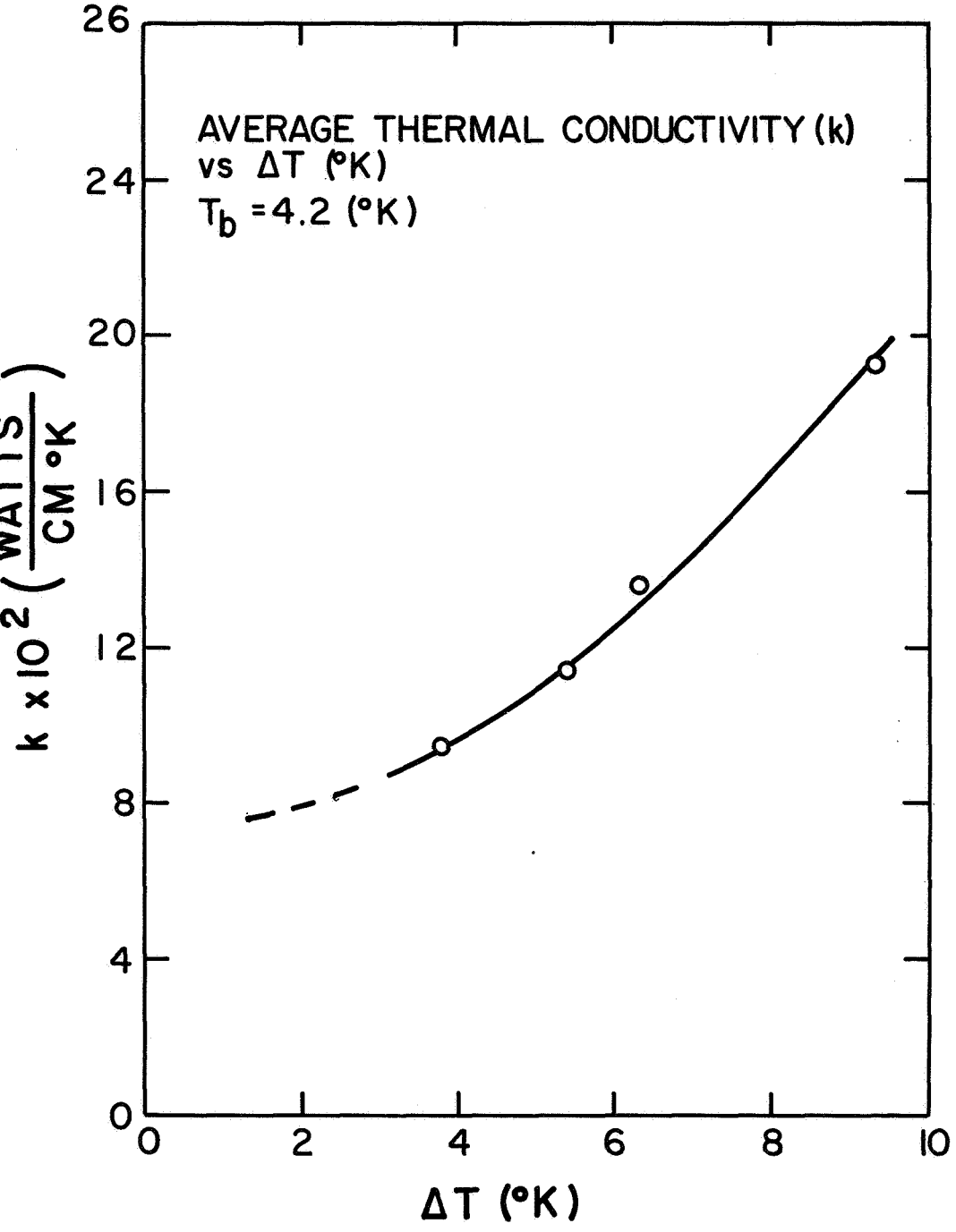

Fig. B-2 The average thermal conductivity of NbTi vs $\Delta T = (T_h - T_b)$

APPENDIX C

This Appendix contains a copy of a paper submitted to the Journal of Applied Physics presenting design consideration and the results of tests concerned with the construction of an 88 kG 51-cm bore diameter solenoid.

RESULTS OF TESTS ON MODELS FOR AN 88 kG 51-CM BORE DIAMETER SOLENOID*

Z. J. J. Stekly, E. Lucas, T. de Winter, B. Strauss, F. Di Salvo
Avco Everett Research Laboratory
Everett, Massachusetts

J. Laurence and W. Coles
NASA Lewis Research Center
Cleveland, Ohio

ABSTRACT

As part of a program to build an 88 kG, 51 cm bore solenoid, two model coils were built to test the conductor characteristics as well as the final coil construction techniques.

The first coil was wound with a square conductor .218 cm on a side, with many strands of Nb-Ti. The coil winding I. D. was 15.24 cm, the O. D. was 22.3 cm, and the length was 10.16 cm. This coil was built using small cooling passages, and its construction was such as to simulate the techniques to be used up to 80 kG in the full size magnet.

The second coil was wound with steel reinforced Nb_3Sn of overall dimensions 1.27 cm by .0292 cm and had a winding I. D. of 12.2 cm and an O. D. of 31.1 cm, and consisted of two pancakes. Its purpose was to simulate the high field windings of the full size coil.

Both coils were instrumented with heaters to determine their stability characteristics. The performance of each coil will be discussed with regard to stability, charge rate, and quench characteristics.

*This work was sponsored jointly by Contract No. NAS 3-9684 under the direction of Dr. James Laurence, NASA Lewis Research Center and Contract No. NAS 8-21037 under the direction of E. Urban and L. Lacey, NASA Marshall Space Flight Center.

Introduction

This paper describes the tests performed on two models of an 88 kilogauss, 51 cm bore superconducting coil system. The full scale coil system is made up of two separate assemblies placed adjacent to each other axially and consisting of three modules each. When both assemblies are operated together the system is designed to produce 88 kilogauss. Each assembly is divided into three modules. The inner module is made with a stainless steel reinforced, copper stabilized flat ribbon Nb_3Sn conductor, and the outer two modules are made with a square copper stabilized Nb-Ti conductor. A schematic of the coil system is shown in Fig. 1 with most of the important dimensions.

Since the conductors and construction methods for both the Nb_3Sn and the Nb-Ti modules were new, model coils with each conductor were built and tested to generate information on construction details as well as to provide information on coil performance. Specifically, information was required on the maximum current before quench, the ability of the coils to recover from disturbances, and the quench time.

Two coils were built for these tests -- one of Nb-Ti copper stabilized conductor and the other of stainless steel reinforced copper

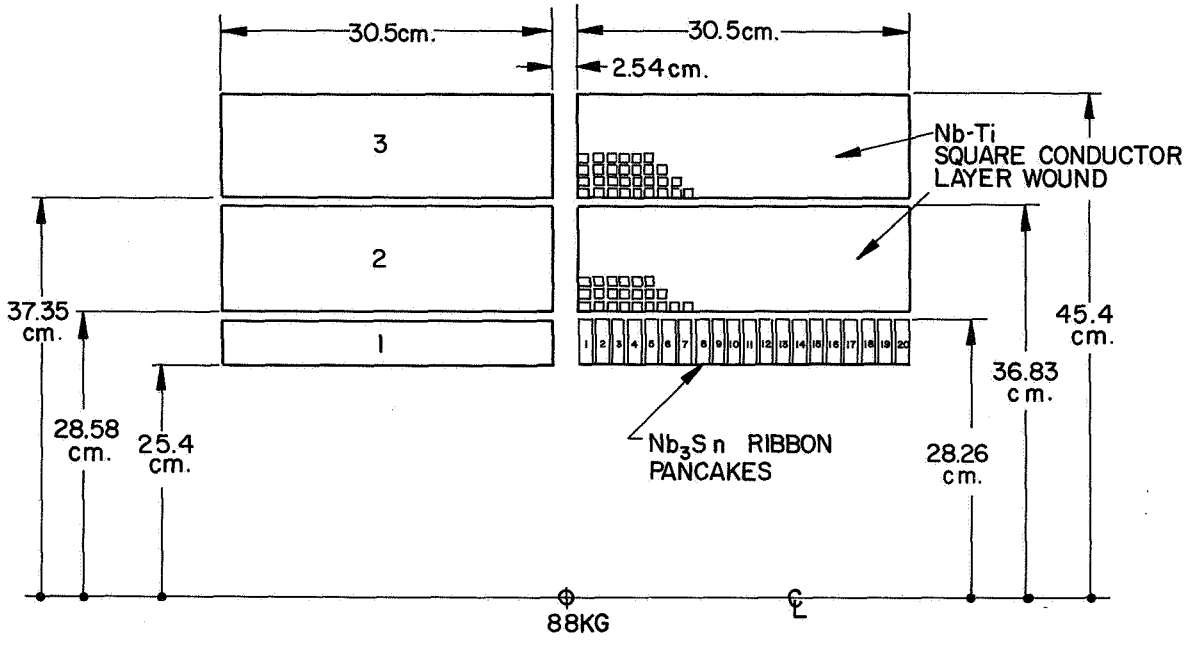

Fig. C-1 Schematic of the 88 kG Coil Assembly

stabilized Nb_3Sn flat ribbon.

A separate test was run for each coil; however the instrumentation and diagnostic techniques were similar.

First each coil will be described, then the performance of each coil will be discussed.

Nb-Ti Coil

The Nb-Ti conductor consisted of 15 Nb-Ti cores approximately .028 cm in diameter in a copper matrix .219 cm by .219 cm. The ratio of copper to superconductor was approximately 2.7 to 1.

This conductor was layer wound into the coil as shown in Fig. 2. Each turn was insulated from the adjacent turn axially by intermittent mylar insulation .018 cm thick and 1.27 cm long placed along the conductor so that the gap between insulation was .635 cm. The layer to layer insulation consisted of G-10 epoxy fiberglass slats .038 cm thick and .159 cm wide placed so that there was a .31 cm gap. The slats were placed at an angle as shown in Fig. 2 to aid in helium convection. With this construction 50% of the conductor surface was exposed to liquid helium.

To determine the coil resistance to thermal disturbances a small heater was wound into the coil. The heater consisted of three turns Nichrome wire .005 cm in diameter. The terminals were soldered to copper leads. The Nichrome wire was wrapped around the square conductor and insulated from it with .0025 cm Mylar. Additional Mylar tape was wrapped around the Nichrome wire so that the path of least thermal resistance would be from the Nichrome wire to the conductor around which it was wound. The overall physical length of the heater was approxi-

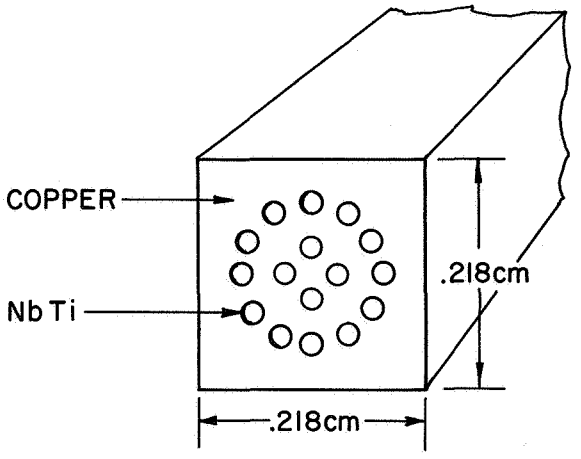

Nb-Ti WINDING SCHEMATIC

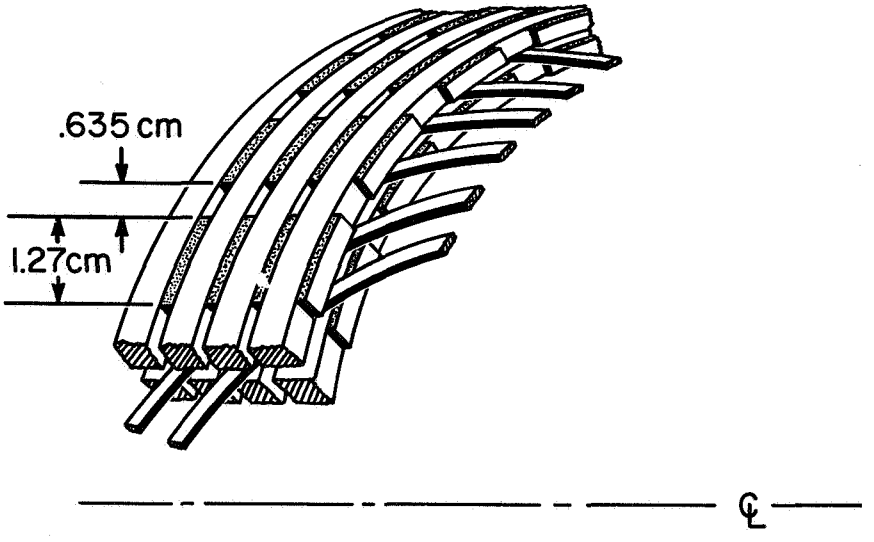

Fig. C-2 Schematic of Nb-Ti Conductor and Coil Windings

A9201
A9203

mately 1 cm. The heater was not placed at the highest field point, but in the fifth layer from the inside, so that the magnetic field at the heater was significantly below the calculated maximum field existing in the windings. A summary of the coil parameters is given in Table I below.

Table I
Nb-Ti Coil Parameters

Inside Winding Dia.	15.4 cm
Outside Winding Dia.	22.4 cm
Winding Length	10.2 cm
Central Field	34.5 Gauss/A
Maximum Field	46.5 Gauss/A
Field at Heater	26.25 Gauss/A
Number of Turns	582
Inductance	.052 H
Conductor Length	346 m
Room Temperature Resistance	1.6 Ω
Fraction of Conductor Surface Exposed to Helium	50%

Nb_3 Sn

The Nb_3 Sn conductor used is shown in Fig. 3. It consists of a Nb_3, Nb_3 Sn core about .002 cm thick manufactured by the General Electric Company. This core is sandwiched between .005 cm of copper and .0071 cm of steel on each side and soldered into one integral conductor. The resulting conductor is 1.27 cm wide and approximately .0305 cm thick.

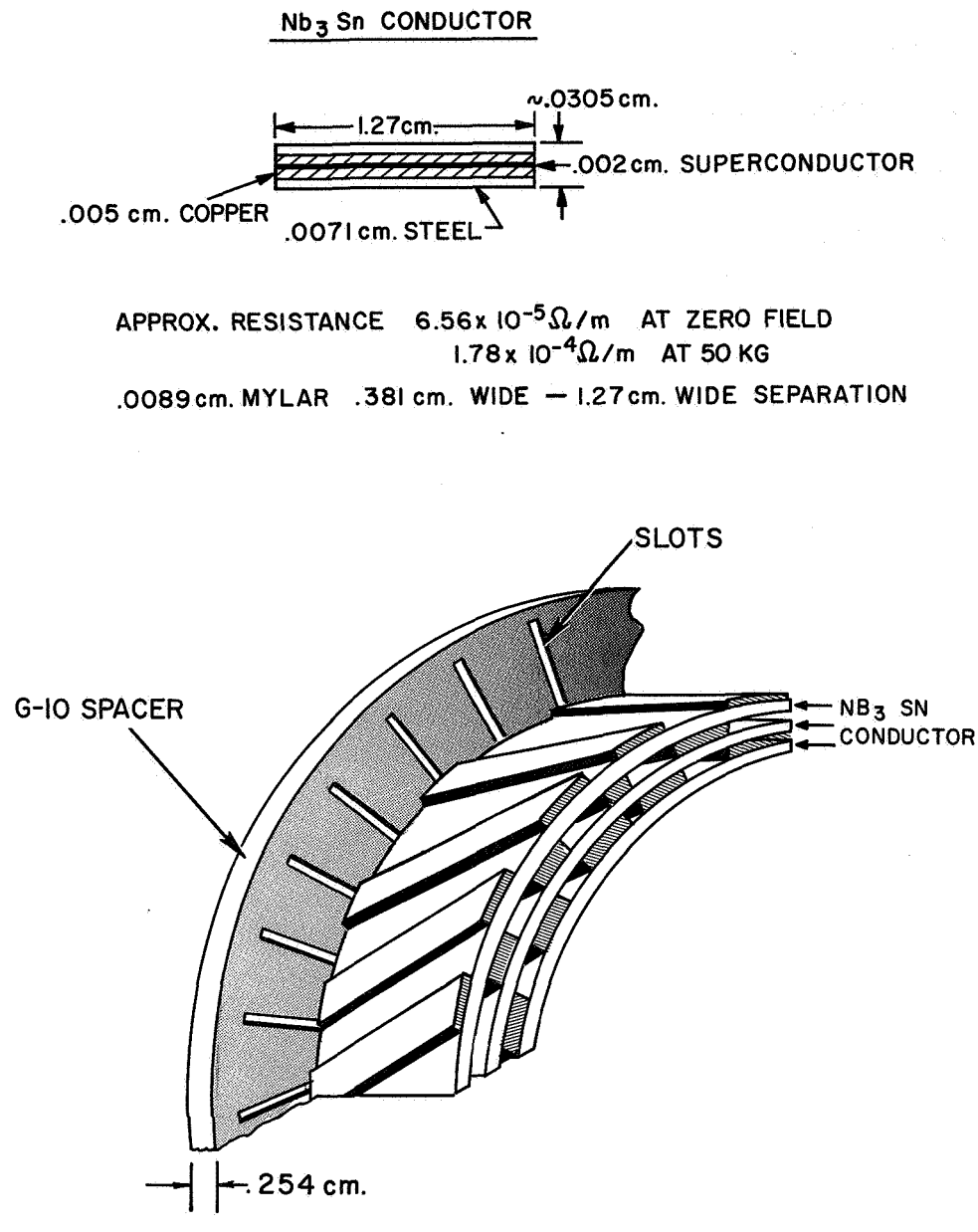

Fig. C-3 Schematic of Nb_3 Sn Conductor and Coil Windings

A9195
A9202

Unlike the Nb-Ti conductor which was layer wound, the Nb_3 Sn conductor was wound into pancakes. The turn to turn insulation was .0089 cm thick Mylar strips, .318 cm wide placed so that there is a .318 cm gap between insulating strips. The insulation was placed on the conductor diagonally as shown in Fig. 3. Two pancakes were wound with this conductor. The pancakes were separated by a G-10 spacer .254 cm thick which was slotted to allow flow of helium.

A heater was also incorporated in the pancakes. The heater consisted of .005 cm Nichrome wire which was wound back and forth into a rectangular shape approximately .318 cm by 1.27 cm. The wire was attached to copper leads and sandwiched between .0025 cm thick Mylar on both sides. The heater was then placed over the full width of the conductor and taped down with 3M type Mylar tape. After the heater was installed, an additional .015 cm of Mylar was added to prevent heat conduction to the adjacent turns.

A summary of the Nb_3 Sn coil parameters is given in Table II below:

Table II

Nb_3 Sn Coils

Inside Winding Dia.	12.2 cm
Outside Winding Dia.	28.7 cm
Width of One Pancake	1.27 cm
Central Field	25.6 Gauss/A
Maximum Field	43.5 Gauss/A
Conductor Length (Each Pancake)	147 m
Number of Turns (Each Pancake)	222
Inductance (Both Pancakes)	.035 H
Spacing between Pancakes	.254 cm
Fraction of Conductor Surface Exposed to Helium	50%

Test Results

Several types of tests were performed on each of the two model coils. The testing procedures and test results will be reviewed below. The main purpose of this paper is to present these testing techniques and the results obtained.

Nb-Ti Coil Heater and Charge Rate Tests

One of the main aims of the testing program was to determine the amount of heat required to generate a detectable normal region and to determine whether this normal region would propagate in an uncontrolled manner. This information was obtained by using the heater within the windings. At a fixed coil current, the heater was energized, and the voltage across the heated section was monitored. Once a voltage appeared across the terminals of the heated section, the heater power was reduced to observe the behavior of the voltage.

Typical data of this type are presented in Fig. 4 for various values of coil current.

At low coil currents (Fig. 4a and 4b) the appearance and disappearance of voltage is gradual and the voltage retraces the same curve on decreasing heater current that it traced on increasing heater current. At 640 amperes coil current a hysteresis exists where the onset of voltage is sudden, and a recovery back to the superconducting state occurs at a lower heater power than the onset. At 660 amperes it takes a finite heater power before onset occurs; however no recovery back to the superconducting state occurs even when the heater current is reduced to zero. At higher currents (800 A) it takes a finite heater

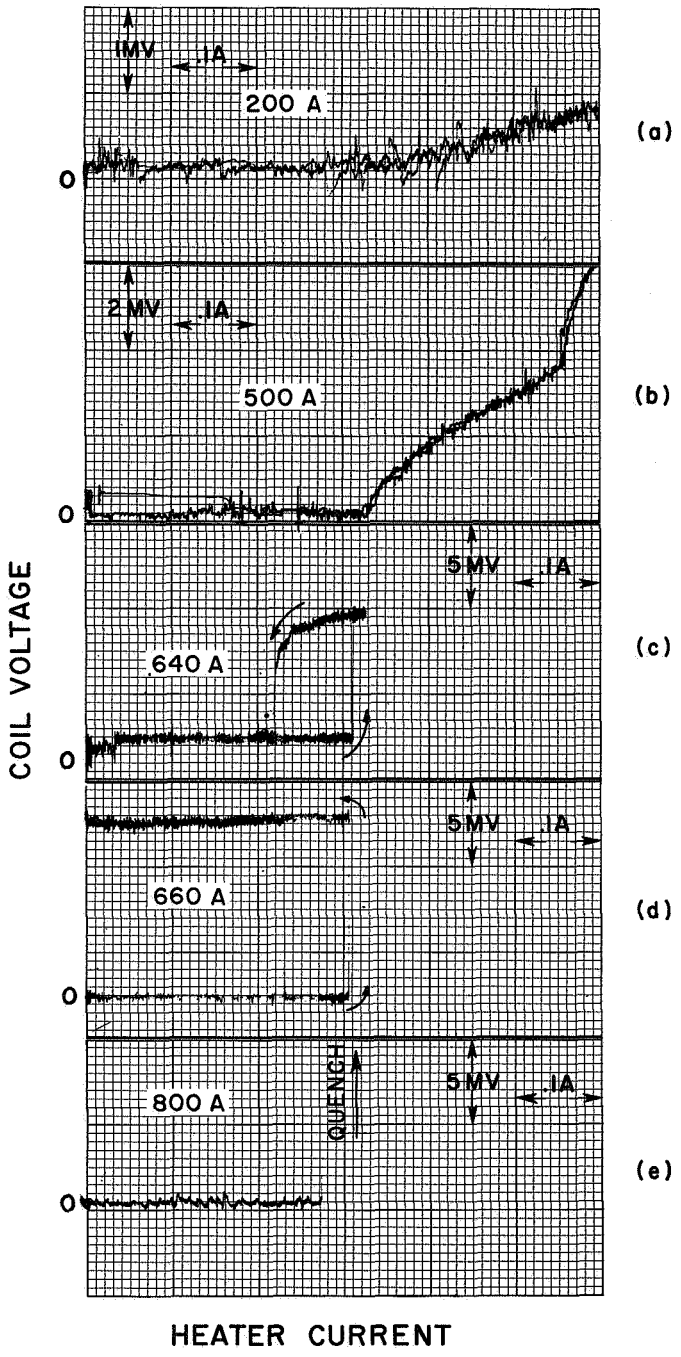

Fig. C-4 Typical Heater Characteristics for the Nb-Ti Coil (Heater #2)

a) At a magnet current of 200 amperes

b) At a magnet current of 500 amperes

c) At a magnet current of 640 amperes

d) At a magnet current of 660 amperes

e) At a magnet current of 800 amperes

current before onset of resistance occurs; however once voltage appears it grows in an uncontrolled manner. Note also that at the sensitivity used (5 mv/in.) no detectable voltage appeared prior to the rapid increase of voltage at the onset of resistance.

The onset of resistance and recovery was determined for the whole operating range of the coil, and in addition at low coil currents heater power was increased considerably beyond that required for resistance. A typical trace is shown in Fig. 4b, which exhibits a sudden change in slope of the coil voltage at a heater current above the onset value. These changes in slope are due to the propagation of resistance to the adjacent turns. This is due to the face that one turn acts as a heater to the adjacent one. It was found that for low currents resistance appeared first in the heated turn, then propagated to one adjacent turn, then the other adjacent turn, and then to the next layer. The propagation of resistance to the adjacent layer coincided with onset of resistance in the adjacent turns, while at currents above 660 A uncontrolled propagation of resistive region coincided with onset of resistance in the heated turn.

The complete heater data is summarized in Fig. 5. At low currents (within the range tested) the onset of resistance is gradual and quench occurs when resistance propagates to the adjacent layer. At higher currents the onset of resistance is still gradual, and quench occurs when resistance propagates to the adjacent turns. At slightly higher currents, onset of resistance occurs at higher heater power than the heater power at recovery from the resistive state and a quench still occurs on propagation of resistance to the adjacent turn. At currents above 660 A the onset of resistance in the heated turn coincides with a quench. As expected the

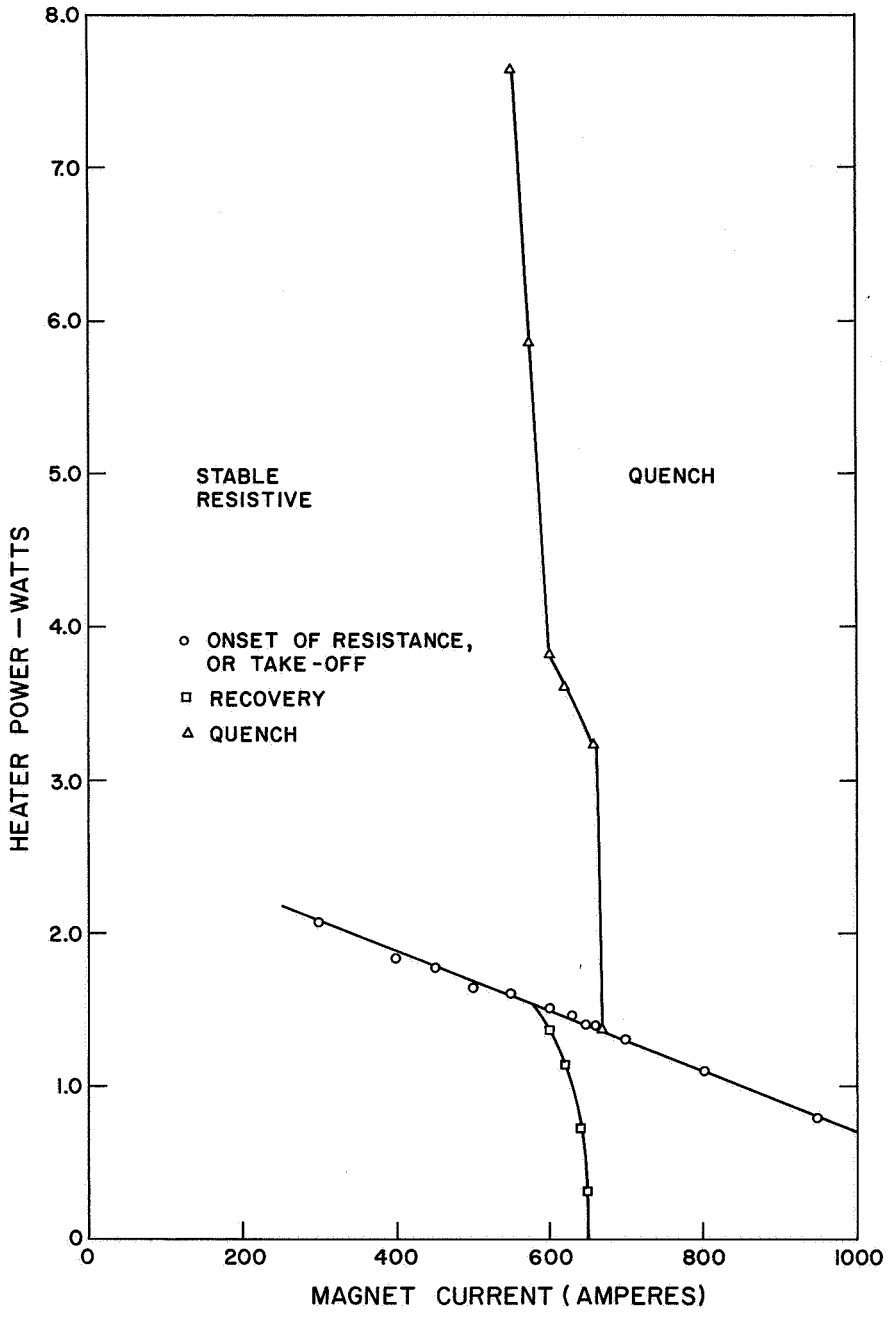

Fig. C-5 Summary of Heater Data for the Nb-Ti Coils

heater power required for onset of resistance decreases with increasing coil current.

The conclusions that can be reached are that for currents above 660 A, the coil (in the vicinity of the heater) is unstable to thermal disturbances large enough to produce a measurable voltage. At lower currents a detectable voltage region exists before uncontrolled propagation of the normal region results. Also the slope of the quench line is very steep; consequently the degree of stability increases very rapidly below 660 A (at the heater).

Now that the effect of thermal disturbances has been determined it is important to determine whether the coil will operate up to the short sample current of the conductor. All that has been determined so far is that above 660 A no recovery from a thermal disturbance large enough to produce a measurable voltage can occur; however the heater power necessary for the onset of resistance is still considerable.

The coil was energized without the heater and the current at quench was measured as a function of charge rate. The results are summarized in Fig. 6.

At charge rates lower than 2.5A/second the coil operated up to its short sample current carrying capacity. At higher charge rates quench occurred at progressively lower currents, but always above the predicted recovery current. The decrease in quench current with increasing charge rate is probably due to heating within the conductor due to shielding currents.

Figure 7 is a summary of all the data. It shows the short sample characteristics for the conductor used, and the load line for the maximum field in the coil. Also shown are data points for the limit of recovery from a thermal disturbance obtained from a small three-layer coil of

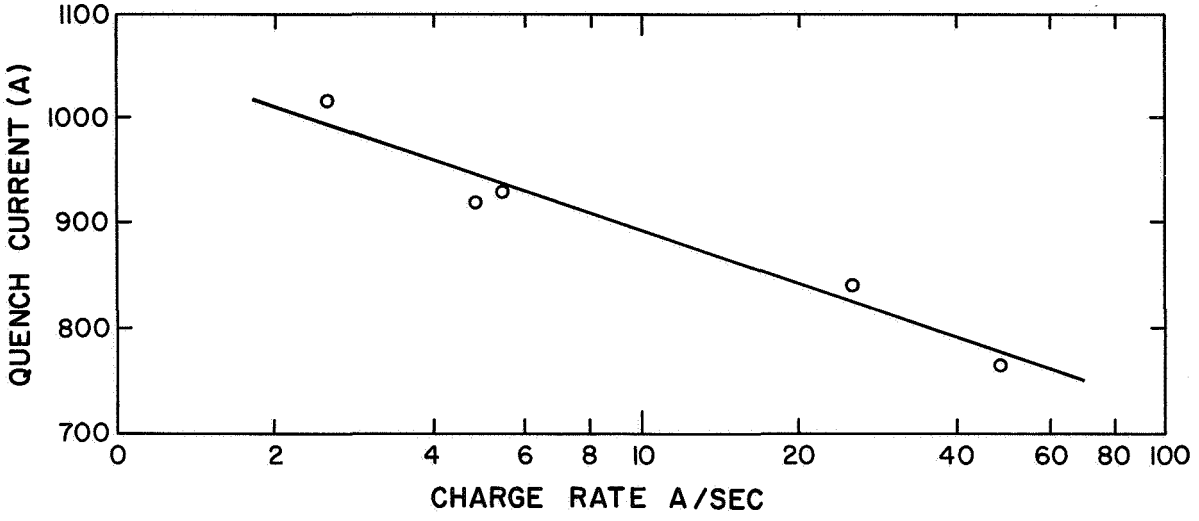

Fig. C-6 Quench current as a function of charge rate for the Nb-Ti coil

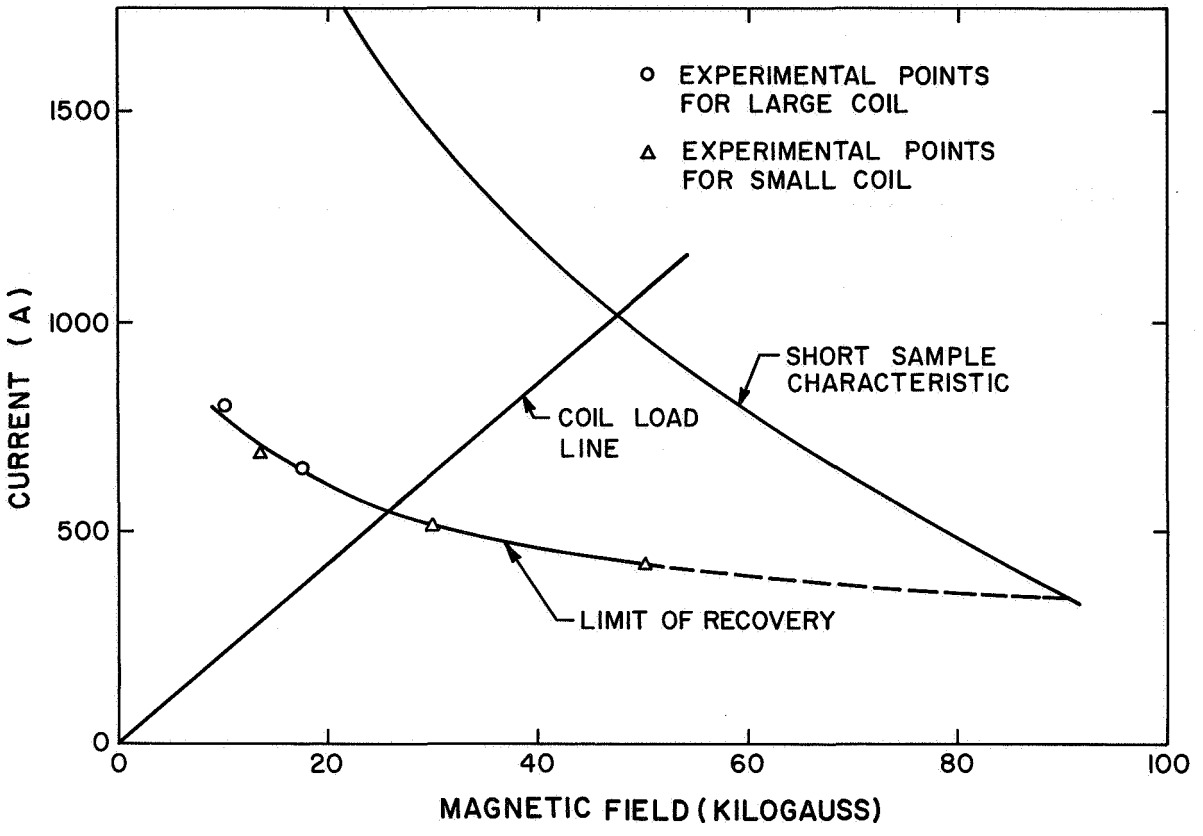

Fig. C-7 Short sample and operating characteristics for the Nb-Ti coil

identical construction instrumented with a heater. The pertinent data for this coil are inside diameter 5.53 cm, outside diameter 7 cm, length 3.96 cm, number of turns 50. This coil was small enough so that it could be operated inside another superconducting coil so that the field at the heater could be varied. The line defining the limit of recovery from a thermal disturbance as determined by the heater test corresponds within experimental error to a heat flux per unit area at the exposed conductor surface of approximately .35 watts/cm^2.

The conclusions are that operation to the full short sample current carrying capacity can be achieved in coils equal in size to the model coil, provided charge rates are kept low enough. Stability against thermal disturbances large enough to produce measurable coil voltages exists at currents somewhat below the short sample current carrying capacity.

When scaling up to larger coils it is expected that coils will operate at least to the limit of recovery from a measurable thermal disturbance. Larger coils in general have larger stored energies, and it is not unreasonable to assume that larger coils might be subjected to greater disturbances. There is evidence that operation of large coils in the presence of disturbances may be limited by the recovery limit referred to above.[1,2,3] However, the coil tested operates very well above this limit.

Nb_3 Sn Coil - Heater and Charge Rate Tests

The tests performed on the Nb_3 Sn coil were similar, but not nearly as extensive as those performed on the Nb-Ti coil.

A typical heater test at low currents is shown in Fig. 8. The onset

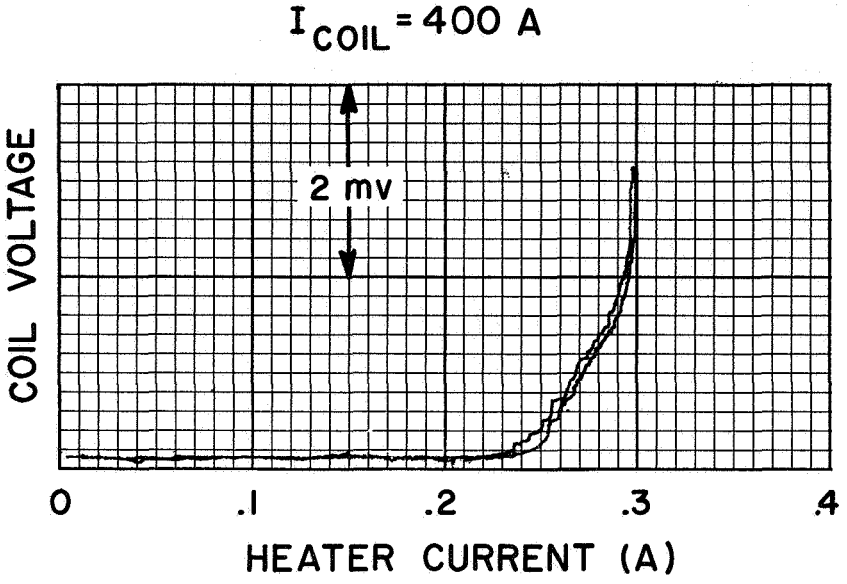

Fig. C-8 Typical heater characteristics for the Nb_3 Sn coil

and disappearance of voltage was gradual and the curve shows negligible hysteresis. As the heater current is increased the slope of voltage increases very rapidly until a quench occurs. For the particular trace shown, the current was lowered before the resistance propagated in an uncontrolled manner.

As the coil current was increased the traces of voltage versus heater current did not exhibit any hysteresis for the currents measured. As the coil current was increased the slope of the voltage trace at onset increased and the range of heater current between onset of resistance and quench decreased. The heater data is summarized in Fig. 9 for the Nb_3 Sn coil.

In interpreting the heater tests for the Nb_3 Sn coil two facts should be borne in mind: (a) the critical temperature is high, and it is necessary to raise the temperature considerably above the transition temperature for nucleate to film boiling, (b) the cooling passages between turns are small and, due to the width of the conductor, can easily become vapor bound.

Because of these reasons, the heater tests are not as meaningful as with the Nb-Ti coil, since vapor binding occurs before onset of resistance (a situation which is not likely to occur under normal coil operation). Once vapor bound, heat transfer from the heated turn occurs by conduction only.

Because of the vapor binding and no hysteresis region it is difficult to directly compare the stability of the Nb_3 Sn and the Nb-Ti coils. The only statement that can be made is that the heater power required to initiate a quench is of the same order of magnitude for the two coils (Figs. 5 and 9).

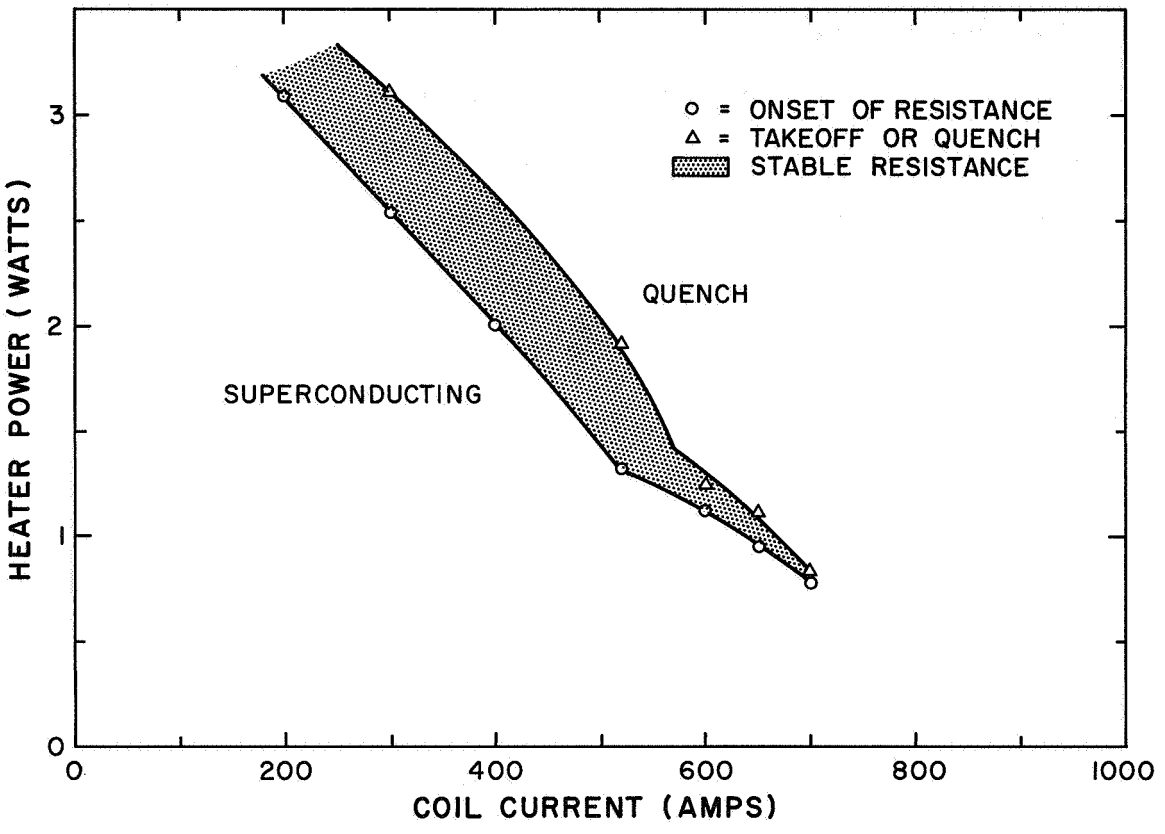

Fig. C-9 Summary of heater data for the Nb_3 Sn coil

The Nb_3 Sn coils were operated mainly to obtain stability data. Operation up to the short sample current carrying capacity of the Nb_3 Sn conductor at the relatively low fields generated by the model coil would result in excessive stresses, so operation was limited to 800 A and below.

No detailed measurements of charge rate versus quench current were done; however to demonstrate that the coil could be rapidly charged it was charged to 500 A at a charge rate of 25 A/sec.

Quench Characteristics

One of the important design considerations in a large coil with a sizeable amount of magnetic energy is the question of what happens if a quench is initiated. The stability or lack of it determines under what conditions a quench might be initiated. The quench characteristics are important mainly from the point of view of preventing damage to the coil or coil system during uncontrolled propagation of a resistive region.

Damage during quench can occur from two causes -- excessive voltage and excessive temperature. An estimate of both the voltage and maximum temperature rise is possible if the quench time can be estimated.

The quench characteristics of each coil were obtained by charging the coil up to a fixed current, then shorting the coil with a room temperature shorting switch. This resulted in a relatively long decay time constant. The heater was then energized to a power level high enough to initiate a quench. The coil current during the quench was measured by a shunt in the circuit, and the rate of change of field was measured by a pickup coil. A typical set of quench data for the Nb_3 Sn coil is shown in Fig. 10.

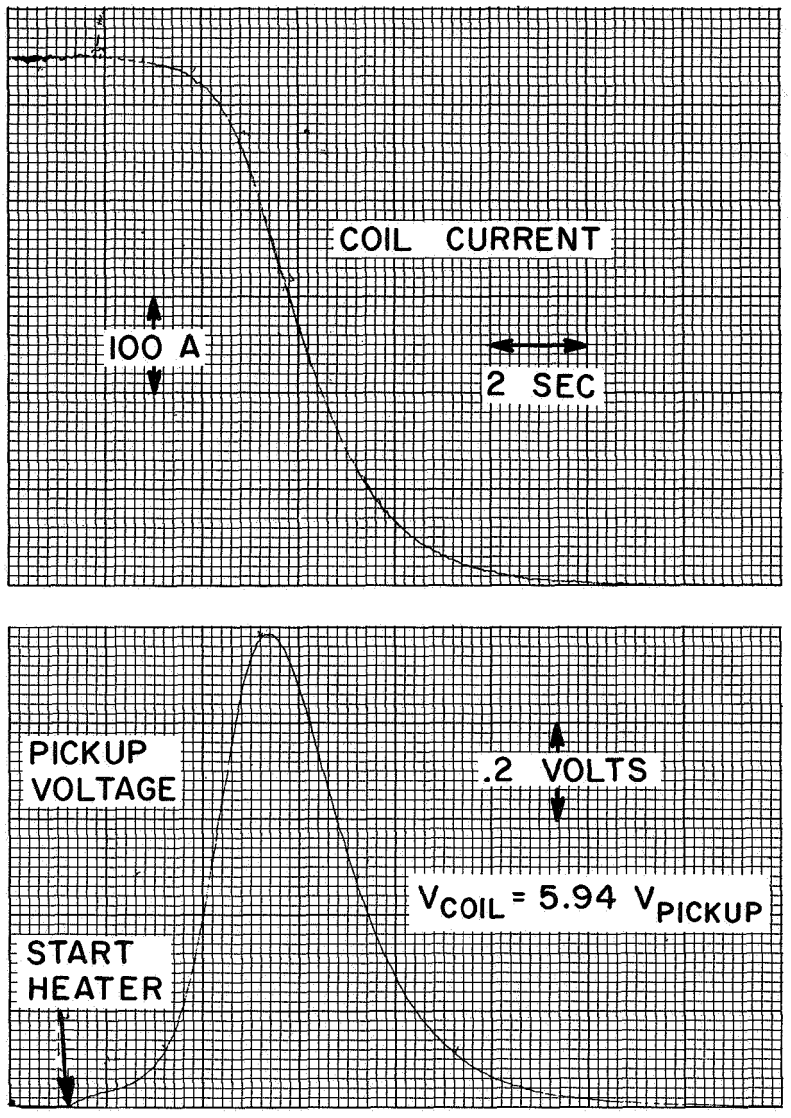

Fig. C-10 Quench characteristics for the Nb_3 Sn coil. The upper curve is a recording of the coil current decay with time, while the lower curve is a trace of the voltage recorded across the terminals of a pickup coil during the quench.

The data for the two coils is summarized in Fig. 11, which shows the quench time as a function of coil current. The quench time is defined as the initial coil current divided by the maximum rate of current decay with time.

The data in Fig. 11 can be extrapolated to the full coil system by methods described in Reference 4.

Concluding Remarks

The data described in this paper were generated for the purpose of obtaining information on construction details and techniques, stability, charge rate, and quench characteristics for the full scale coil system.

Both the Nb-Ti and Nb_3 Sn coils made use of new conductors and new construction techniques.

From the test data on stability and charge rate it can be concluded that both the Nb-Ti and the Nb_3 Sn coils can withstand sizeable thermal disturbances, as well as rapid charge rates without quenching.

There were no results of a negative nature obtained during the testing program on either of the coils, and the full scale coil system is being built using the same construction.

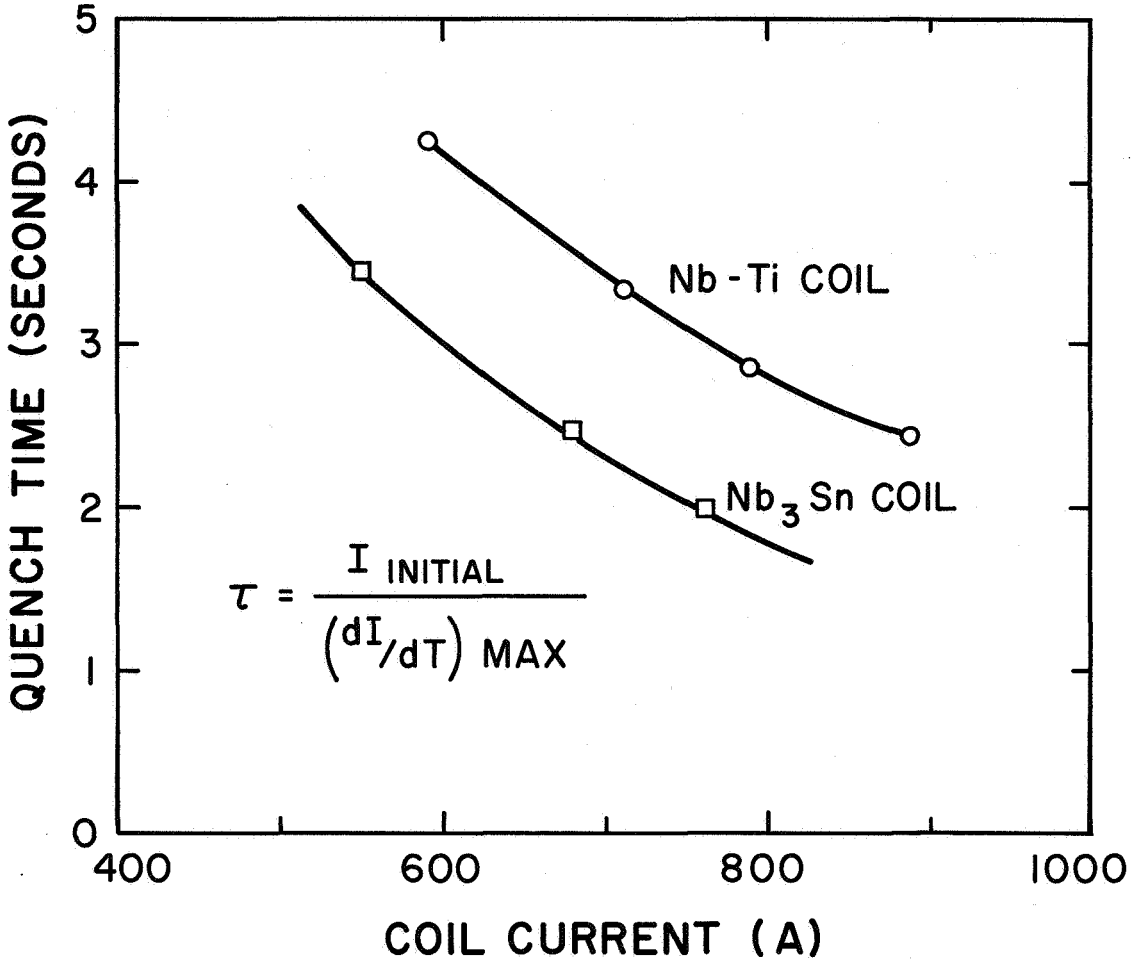

Fig. C-11 Quench time as a function of coil current for the Nb-Ti and Nb_3 Sn model coils

REFERENCES

1. Stekly, Z. J. J., "The Performance of a Large MHD-Type Stable Superconducting Magnet." Presented at the International Conference on High Magnetic Fields, Grenoble, France, September 12-14, 1966.

2. Stekly, Z. J. J., "Large Superconducting Magnets for MHD." Presented at the International Cryogenic Engineering Conference, Kyoto, Japan, April 1967.

3. Boom, R. W. and Nuding, J. M., "Force Reduced Superconductor Toroid." Presented at the International Conference on Magnetics, Stuttgart, Germany, April 20-22, 1966.

4. Stekly, Z. J. J., "Theoretical and Experimental Study of an Unprotected Superconducting Coil Going Normal," BSD-TDR-62-116, Avco Everett Research Laboratory Research Report 135, May 1962.